7-1-2015

Hydrologic Controls of Coastal Groundwater Discharge in Southern Taylor Slough, Everglades National Park, Florida

Edward Linden
Florida International University, elind014@fiu.edu

DOI: 10.25148/etd.FIDC000093

FLORIDA INTERNATIONAL UNIVERSITY

Miami, Florida

HYDROLOGIC CONTROLS OF COASTAL GROUNDWATER DISCHARGE IN SOUTHERN TAYLOR SLOUGH, EVERGLADES NATIONAL PARK, FLORIDA

A thesis submitted in partial fulfillment of

the requirements for the degree of

MASTER OF SCIENCE

in

GEOSCIENCES

by

Edward Linden

2015

To: Dean Michael R. Heithaus
College of Arts and Sciences

This thesis, written by Edward Linden, and entitled Hydrologic Controls of Coastal Groundwater Discharge in Southern Taylor Slough, Everglades National Park, Florida, having been approved in respect to style and intellectual content, is referred to you for judgment.

We have read this thesis and recommend that it be approved.

_____
Dean Whitman

_____
William T. Anderson

_____
René M. Price, Major Professor

Date of Defense: June 30, 2015

The thesis of Edward Linden is approved.

_____
Dean Michael R. Heithaus
College of Arts and Sciences

_____
Dean Lakshmi N. Reddi
University Graduate School

Florida International University, 2015

DEDICATION

I dedicate this thesis to my parents, Charles and Diana. They have fostered learning and exploration throughout my life, helping to inspire me to succeed at everything I set out to accomplish.

ACKNOWLEDGMENTS

I would like to thank the following individuals for the help that they gave me throughout this project: Dr. David Lagomasino and Adriana Sanchez for teaching me both lab and field techniques; Dr. Jordan Barr, Josh Allen, Hilary Flower, and Rafael Travieso, for helping me with fieldwork; Adam Heins, Olga Sanchez, and Dr. Tiffany Troxler's entire lab and field staff for providing samples from the autosamplers at TS/Ph-3 and TS/Ph-6a and helping me make sense of the nutrient data for the sites; Mark Zucker from the USGS and Kevin Kotun from Everglades National Park, for their assistance with physical data acquisition and analysis. I also would like to thank my committee members, Dr. Dean Whitman and Dr. Bill Anderson for their advice and input on this project. And finally, Dr. René Price is due the most thanks for her all of her help with the countless problems that I encountered and questions that I asked of her throughout the duration of this project.

This project was made possible by long term datasets provided by the United States Geologic Survey, Everglades National Park, the South Florida Natural Resources Council, and the Florida Coastal Everglades Long Term Ecological Research Project. Funding was provided through NSF grant # DEB-1237517.

ABSTRACT OF THE THESIS

HYDROLOGIC CONTROLS OF COASTAL GROUNDWATER DISCHARGE IN SOUTHERN TAYLOR SLOUGH, EVERGLADES NATIONAL PARK, FLORIDA

by

Edward Linden

Florida International University, 2015

Miami, Florida

Professor René M. Price, Major Professor

This project empirically determined the controls of groundwater discharge potential and surface water chemistry in southern Taylor Slough, Everglades National Park, Florida. Potential for groundwater discharge was calculated as the difference in equivalent freshwater stage between groundwater and surface water on a daily basis for two sites (upland and coastal) along southern Taylor Slough. Upstream water stages were shown to vary most similarly to the timing of groundwater discharge potential in coastal Taylor Slough. Surface water major ion chemistry did not apparently change as a result of groundwater discharge potential. Surface water major ion chemistry at the coastal site was controlled by surface water flow direction, while at the more inland site surface water major ion chemistry was controlled by upstream water levels and evapotranspiration. Surface water phosphorus concentrations at the coastal site were controlled by groundwater discharge and flows of local surface water.

TABLE OF CONTENTS

LIST OF TABLES

LIST OF FIGURES

FIGURE PAGE

INTRODUCTION

Groundwater (GW) discharge from coastal aquifers to near-shore environments occurs in many diverse regions around the globe (Tobias et al. 2001). Discharge of GW can contribute a significant volume of water and entrained constituents to the regions in which the discharge occurs (Burnett et al. 2003; Moore 2006; Tobias et al. 2001; Price et al. 2006; Winter et al. 1998). The term submarine GW discharge is used when GW discharge occurs seaward of the shoreline, with the greatest GW discharge typically found near the shoreline (Winter et al. 1998). In aquifers with extremely shallow hydraulic gradients that are affected by saltwater intrusion, such as in south Florida's coastal Everglades, GW discharge can occur inland of the coastline in a process known as coastal GW discharge (Price et al. 2006; Zapata-Rios & Price 2012).

Density-driven intrusion of brackish marine waters into coastal freshwater aquifers creates a wedge-shaped brackish mixing zone inland of the saltwater intrusion front (Figure 1) (Cooper 1959; Kohout 1960). Numerous geochemical reactions have been reported in the brackish mixing zone including: water-rock interactions including mineral dissolution and precipitation; acid-base reactions; sorption and ion exchange reactions; redox reactions; biodegradation reactions; and gas exchange. (Moore 1999; Price et al. 2006; Valiela et al. 1990; Valiela et al. 1992; Winter et al. 1998). The interaction of the brackish GW discharge and the receiving surface water (SW) facilitates the exchange of chemical constituents and nutrients between the two water reservoirs that has been linked to ecosystem responses of increased metabolic activity as a result of changes in SW chemistry (Koch et al. 2012; Valiela et al. 1992; Zapata-Rios & Price 2012).

Hydraulic gradient is often cited as the driving mechanism of GW discharge and has both marine and terrestrial forcing components. Tidal pumping, in combination with storm occurrence, wave action, and buoyancy differences can lead to exchange of water across the SW-sediment interface (Moore & Wilson 2005; Wilson & Morris 2012; Li et al. 1999). Recharge of terrestrial aquifers causes GW to flow to the coastline (Burnett et al. 2006), and seasonality in the recharge can result in seasonal pulses of GW discharge at or near the coastline (Michael at al. 2005).

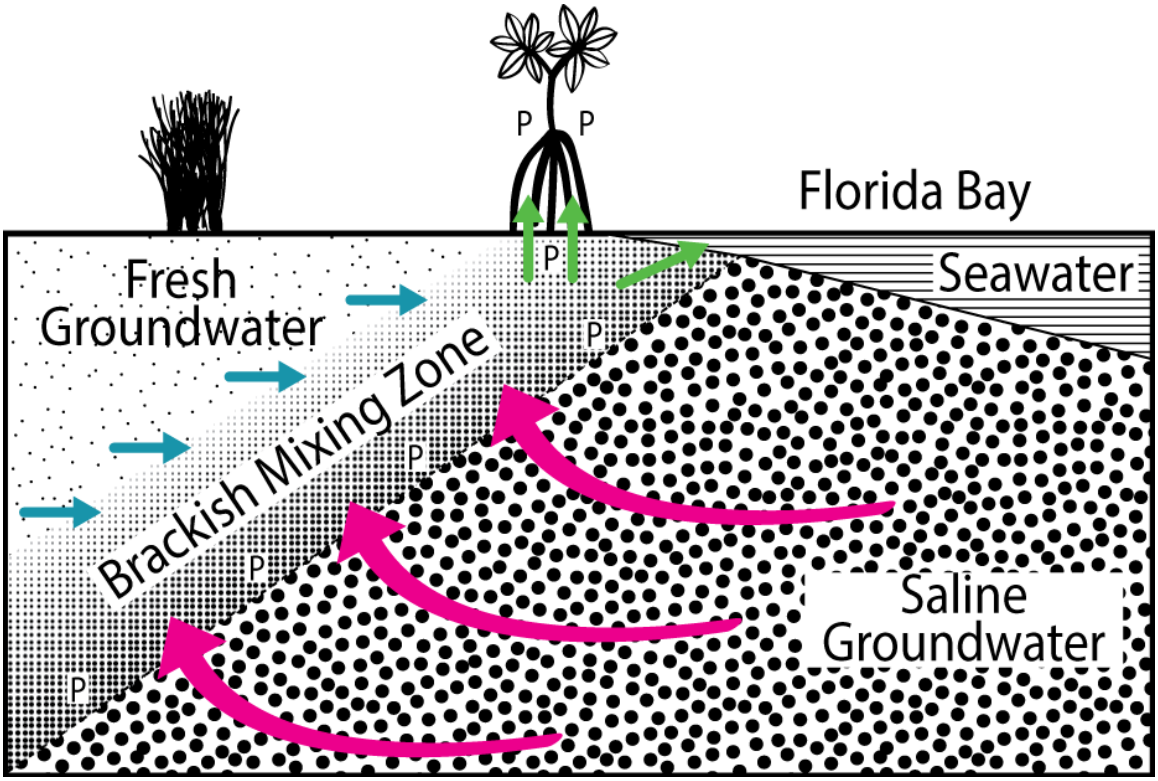

Figure 1: Conceptual diagram of a saltwater intrusion wedge beneath a terrestrial aquifer, creating a brackish mixing zone and driving coastal and submarine groundwater discharge with associated phosphorous (P)-derived productivity peak. Vertical dimensions are greatly exaggerated. Following Price et al. (2006).

Along the southern Everglades coastline, particularly along the boundary with northeastern Florida Bay, tides and waves are minimal (Holmquist et al. 1989), therefore, seasonal forcing mechanisms may be more important in the timing and quantity of GW discharge. Previous GW discharge related work in the region focused on water balance techniques (Zapata-Rios & Price 2012; Sandoval 2013); thermally-based, flux modeling (Spence 2011); and small scale water balanced augmented by numerical modeling of the Slough's GW (Michot et al. 2011). Those projects determined that GW discharge was an important contributor to Taylor Slough's water (Zapata-Rios & Price 2012, Sandoval 2013) and phosphorus (P) budgets (Koch et al. 2012). As yet, no attention was given to the driver(s) of the GW contribution. As a principle driving force of the Everglades' ecosystem (DeAngelis & White 1994), the hydrology and the forcing mechanisms behind the hydraulic processes of the region must be well defined in order to form more regionally accurate hydrological and chemical models and to make informed water

management decisions that can protect waters (Kalbus et al. 2006) and prevent detrimental effects of water management actions in spatially distant regions. This project attempts to determine the specific forcing mechanisms from a variety of potential hydrologic drivers of GW discharge in a shallow hydraulic gradient region that experiences only minor tides and waves. Since GW discharge has also been shown to be an important contributor of not only brackish water but also nutrients to the receiving SW body (Burnett et al. 2003; Moore 2006; Tobias et al. 2001; Price et al. 2006; Winter et al. 1998), the influence of GW discharge on the SW of the southern Everglades was also investigated. A better understanding of the interactions between GW and SW can help support research on nutrient cycling (Sutula et al. 2001) because GW and SW interactions are an important component of the hydrologic cycle (Winter et al. 1998). The objectives of this research were to determine the dominant forcing mechanism(s) driving GW discharge along coastal Taylor Slough and to evaluate the effects of GW discharge on SW chemistry along coastal Taylor Slough. I hypothesized that the dominant forcing mechanisms that drive GW discharge along coastal Taylor Slough are upstream and downstream water levels. I further hypothesized that GW discharge increases the concentration of major ions and phosphorus in the overlying SW. Investigation of these hypothesis will lead to a more complete understanding of the Everglades' hydrology in terms of both forcing mechanisms and resultant chemical changes, which is necessary to understand and predict the effects of sea level rise and water management actions.

STUDY AREA

Anthropogenic influences on the Everglades began in the early 20th century with the construction of a system of canals, dikes, and levees that were intended to drain the region for human utilization (Davis & Ogden 1994). These drainage efforts intensified in the middle of the century in response to flooding that occurred in 1948 with the addition of water storage areas, among other modifications (Light & Dineen 1994). These changes led to drainage of nearly half of the historical Everglades (Davis & Ogden 1994). As hydrologic processes within the region deviated from their natural patterns, human settlement and agriculture increasingly encroached and largely surrounded the area, further intensifying the hydrologic changes that had already occurred. Anthropogenic modification has produced significant differences in the volume of SW and GW flows in terms of both timing and quantity, with a smaller spatial extent and a lesser amount of flow now occurring (Fennema et al. 1994). Consequentially, wetlands became dehydrated and threatened (Davis & Ogden 1994; Light & Dineen 1994).

The modern Everglades is one of the most endangered ecosystems in the country (Light & Dineen 1994). Much of the Everglades that persists upstream from developed areas has been sectioned into diked impoundments, the water conservation areas. These areas and the canals that dissect much of South Florida are currently managed with the goals of maintaining a steady supply of water for the region's residents and reducing the potential of flooding for South Florida's continuously expanding population, while simultaneously addressing environmental concerns for water level, flow, and quality. South Florida is currently home to nearly 7 million residents who rely of a supply of potable GW that is locally replenished through GW recharge that partly occurs within Everglades National Park (ENP) (Fish & Stewart 1991). Many tourists visit the Everglades and Everglades-dependent ecosystems every year and many fisherman fish in and around the Everglades, making the Everglades' health important to maintenance of the region's population and economy.

The Everglades is an oligotrophic wetland (Noe et al. 2001) that is metabolically limited by P (Gaiser et al. 2006). Everglades National Park occupies the southern tip of the Florida

peninsula and bounds only one-fifth of the historical Everglades (Light & Dineen 1994). The plant and animal communities within ENP, including sawgrass (*Cladium jamaicense*) prairie, tree islands, pine (*Pinus elliottii*) rocklands, and mangrove forests have adapted to the seasonal wet-dry cycle as well as the low nutrient conditions. Differences in the occurrence of these communities are a function of water flow, slight elevation differences, timing of inundation, nutrient availability, and salinity.

Within ENP there are two major waterways: Taylor Slough and Shark River Slough (Figure 2). These two waterways are hydraulically isolated from one another by a limestone ridge with elevations of 1.5 to 2.5 m known as the Rocky Glades (Price & Swart 2006) (Figure 2). Despite Taylor Slough's smaller size relative to Shark Slough, Taylor Slough is a critical component of the Everglades ecosystem; the slough acts as an important regional hydraulic link between freshwater uplands and estuaries (Armentano et al. 2006). In this way, the slough helps maintain the health of ENP and Florida Bay (Briceño et al. 2014). The eastern edge of Taylor Slough abuts the urban and agricultural sprawl of South Florida and represents a unique natural laboratory for studying the response of wetlands to restoration along such a margin (Sullivan et al. 2014). A thorough understanding of Taylor Slough's hydrologic conditions is thus key to successful management, restoration, and preservation of ENP and associated ecosystems.

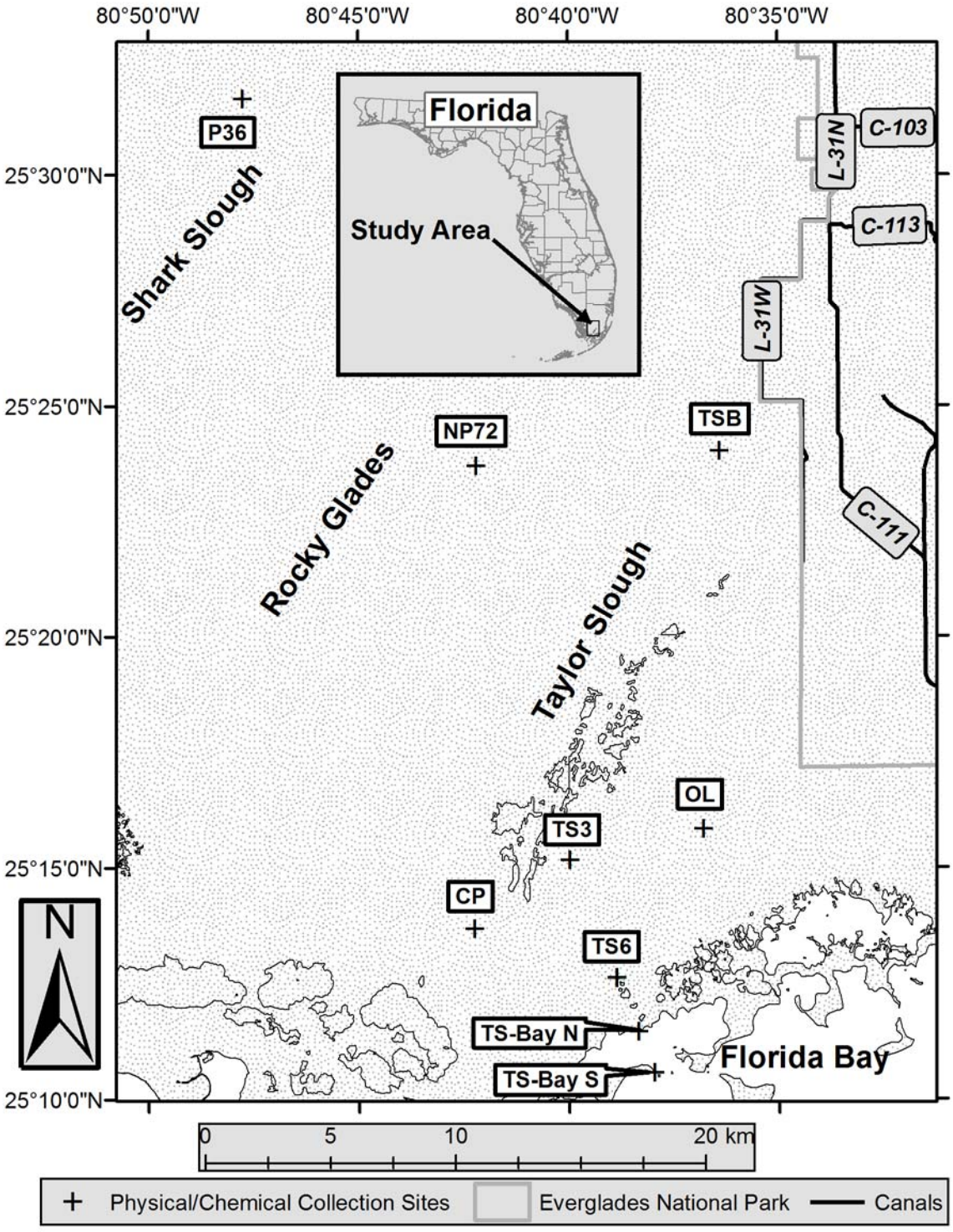

Figure 2: Physical and chemical data collection sites in and around Taylor Slough. The TS3 site includes E146, G3776, G3777, and TS/Ph-3; while the TS6 site includes Upstream Taylor Slough, G3763, G3764, TS/Ph-6a, TS/Ph-6b.

Previous studies in Taylor Slough have largely been ecologically focused (e.g., Childers et al. 2006; Davis et al. 2001; Gaiser et al. 2006). A primary productivity peak arises in the mangrove ecotone region of southern Taylor Slough that is attributed to GW discharge (Childers 2006). Net primary productivity in the mangrove ecotone is P-limited and controlled by salinity, the timing of SW flows, and GW discharge (Koch et al. 2012). Taylor Slough's primary source of water and P is atmospheric deposition (Sandoval 2013; Sutula et al. 2001), but GW discharge may be another significant source of P (Price et al. 2006).

Thermal modeling has demonstrated that GW discharge does occur in Taylor Slough's mangrove ecotone (Spence 2011), which agrees with the findings of both single and multiple technique water balance approaches (Sandoval 2013; Zapata-Rios & Price 2012). Another study that used a water budget technique that was augmented by numerical modeling of GW in southern Taylor Slough similarly found that GW discharge was an important contributor, but that GW discharge occurs most of the time (Michot et al. 2011). Michot et al.'s (2011) work additionally showed that the contribution of GW discharge is more important during the dry season and insignificant during the wet season, relative to SW flow. These research projects have all concluded that GW is an important contributor to Taylor Slough, but none have investigated the drivers of GW discharge in the highly productive mangrove ecotone of southern Taylor Slough.

Water currently enters Taylor Slough through a variety of routes. Precipitation is the dominant freshwater contributor (Sandoval 2013; Sutula et al. 2001; Zapata-Ríos & Price 2012), while GW discharge and inputs from Florida Bay contribute brackish water (Price et al. 2006). Water leaves the slough primarily via evapotranspiration (ET) and to a lesser degree, outflows into Florida Bay (Sandoval 2013; Zapata-Rios & Price 2012). Drainage is affected both tidally and seasonally; southward flows occur during the wet season, whereas stagnation and flow reversals occur during the dry season (Sandoval 2013; Sutula et al. 2001). After being cut off from the greater Everglades because of upstream levee construction, the slough has experienced over-drainage throughout much of the managed history (Kotun & Renshaw 2014). A series of

successful managerial responses to dehydration have resulted in restoration of the slough's water level, flow, and marsh hydroperiod towards improved conditions (Kotun & Renshaw 2014).

The South Florida Everglades ecosystem is characterized by a tropical climate with distinct wet and dry seasons (Duever et al. 1994). The wet season of the greater Everglades typically spans from May to October and the dry season extends from November through April (Kotun & Renshaw 2014). Southern Taylor Slough's wet and dry seasons have been defined in a different manner by Koch et al. (2012), using the timing of freshwater pulses through the slough as the determinant. Following this alternative methodology, Taylor Slough's wet season was defined as September through February and the dry season as March through August (Koch et al. 2012).

Historical annual rainfall totals at the Royal Palm Ranger Station (RPL) located near the Taylor Slough headwaters average close to 140 cm (Kotun & Renshaw 2014). Approximately 70% of precipitation at RPL occurs during the Everglades' wet season while the remaining 30% occurs during the dry season (Kotun & Renshaw 2014). The strong contrast in rainfall between the wet and dry seasons creates drastic seasonal contrasts in the hydrology, salinity distribution, and nutrient distribution of the region (Armentano et al. 2006, Childers et al., 2006; Harvey et al. 2004). These seasonal differences make long-term research studies essential to properly understanding the ecologic and hydrologic conditions of a system (Gaiser et al. 2012). As a part of the Florida Coastal Everglades Long Term Ecological Research Project (FCE-LTER), this research project addresses one of the FCE-LTER's core hypotheses regarding the effects of water management activates on GW discharge and seawater intrusion in the mangrove ecotone (Gaiser et al. 2012).

In much of the Everglades, GW is not well isolated from the SW (Harvey et al. 2004). A layer of peat and marl overlies much of the region's bedrock (Fish & Stewart 1991), and acts as a subtle aquitard, reducing interactions between SW and GW. In many parts of the Everglades, including in this study area, SW primarily flows in channelized depressions that have little to no

peat or sediment cover. These channels may provide a lower-resistance flow path for discharging GW to be released.

In Taylor Slough, GW capable of interacting significantly with SW occurs within an unconfined group of aquifers known as the superficial Aquifer System (SAS) (Fish & Stewart 1991). The SAS represents a critically important source of drinking water for many residents of South Florida and is characterized by extremely high transmissivities and hydraulic conductivities (Fish & Stewart 1991). Beneath Taylor Slough, the SAS extends from the ground surface to between 46m and 122m in depth and is stratigraphically divided into the Biscayne Aquifer and the gray limestone aquifer (Fish & Stewart 1991). The Biscayne Aquifer underlies the entirety of Taylor Slough and the gray limestone aquifer occupies all but the easternmost extent (Fish & Stewart 1991). The Biscayne Aquifer is the shallower of the two aquifers under Taylor Slough and is karstic. The aquifer varies in depth and thickness across Miami-Dade County, with a basal depth that varies from approximately 6m to at least 57m below sea level in the eastern portion of the county (Fish & Stewart 1991).

There is a shallow hydraulic gradient of approximately 0.00005 over the region (Price et al. 2006), a product of the extremely gentle topography and low elevation. The gentle slope produces gradual drainage and slow movements of SW (Sandoval 2013). As a result of the contact and interaction between SW and the limestone bedrock, Everglades' SW is chemically characterized as calcium-bicarbonate type (Price & Swart 2006).

METHODS

GROUNDWATER DISCHARGE POTENTIAL

Comparisons of GW heads and SW levels were made at two locations in Taylor Slough: TS3 and TS6 (Figure 2). Two GW wells, one shallow (<4 m) and one deep (6-9 m) along with one SW gaging station were present at both sites. At TS3, the GW wells (G3776 – 8.58 m depth; G3777 – 3.02 m depth) were located 131 m south of the E146 SW gage (SFNRC 2015; USGS 2015a-d) (Figure 2). The TS6 GW wells (G3763 - 6.83 m depth; G3764 - 3.89 m depth) were located 198 m south of the Upstream Taylor River SW gage. Each of the wells at TS3 and TS6 have two inch diameter casings. Both YSI 600 LS and In Situ Aqua Troll 200 pressure transducers were installed in each of the GW wells and made measurements of water depth, specific conductance, and water temperature at fifteen-minute intervals. Measurement errors associated with the pressure transducers are +/- 0.30 cm for the YSI pressure transducers and +/- 1.15 cm for the In-Situ pressure transducers (Zapata-Rios & Price 2012).

Measurements of SW at the Upstream Taylor River site (TS6) were made with a shaft encoder, float, and tape with an accuracy of +/- 0.30 cm. At E146, SW was gaged with an analog float and pulley system and potentiometer, and later on a WaterLog 3311 digital shaft encoder; accuracy is at least +/- 0.76 cm. All water elevations not already measured in centimeters (cm) relative to North American Vertical Datum of 1988 (NAVD88) were converted to cm NAVD88. Data collection at each of the four GW wells began in October of 2007 and ceased for G3763 in October 2010 and for G3776 and G3764 in November 2010, when the pressure transducers were removed from the wells. Measurements are still being collected as of this publication at all of the SW gaging stations and at the shallower GW well at TS3 (G3777), but the analyzed data in this project only continue through January 31, 2015. Mean daily water levels were determined for all of the GW and SW stations using the 15 minute data.

The potential for GW discharge (PGD) at each of the sites was first calculated from the daily water level data by subtracting the SW level from the GW head of either the shallow or deep well. Positive PGD values corresponded to higher GW levels compared to the SW level, while

negative values indicate higher SW levels than the GW. Equivalent freshwater head (EFW) must be considered when determining GW flow direction because water density differences can create differential pressures, driving flow and mixing of waters (Langevin et al. 2008). The density of water changes as a function of temperature, salinity, and pressure (Maidment 1992; Langevin et al. 2008). A density conversion based on temperature and salinity was made using the equations found in Maidment (1992).

$$\rho_p = \rho_f + (a * Salinity) + (b * Salinity^{\frac{3}{2}}) + (0.00048314 * Salinity^2) \quad (1)$$

$$\rho_f = 1000 * (1 - \frac{T+288.9414}{508929.2*(T+68.12963)} * (T - 3.9863)^2 \quad (2)$$

$$a = 0.824493 - 0.0040899 * T + 0.000076438 * T^2 - 0.00000082467 * T^3 + 0.0000000053675 * T^4 \quad (3)$$

$$b = -0.005724 + 0.00010227 * T - 0.0000016546 * T^2 \quad (4)$$

In Equations 1-4, ρ_p represents the density of water as a function of both salinity and temperature, ρ_f represents the density of water as a function of temperature, *a* and *b* are temperature based correction factors, *Salinity* is in psu, and *T* is temperature in Celsius (Maidment 1992). Density changes caused by pressure at depth were not considered because the wells used in this project are relatively shallow (<10m). The EFW corrections to GW stages were made with the assumption that the water column length in each well could not exceed the depth of the well, plus the height of the well casing above the land surface. The EFW corrections for the Upstream Taylor River SW at TS6 were made assuming a maximum water column length of 91.44 cm (3 feet), which is the approximate depth of water at the Upstream Taylor River gage. No EFW correction was made for the SW at TS3 (E146) as the salinity at this site was generally very low (< 5 psu).

The difference calculation was made for each of the GW wells at TS3 and TS6 (Figure 2) and was made on an hourly interval for all of the wells, using hourly means calculated from the

15-minute measurements or with hourly measurements as in the case of TS3 SW. A positive number from this calculation is indicative of a potential for upward movement of GW relative to SW, or PGD. Conversely, a negative number from this calculation implies a potential for GW recharge from the overlying SW.

Density corrected GW discharge potential (PGD EFW) at TS6 was calculated by subtracting TS6 SW EFW stage from GW EFW stage for the shallow and deep GW wells at TS6. At TS3, PGD EFW was calculated by subtracting TS3 SW stage from GW EFW stage for the shallow and deep GW wells at TS3. As a result of both instrument malfunction and measured values that were markedly different from the seasonal variability that occurred over the same period in every other year, data from December 2011 through May 2012 at TS3 was not used in this analysis.

DETERMINATION OF POTENTIAL HYDROLOGIC DRIVERS

Potential drivers of GW discharge were selected based on their relevance to Taylor Slough's water budget. Selected drivers included upstream and downstream water stages, upstream and mangrove ecotone SW discharge, rainfall, and ET. South Florida's Everglades are one of the most heavily instrumented and monitored environments in the world, offering numerous long-term data series (Gaiser et al. 2012; USGS 2015a-d; SFNRC 2015; SFWMD 2015), allowing researchers when designing experiments in south Florida a plethora of environmental data to select from for use in research projects. For this project, SW stage sites were selected from NPS, USGS, and SFWMD maintained sites. Upstream SW gaging sites were initially selected from the USGS' EDEN database (USGS 2015a) based on the approximate boundaries of Taylor Slough; south of water management structures that pump water into Taylor Slough (S332B_T), east of the Rocky Glades (P38), north of the mangrove ecotone (CP), and west of US 1 (EP1R) (Figure 3). The coordinates corresponding with these sites (25°13'38"N, 80°27'10"W and 25°32'59"N, 80°50'00"W) were used as boundary locations for selection of SW gaging sites. Sites within these boundaries that had incomplete data series were omitted from the

comparison. There were 51 resultant SW gaging sites without missing observations that occur within these spatial boundaries (Figure 3), in addition to E146, which was not included in the correlation matrix because it was used for PGD EFW calculations at TS3. Downstream stage in Florida Bay, recorded in Little Madeira Bay (TS-Bay S), was recorded as a daily average (Figure 2) (SFNRC 2015). Any datasets acquired in Sea Level Datum of 1929 (NGVD29) were converted to North American Vertical Datum of 1988 (NAVD88). All stage measurements not recorded in units of centimeters were converted to centimeters.

Upstream SW stage measurements were selected for use as potential hydrologic drivers in this project through use of a correlation matrix, which was generated to facilitate removal of highly correlated sites. The step was performed to reduce the total number of sites that were used in later analyses and to reduce colinearity between the sites. The initial correlation analysis was performed on the daily median water stage for each of the 51 SW gaging sites that fall within the spatial boundary conditions outlined above, as published on the USGS's EDEN website, from October 1, 2007 through January 31, 2015.

To eliminate a highly correlated site, the following procedure was used: first, the highest correlation value in the matrix was located; next, the two sites that comprised the pair having the highest correlation were compared to each other by calculating the mean correlation for each of the two sites with every other site remaining in the correlation matrix; from the pair with the highest correlation, the site with the higher overall mean correlation was removed from the matrix. The elimination procedure was repeated for the remaining sites in the correlation matrix until 6 upstream stage sites remained. Once the correlation matrix comparison was completed, the 6 remaining gaging sites were examined and sites that were discovered to have periods of invariable and rapidly fluctuating water levels were removed. Fluctuations such as those were observed in two of the resultant sites, S332B_T and S332_T. The gaging sites S332B_T and S332_T are canal gaging sites located immediately downstream of water control structures and

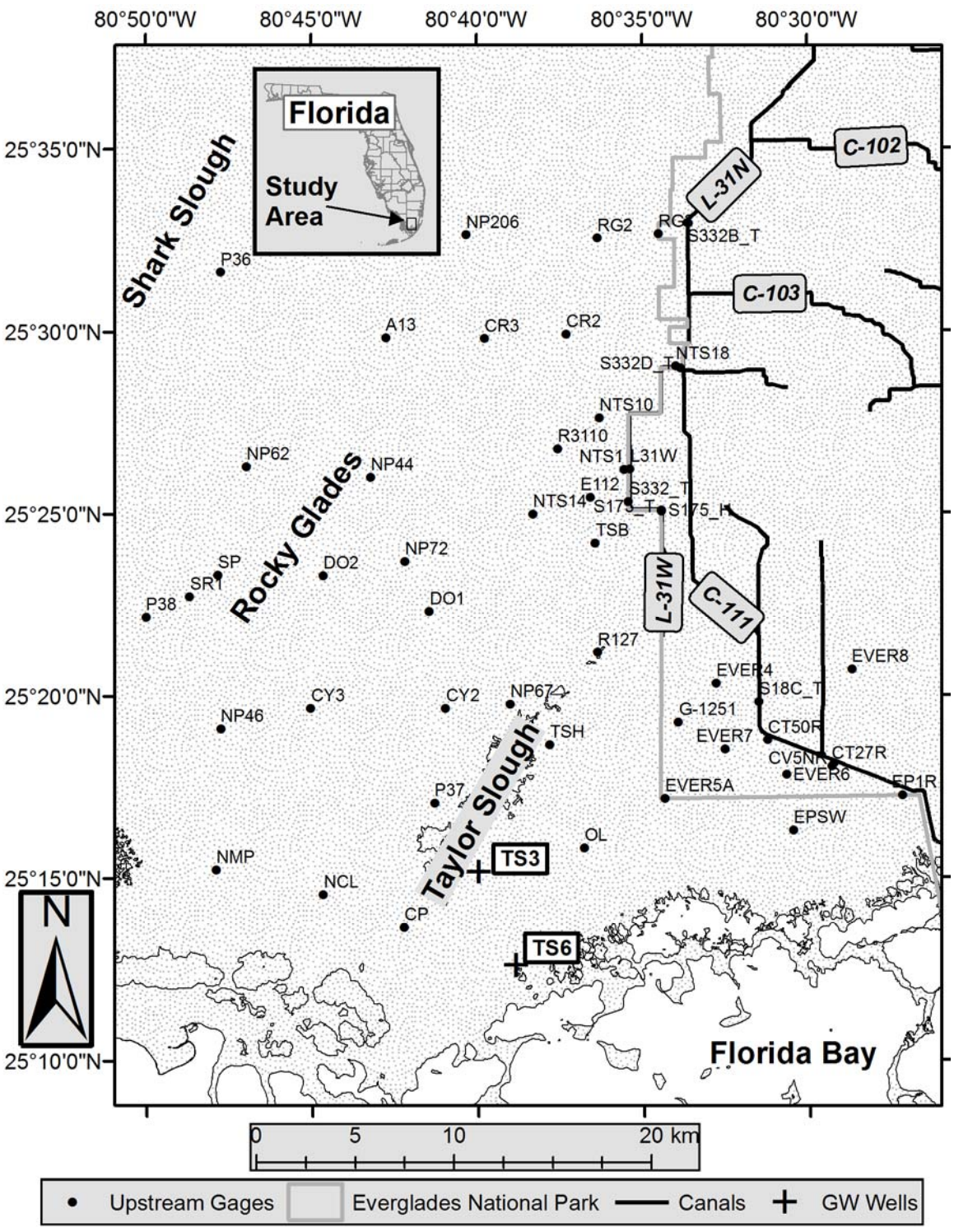

Figure 3: Surface water (SW) gaging stations used as inputs for the correlation matrix.

the fluctuating water levels observed at those stations were most likely representative of operation of the nearby water control structure. The canal gaging sites S332B_T and S332_T were therefore not included in subsequent comparisons.

The spatial relationships between surrounding water levels and PGD EFW calculations at TS6 and TS3 were investigated using a combination of correlation and spatial analysis. Pearson correlations coefficients were calculated between all 51 SW gage stations' (Figure 3) daily water levels over the study period and the four PGD EFW calculation series from TS6 and TS3. Correlations between each of the PGD EFW calculations and SW stages at TS6, TS3, and Florida Bay were also calculated. Spatial analysis of the resulting Pearson correlation coefficients was then performed using the Simple Kriging tool in ESRI ArcGIS 10.2.2, which is an inexact geostatistical interpolator. The z-value inputs for the Simple Kriging tool were the Pearson correlation coefficients between each SW gaging site and each of the four PGD EFW calculation series from TS6's and TS3's deep and shallow GW wells.

Fluctuations in SW and GW stages can be produced by ET (White 1932), and in coastal wetlands, ET can remove water directly from GW because the roots of plants in such environments are capable of transpiring shallow GW at close to the full potential rate (Winter et al. 1998). As a result of the potential for ET directly from GW and the high rate of ET that occurs in the Everglades (Sandoval 2013; Zapata-Rios & Price 2012), ET was considered as a potential hydrologic driver in this project. Similarly, rainfall was considered as a potential hydrologic driver because rainfall is a major contributor to the water budget of Taylor Slough (Sandoval 2013; Zapata-Rios & Price 2012). Inputs of rainfall to the SW serve to directly influence the hydraulic gradient. Rainfall was also investigated because atmospheric deposition represents an important source of P to the Everglades, and atmospheric deposition of P is 50% higher during the wet season than in the dry season (Sutula et al. 2001).

Rainfall and ET data were obtained from the USGS sites E146 for the TS3 wells, and from UTR for the TS6 wells (USGS 2015b & 2015c). As a result of the highly intermittent occurrence of rainfall at the sites studied in this project, 3-day, 7-day, and 14-day cumulative

antecedent moving windows were applied to the TS3 and TS6 rainfall measurements for use in later analyses, in addition to the original daily total rainfall observations. The ET measurements used in this project were of daily potential ET and calculated with the Priestley-Taylor method, using Geostationary Operational Environmental Satellite (GOES) imagery (USGS 2015b); no further processing was performed on the potential ET measurements.

The ET measurements at TS3 were only available through the end of 2013, so a daily averaging procedure was used to supplement ET observations from January 2014 through January 2015, based on the observations at TS3 between January 2004 and December 2013. Following this averaging procedure, average daily ET and rainfall values were summarized into monthly averages by calculating the mean daily total ET and rainfall during each month. Mean daily totals for ET and rainfall were calculated rather than monthly totals because monthly totals would disproportionately weight months with a larger number of days, relative to shorter months. Monthly basinwide area-weighted rainfall values for Taylor Slough from Sandoval (2013), calculated using the Thiessen polygon method, were also utilized when monthly comparisons were made.

Inflow to the headwaters of Taylor Slough was monitored because this input is indicative of water management activity. Water management activities have dramatically changed the hydrologic regime of the historic Everglades into its current state (Davis & Ogden 1994), but upstream inflows remain an important contributor to Taylor Slough's water budget (Kotun & Renshaw 2014; Sandoval 2013) and were therefore considered as a potential driver of PGD in this study. Upstream inflow under Taylor Slough Bridge (TSB) was recorded as a volumetric daily average rate in cubic feet per second and converted to cubic meters per second (m^3/s) (SFNRC 2015) (Figure 2). When upstream SW discharges were averaged to monthly values, the mean daily rate for each month was calculated. The SW discharge at TS6, recorded at Upstream Taylor River, was collected via acoustic Doppler current profiler deployed in the main channel of Taylor River (USGS 2015d). The SW discharge measurements at TS6 were recorded in cms at 15-minute intervals and averaged to daily and monthly average flow rates in m^3/s.

Once the independent variables were selected for upstream stage, downstream stage, ET, rainfall, upstream flow, and TS6 SW discharge, statistical analyses were conducted using Excel 2013 (Version 15.0, Microsoft Corp., 2012), Sigmaplot (Version 11.2, Systat Software Inc., 2008), and SPSS Statistics for Windows (Version 22.0, IBM Corp., 2013). Descriptive statistics, correlation, regression, and cross-correlation analyses were conducted in addition to qualitative examination of the data, with the goal of discerning direct and significant relationships between the chosen potential hydrologic drivers and PGD EFW in each of the wells at TS6 and TS3. Cross-correlation analyses were conducted for daily values with a lag window of +/- 100 days (approximately 3 months). All reported standard errors were calculated by dividing the sample standard deviation by the square root of the count of observations and do not include measurement errors.

CHEMICAL ANALYSES OF SURFACE WATER

The transfer of chemicals between SW and GW can indicate the direction of water movement at the SW/GW interface (Winter et al. 1998). During periods of GW discharge, SW can be expected to have chemical constituent concentrations influenced by those of the underlying GW. The SW in the southern Everglades can become enriched in ions and salinity independently of GW discharge as a result of evaporation and tidal inflows (Price et al. 2006). Enrichment in calcium relative to other major ions because of dissolution from the underlying limestone bedrock can indicate a GW source (Price et al. 2006). Thus by comparing the relative ionic concentrations of the SW and GW at a site, the influence of GW discharge on SW chemistry can be determined.

Manually collected SW, peat GW, and bedrock GW samples were obtained intermittently from July 2008 through December 2014 at TS/Ph-6b (TS6 - Peat-GW (from C1 and C3 GW wells (Zapata-Rios & Price (2012)), Taylor Slough Bridge (TSB SW), and southern Little Madeira Bay (TS-Bay S SW) (Figure 2). Manually collected samples are from this study, Zapata-Rios & Price (2012), Sandoval (2013), and previously unpublished data. Manually collected samples were pumped with peristaltic pumps through chemically inert polymer tubing into 10% HCl washed HDPE bottles. At least three well volumes were purged from GW wells whenever GW was sampled. All of the manually collected samples were analyzed for major ions (Na^+, Mg^{2+}, K^+, Ca^{2+}, Cl^-, SO_4^-) in the FIU Hydrogeology lab using Dionex DX-120 and ICS-1000 ion chromatographs. Most of the manually collected samples were also analyzed for total P (TP). The P analyses were performed in FIU's Southeast Environmental Research Center (SERC) Nutrient and Soil/Sediment Biogeochemistry laboratories. Alkalinity of the manually collected samples was analyzed in FIU's Hydrogeology lab with a Brinkman potentiometric acid titrator and calculated using a Gran function and calculating for bicarbonate alkalinity (HCO_3^-) (Price 2001).

Automated SW sampling occurred continuously when adequate SW was present, with each sample collected as an 18-hour composite (Gaiser et al. 2012) at TS/Ph-3 and at TS/Ph-6a using ISCO 6172 Full-Size Portable Samplers. In addition to the normal schedule of automatic sampling, the autosampler at TS/Ph-3 collected SW samples whenever local rainfall was

occurring. The automatically collected samples were also analyzed for TN and TP concentrations as well as each of the major ions, but not for alkalinity. These autosampler TN and TP data were sourced from the same dataset that is partially available on the Signature Datasets section of the FCE-LTER website (http://fcelter.fiu.edu/data/FCE/signature_datasets.htm). The automatically collected samples were not analyzed for alkalinity because the samples are not immediately available once collected and may sit for up to a month prior to their receipt, greatly exceeding the maximum 48-day holding time for alkalinity analysis.

Grab samples were also collected at the autosamplers at TS/Ph-3 and TS/Ph-6a once per month when adequate SW was present, but were analyzed in the same manner as the rest of the automatically collected samples and included with the automatically collected samples' monthly averages; without alkalinity analyses. A coarse polymer-mesh pre-filter was used for the manually collected SW samples obtained at the sites without autosamplers to remove floating debris such as periphyton and other large particulate matter from the incoming water. All manually collected samples destined for analysis of alkalinity, major ions, and dissolved nutrients were filtered with a chemically inert .45µm filter. Manually collected samples analyzed for total nutrients were not filtered. All manually collected samples collected for major cation and total nutrient analyses were acidified with ~10% HCl to a pH of less than 2 (Price & Swart 2006). Charge balances were calculated for the manually collected samples not included with autosampler data using each of the quantified major ions and bicarbonate alkalinity. Manually collected samples with charge balances errors of greater than 5% were rejected and their ionic concentrations were not used in subsequent analyses. Charge balances were not calculated for the automatically collected samples because they lacked alkalinity measurements.

CONTROLS OF SURFACE WATER CHEMISTRY

Controls of GW salinity at TS6 and TS3 as well as controls of SW salinity at TS6 were explored utilizing most of the same physical measurements considered as drivers of PGD: local and regional SW and GW stages; PGD EFW at TS6 and TS3; local rainfall; and SW discharge upstream (TSB) and at TS6 (Figure 2). Mean daily values for GW and SW salinity at TS6 were compared with each other qualitatively and with correlation, regression, and cross-correlation analyses to determine their interactions. The TS6 GW and SW salinities were further analyzed using the same methods, in comparison with the physical measurements. Identical analyses were conducted for TS3 GW, but TS3 SW salinity was not considered because of the poor record and low salinity (<5 psu) at TS3 for SW.

Monthly mean values of the calcium/chloride (Ca/Cl) ratios of the automatically collected SW samples collected at TS6 and TS3 were qualitatively compared to the Ca/Cl ratio averages of manually collected, charge-balanced GW and SW samples collected at Taylor Slough Bridge (TSB SW), TS/Ph-6b (TS6 - Peat-GW (from C1 and C3 GW wells (Zapata-Rios & Price (2012)), and southern Little Madeira Bay (TS-Bay S), in northern Florida **Bay** (Figure 2). The monthly chemistry averages from the automatically collected samples at TS6 and TS3 were compared qualitatively and through correlation, regression, and cross-correlation analysis over time with each other and with monthly means of the spatially coincident deep and shallow PGD EFW calculations; local GW and SW stages; the SW discharge measurements at Taylor Slough Bridge and TS6, basinwide rainfall values from Sandoval (2013), and local rainfall at each site.

Monthly mean concentrations of TP in automatically collected SW samples from TS6 and TS3 were analyzed over time, seeking relationships between TP concentration in TS6 SW, TS3 SW, and the same physical measurements to which the Ca/Cl ratios in SW were compared. Correlation, linear regression, and cross-correlation analyses were also used for the TP comparisons in the same manner that the same statistical analyses were applied to the monthly Ca/Cl ratios of TS3 SW and TS6 SW.

A time series of SW Ca/Cl ratios at TS6 SW and TS3 SW was investigated from about 2007 to 2013. The time series was compared to average Ca/Cl ratios of upstream fresh Everglades SW and the marine water from Florida Bay (TS-Bay S) using SW samples collected in this investigation as well as published in Price (2008). In addition, a trilinear mixing model using TP and salinity was developed for the TS6 SW samples. The mixing model used monthly-averaged TP and salinity values of the TS6 SW collected from the autosampler between October 2007 and January 2015. Averaged TP and salinity endmember values were from TSB SW, bedrock GW from TS6 (Price et al. 2006), and Florida Bay SW (TS-Bay S SW and samples from Price (2008)).

RESULTS

CONTROLS OF GROUNDWATER DISCHARGE

Water Stages

Stages of SW and GW at TS6 were highly correlated with each other and demonstrated strong seasonality with seasonal maximums occurring between August and October and seasonal minimums occurring over a broader period, between January and April (Figure 4, Table 1). At TS3, SW and GW stages similarly demonstrated strong seasonality, though the seasonal highs in TS3 stages occured in September and October from 2007 through 2011 and in 2014 (Figure 5, Table 1). In 2012 and 2013, seasonal highs in TS3 stages occurred earlier in the year, in June and July, respectively (Figure 5). Seasonal lows in TS3 stages tended to occur in in May and June with the exception of the seasonal low of 2013, which occurred in March (Figure 5). At TS6, the range of GW and SW stages was smaller than those of TS3's GW and SW (Table 1).

The mean daily PGD for the shallow and deep wells at TS6 ranged from 0.12 to 18.48 cm and from -2.26 to 18.25 cm, respectively (Figure 6, Table 2). The daily uncorrected GW stage in the shallow well at TS6 was consistently higher than the SW stage (Figure 6). With the exception of a few days, the daily uncorrected GW stage in the deep well at TS6 was also consistently higher than the SW stage (Figure 6). The shallow GW stage at TS6 was generally higher than the deep GW stage, with the exception of a few periods varying from one day to approximately two months (Figure 6).

At TS3, the mean daily values of PGD as determined from the uncorrected stage values from the shallow well ranged from -5.58 to 5.98 cm, with most of the values positive except for a few negative instances in June 2011; March, September, and October 2014; and at the end of the study period, in January 2015 (Figure 7, Table 2). For the deep GW well at TS3, the values of daily PGD as determined from the uncorrected stage data ranged from -8.16 cm to 2.97 cm (Figure 7, Table 2). Shallow GW at TS3 was higher than TS3 SW for a greater portion of this study than deep GW at TS3 (Figure 7). At TS3, the shallow GW stage was higher than deep the GW stage for all 4 years of coincident measurements (Figure 7).

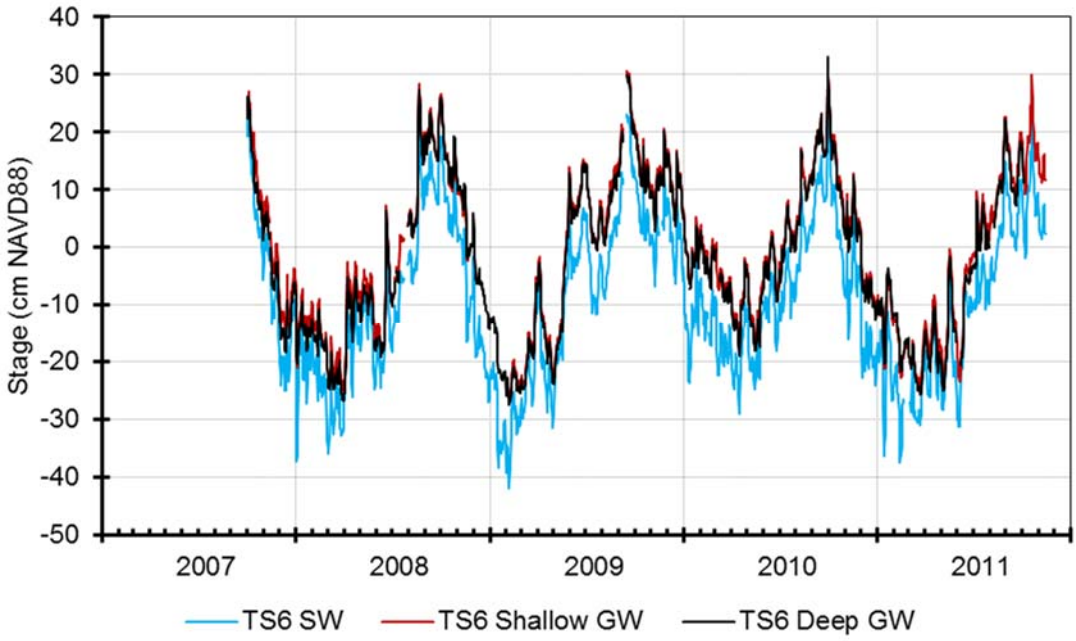

Figure 4: Daily surface water (SW) and groundwater (GW) stages observed over time at TS6.

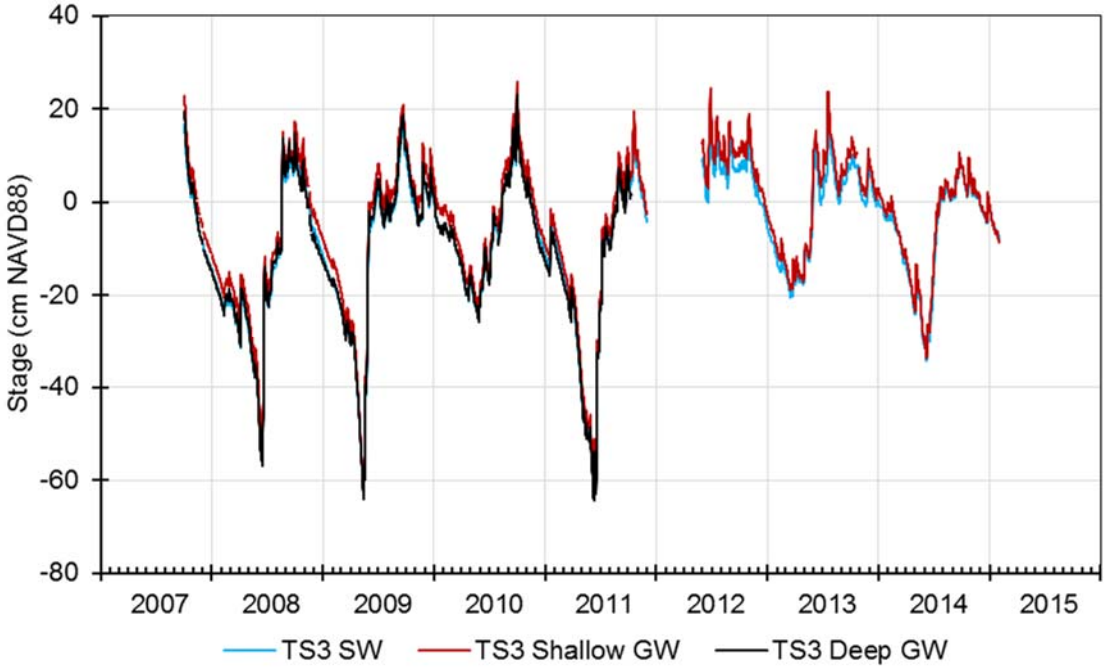

Figure 5: Daily surface water (SW) and groundwater (GW) stages observed over time at TS3.

Table 1: Daily mean, minimum, maximum, and difference values for surface water (SW) stages, groundwater (GW) stages, and density corrected (EFW) stages over time at TS6 and TS3.

Stage / Stage Difference	Mean	Minimum	Maximum	# of Observations
TS6 SW (cm NAVD88)	-9.25	-41.87	26.49	1473
TS6 SW EFW (cm NAVD88)	-8.59	-41.80	26.54	1467
TS6 Shallow GW (cm NAVD88)	-0.53	-27.24	32.91	1415
TS6 Shallow GW EFW (cm NAVD88)	5.03	-21.57	39.92	1321
TS6 Deep GW (cm NAVD88)	-2.45	-27.39	32.99	1400
TS6 Deep GW EFW (cm NAVD88)	10.66	-14.80	46.89	1356
TS6 Deep GW - Shallow GW (cm)	-1.09	-5.98	1.50	1316
TS6 Deep GW EFW - Shallow GW EFW (cm)	6.44	3.38	9.85	1207
TS3 SW (cm NAVD88)	-7.34	-56.48	21.64	2488
TS3 Shallow GW (cm NAVD88)	-4.91	-62.05	25.83	2479
TS3 Shallow GW EFW (cm NAVD88)	-4.35	-61.33	26.74	2425
TS3 Deep GW (cm NAVD88)	-11.67	-64.50	23.04	1452
TS3 Deep GW EFW (cm NAVD88)	-5.27	-56.86	31.66	1327
TS3 Deep GW - Shallow GW (cm)	-3.12	-5.46	-0.65	1451
TS3 Deep GW EFW - Shallow GW EFW (cm)	4.15	2.12	6.67	1315

Table 2: Mean, minimum, and maximum daily values for uncorrected (PGD) and density corrected (PGD EFW) discharge potential over time at TS6 and TS3.

	Mean	Minimum	Maximum	# of Observations
TS6 Shallow PGD	8.18	0.12	18.48	1401
TS6 Shallow PGD EFW	13.12	3.38	22.50	1306
TS6 Deep PGD	7.22	-2.26	18.25	1384
TS6 Deep PGD EFW	19.83	8.86	31.12	1341
TS3 Shallow PGD	2.67	-5.58	5.98	2470
TS3 Shallow PGD EFW	3.36	-5.07	6.56	2425
TS3 Deep PGD	0.01	-8.16	2.97	1443
TS3 Deep PGD EFW	7.86	-0.77	11.02	1327

Upon application of the density-based equivalent freshwater head correction (EFW) to each of the water stages at TS6 and TS3, SW stages and GW stages were raised by a small amount (Figure 8, Figure 9, Table 1). Given its generally low salinity (<5 psu) no correction was applied to the SW at TS3. The EFW corrections were greatest for the deep GW and least for the SW at both TS6 and TS3; as a result, the density-corrected stages in the deep GW wells were consistently higher than the SW and higher than the shallow GW most of the time (Figure 8, Figure 9).

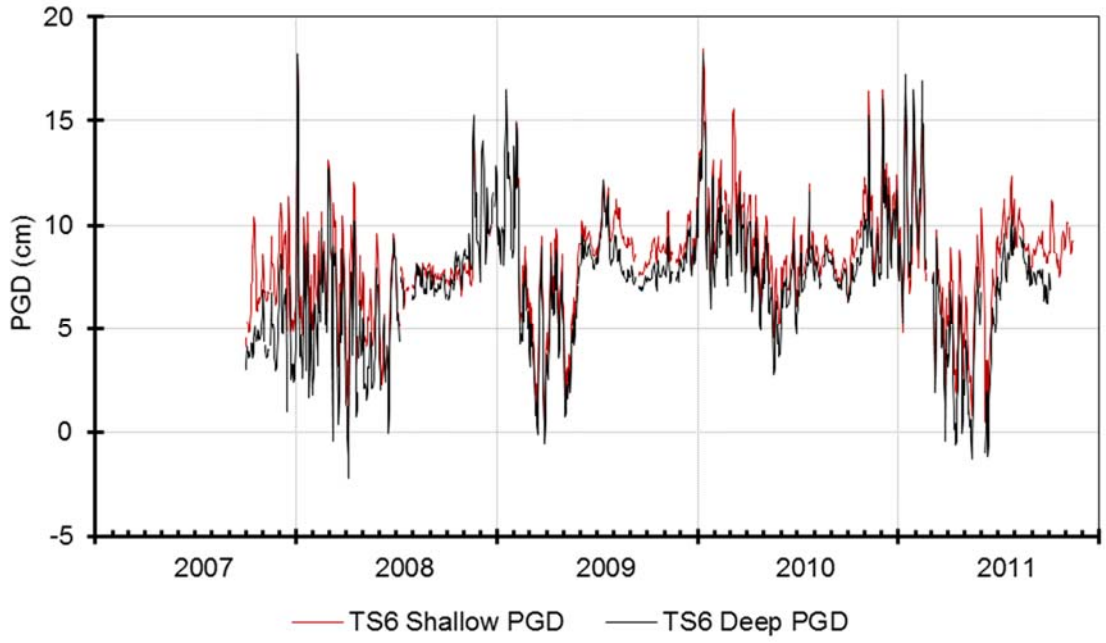

Figure 6: Daily values of groundwater discharge potential (PGD) determined from uncorrected stage measurements for shallow and deep wells over time at TS6.

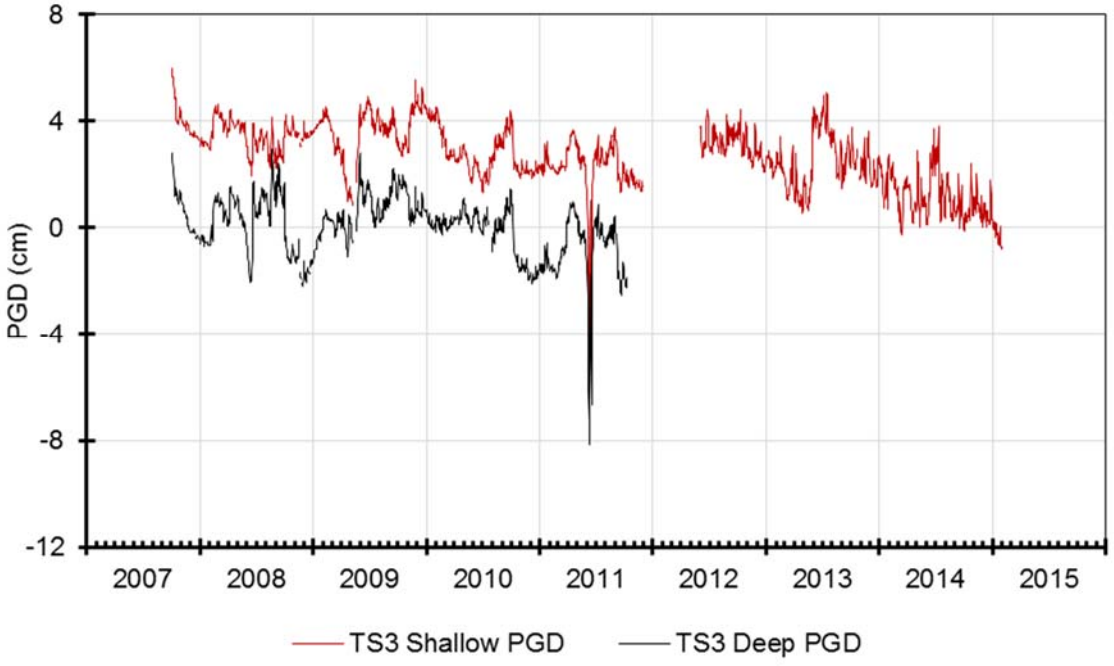

Figure 7: Daily values of groundwater discharge potential (PGD) determined from uncorrected stage measurements for shallow and deep wells over time at TS3.

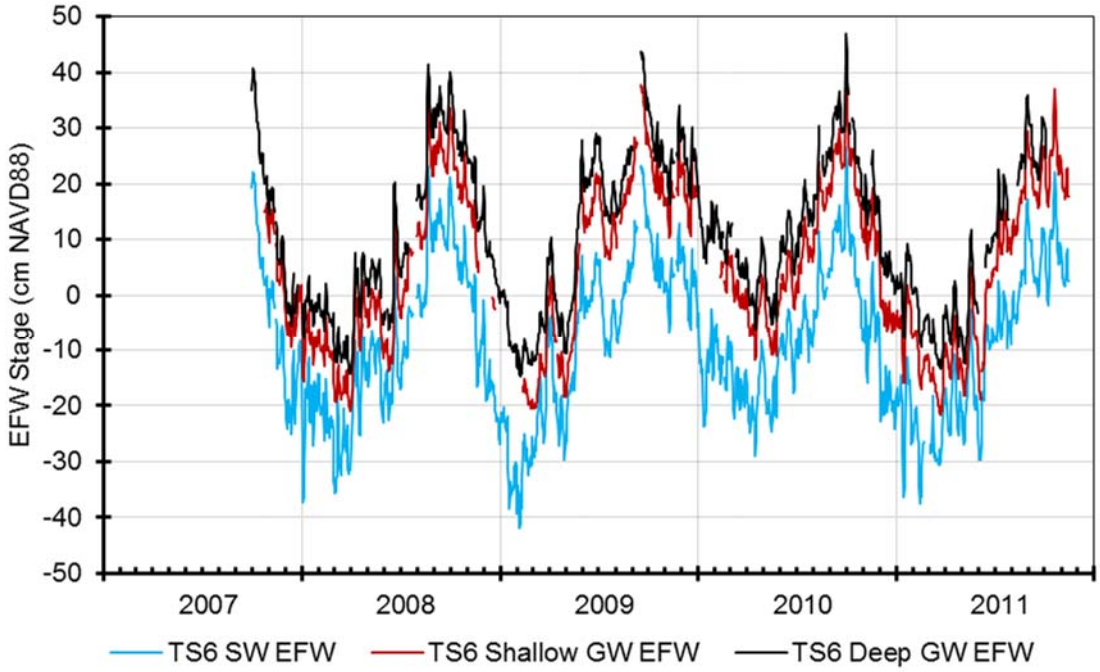

Figure 8: Density corrected (EFW) surface water (SW) and groundwater (GW) stages as determined on a daily basis over time at TS6.

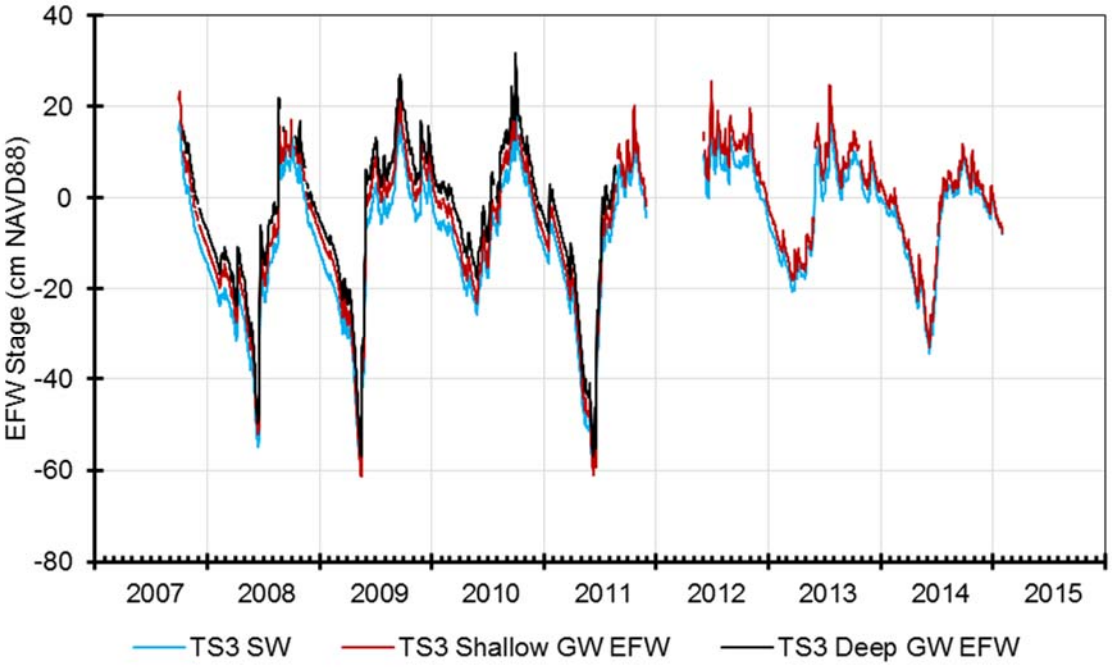

Figure 9: Density corrected (EFW) surface water (SW) and groundwater (GW) stages as determined on a daily basis over time at TS3. No correction was applied to the SW stage at TS3 because of the generally low salinity (<5 psu).

Calculation of PGD EFW following application of EFW corrections to the SW and GW stages at TS6 resulted in consistently positive values, with higher values in the deeper well than in the shallower well (Figure 10). At TS3, the PGD EFW values were positive during the majority of the study period for both deep and shallow GW measurements, but decreased briefly to negative values in May 2009 and June 2011 (Figure 11). Trends and seasonality are not apparent in either of the site's deep minus shallow GW stage differences, with and without density corrections. The highest PGD EFW values at TS6 shallow occurred in November and the lowest values occurred in May (Figure 10). At TS6 deep, the highest PGD EFW values occurred in January and the lowest values occurred in May (Figure 10). The highest PGD EFW values at TS3 shallow occurred in July and the lowest values occurred in May (Figure 11). At TS3 deep, the highest PGD EFW values at TS3 deep occurred in September and the lowest values occurred in December (Figure 11).

Peaks in shallow TS6 PGD EFW tended to lag behind peaks in shallow GW stage each year by approximately 1 to 3 months (Figure 12). Lows in shallow PGD EFW at TS6 tended to lag behind the seasonal lows observed in shallow GW stage by about 0-2 months (Figure 12). Shallow GW stage at TS6 tended to fall from wet season highs more rapidly and earlier in the year than the seasonally falling limbs the occurred in shallow PGD EFW (Figure 12). Shallow TS3 PGD EFW did not have a consistent relationship with TS3 shallow GW stage through January 2012 (Figure 13). However, from June 2012 to January 2015, the PGD EFW tended to co-vary with the shallow GW stage at TS3, albeit with greater variability (Figure 13). At TS3, shallow PGD EFW generally decreased throughout the study period (Figure 13).

Peaks in deep PGD EFW at TS6 tended to lag behind those of deep GW stage each season by approximately 1 to 4 months, similar to the lagged peaks between shallow GW and shallow PGD EFW (Figure 14). Lows in deep PGD EFW and deep GW stage at TS6 were also lagged by about 0 to 2 months, with deep PGD EFW lows consistently occurring subsequent to the lows in deep GW stage (Figure 14). Deep GW stage at TS6, like shallow GW stage, tended to fall from wet seaon highs more rapidly than shallow PGD EFW (Figure 14). Deep TS6 PGD EFW

exhibited less variability than shallow TS6 PGD EFW (Figure 12, Figure 14). Deep TS3 PGD EFW had a slightly smaller range than than shallow TS3 PGD EFW, less variability, and similarly exhibited a decrease over the study period (Figure 13, Figure 15,Table 2). As with shallow TS3 PGD EFW and TS3 shallow GW stage, a consistent relationship with deep GW stage and deep PGD EFW was not apparent (Figure 15).

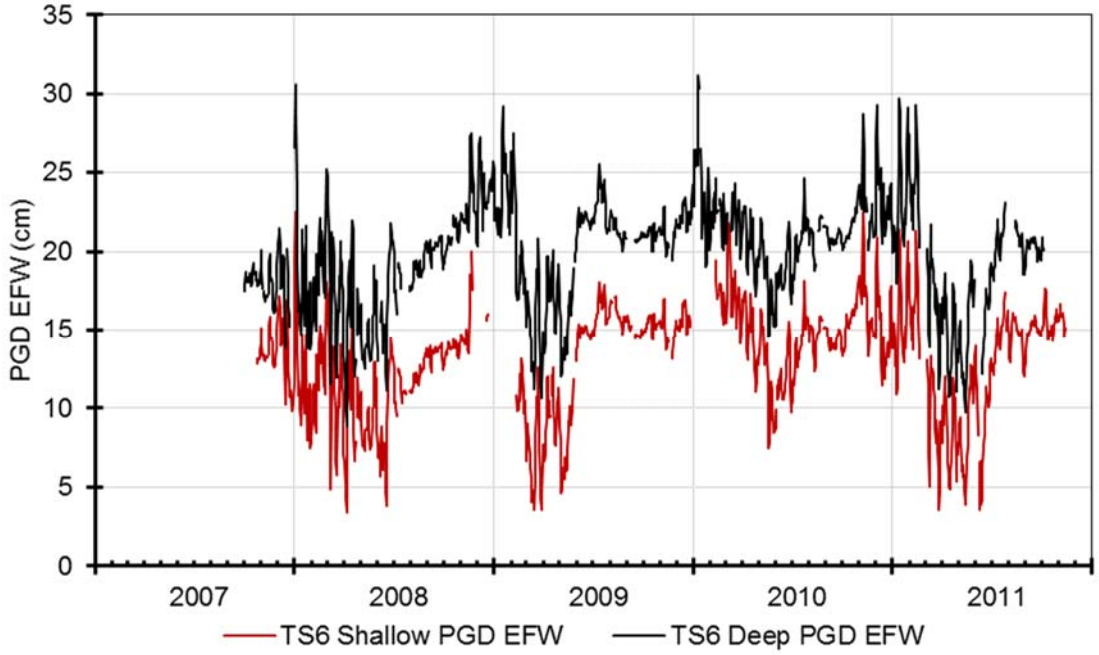

Figure 10: Daily density corrected groundwater discharge potential (PGD EFW) over time at TS6.

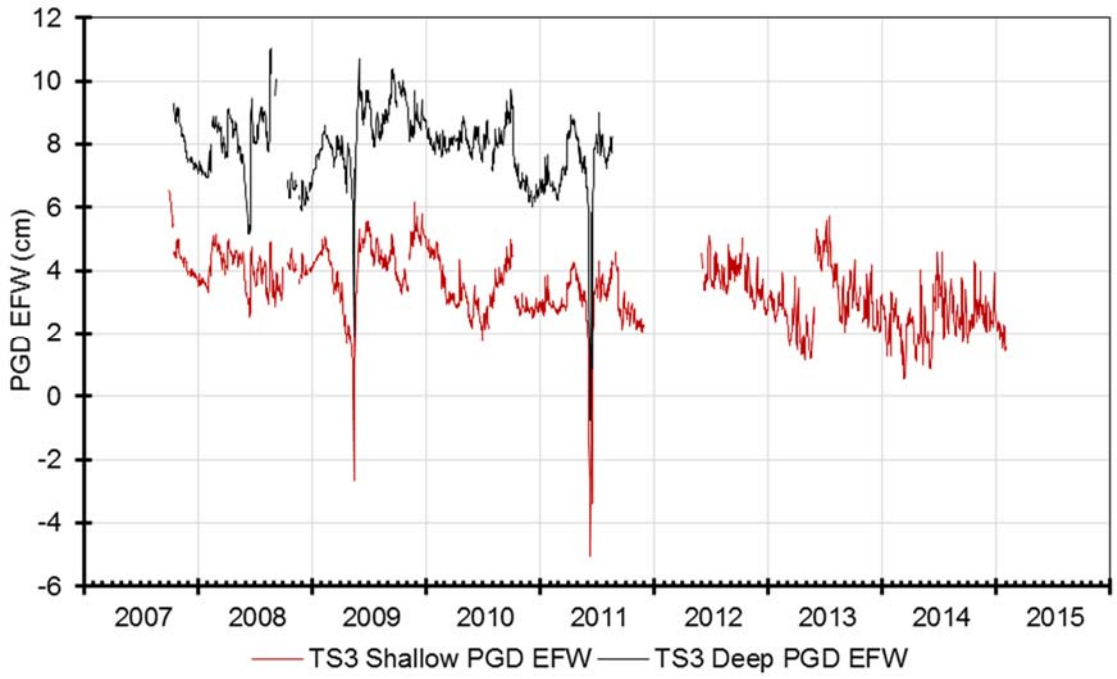

Figure 11: Daily density corrected groundwater discharge potential (PGD EFW) over time at TS3.

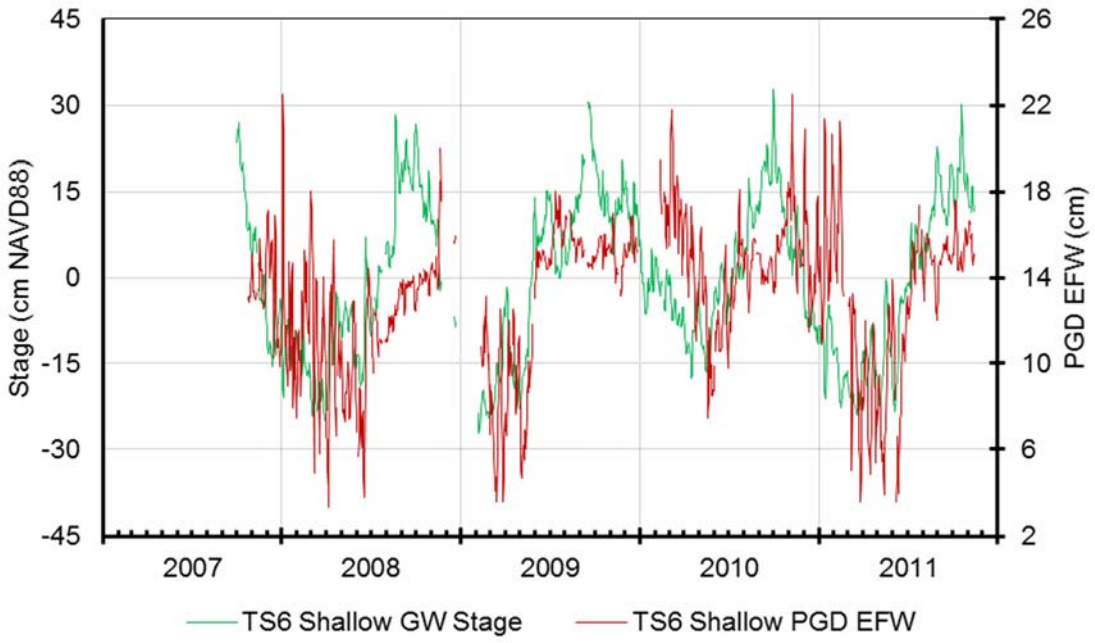

Figure 12: Daily shallow groundwater (GW) stage and density corrected shallow groundwater discharge potential (PGD EFW) over time at TS6.

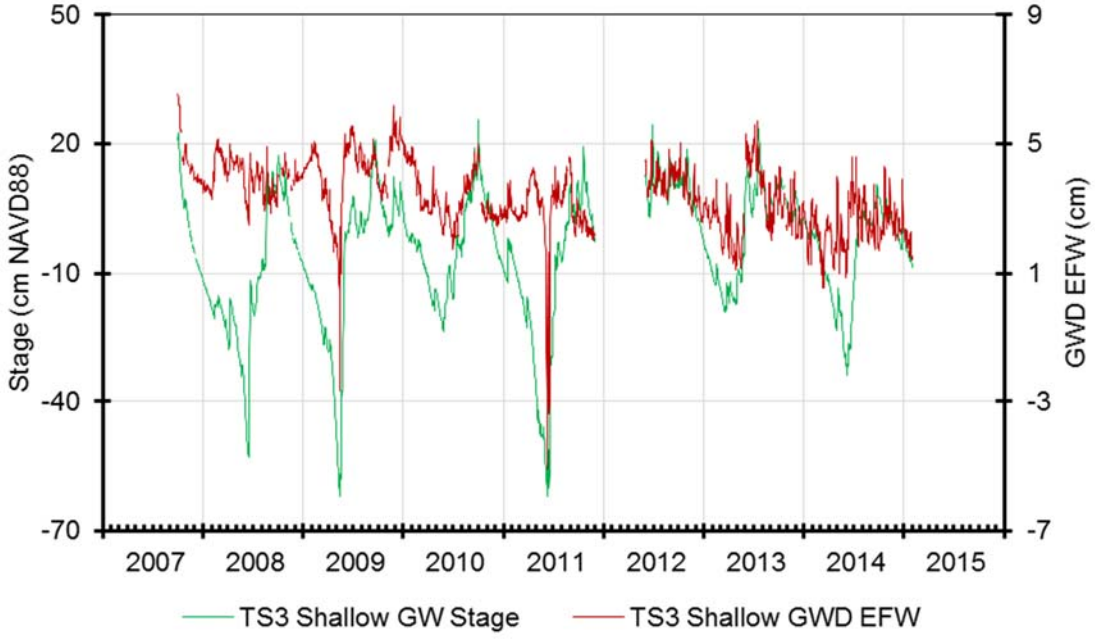

Figure 13: Daily shallow groundwater (GW) stage and density corrected shallow groundwater discharge potential (PGD EFW) over time at TS3.

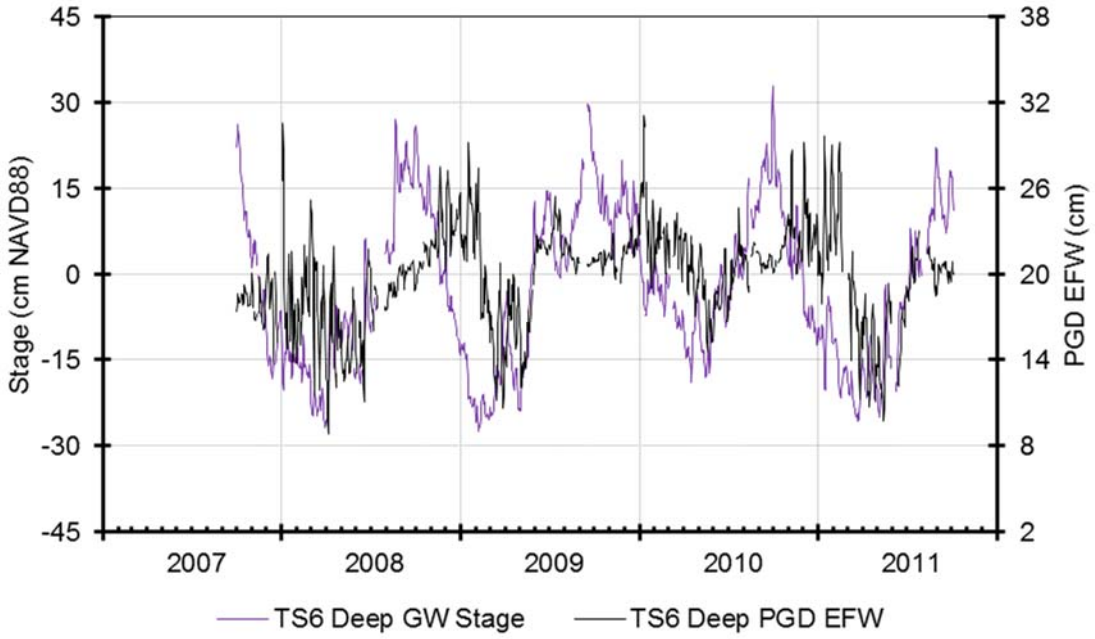

Figure 14: Daily deep groundwater (GW) stage and density corrected deep groundwater discharge potential (PGD EFW) over time at TS6.

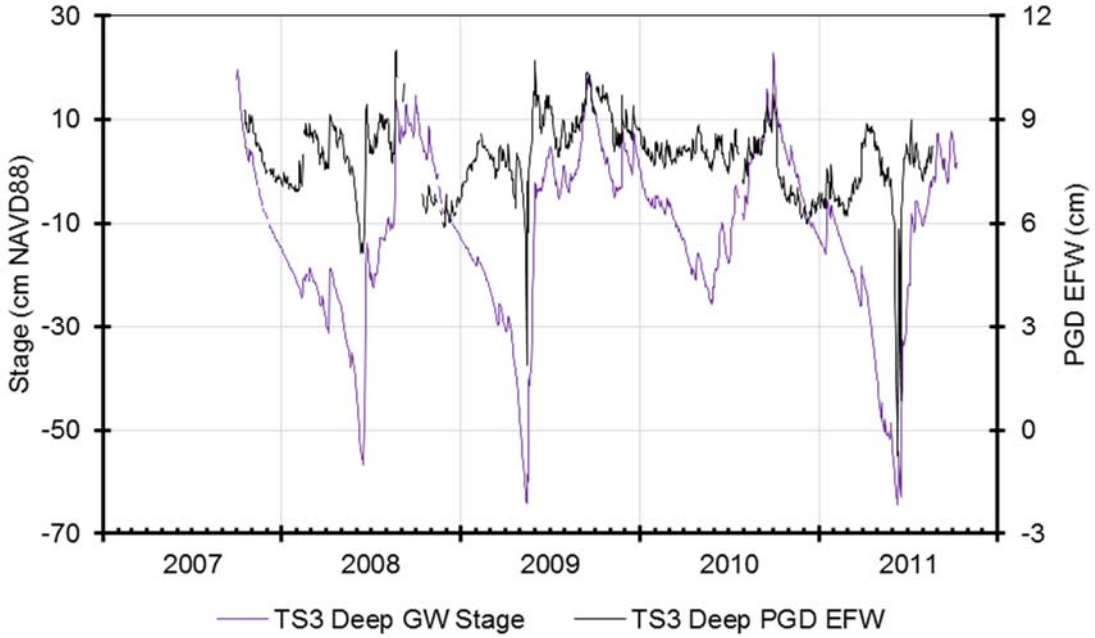

Figure 15: Daily deep groundwater (GW) stage and density corrected deep groundwater discharge potential (PGD EFW) over time at TS3.

Results from the spatial correlation analyses indicate that shallow and deep TS6 PGD EFW are most similar to upstream gages in a longitudinal band of stations approximately halfway between TSB and Florida Bay that occurs between NP46 and G-1251 (Figure 16), and to a lesser extent to gages located in the Rocky Glades (Figure 2) and in the canal region to the east of Taylor Slough. Observed stages at TS6 and Florida Bay are dissimilar to shallow and deep PGD EFW at TS6 (Figure 16). Considerably weaker correlations existed between the regional stage measurements and both shallow and deep TS3 PGD EFW (Figure 16). A consistent spatial pattern of strong correlations was not observed with either the shallow or the deep TS3 PGD EFW calculations (Figure 16).

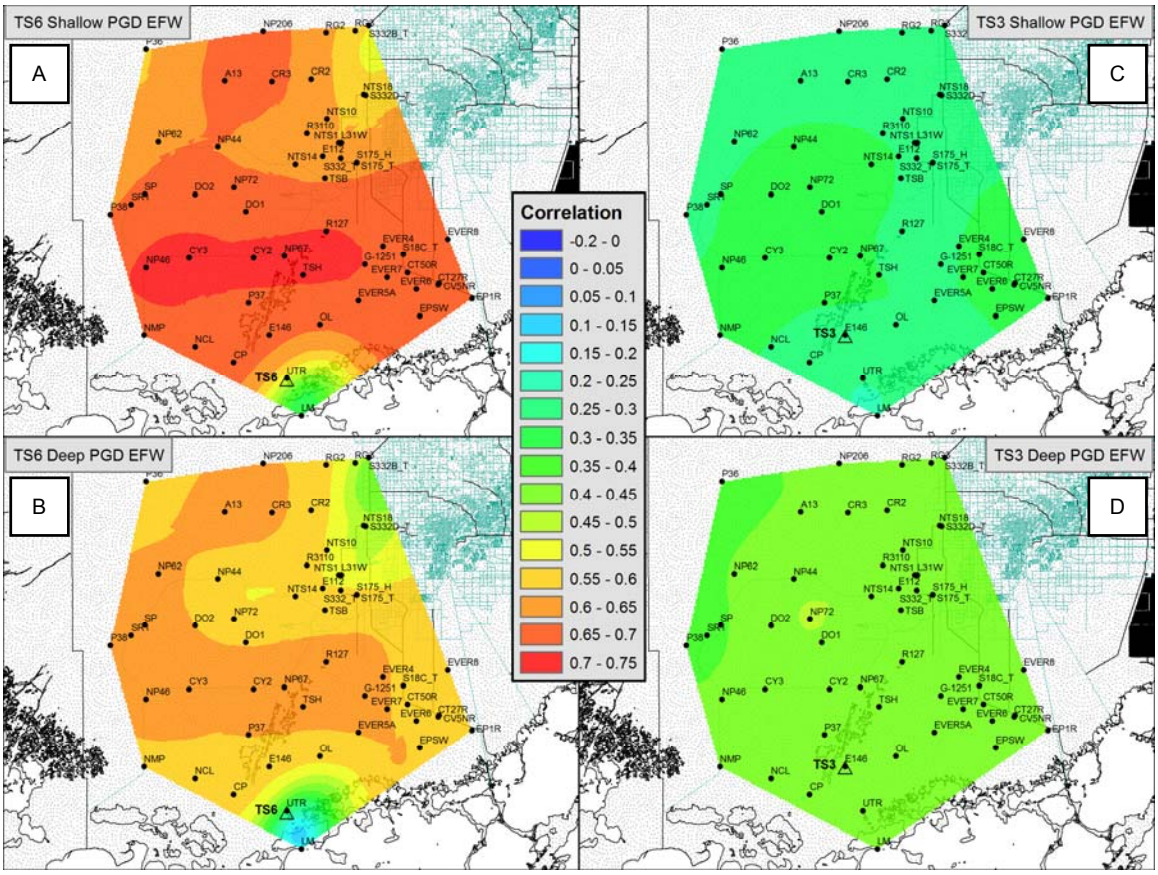

Figure 16: Results from Simple Kriging interpolation, depicting correlations between observed water stages and density-corrected groundwater discharge potential (PGD EFW) at (A) TS6 shallow, (B) TS6 deep, (C) TS3 shallow, and (D) TS3 deep over time.

The correlation matrix analysis of upstream SW levels yielded four stations with the lowest possible correlations amongst each other. The resulting SW gaging stations, listed alphabetically, were CP, NP72, OL, and P36 (Figure 2). Many of the SW and GW stages were strongly and positively correlated, with no lags observed except for between two upstream SW stage sites (CP and P36) and Florida Bay SW stage (Table 3, Table 4). The SW and GW stages studied in this project conformed to Tobler's first law of geography; sites that are closer together were more closely related than those that are further away (Tobler 1970).

Of the selected upstream SW stages, the highest stages tended to occur in October and September and the lowest mean stages were observed in May and April (Figure 17). Florida Bay and TS6 SW stages tended to be highest in September and lowest in March (Figure 18). At TS6, SW and GW stages were most similar to each other and to Florida Bay stage, but less so to upstream stages (CP, NP72, OL, P36, TS3 SW) (Table 3, Table 4). At TS3, SW and GW stages were most similar to each other and also correlated strongly to TS6 GW and SW and to upstream stages (CP, NP72, OL, P36) (Table 3, Table 4). The TS3 SW and GW stages only moderately correlated with Florida Bay stage (Table 3, Table 4).

When density-corrected differences between GW heads and SW stages were considered, or PGD EFW, different spatial relationships emerged. At TS6, PGD EFW compared between the two GW wells was highly correlated without a lag (Table 3, Table 4). Calculated PGD EFW values in both GW wells at TS3 was also strongly correlated, without a lag (Table 3, Table 4). At TS6, PGD EFW lagged TS6 GW and SW stage by 17 to 19 days (Table 4). At TS3, PGD EFW did not lag TS3 GW or SW stages (Table 4). Without a lag time included, TS6 SW did not correlate with deep TS6 PGD EFW and only very weakly with shallow TS6 PGD EFW (Table 4). At TS3, SW had stronger correlations with deep and shallow TS3 PGD EFW than TS6 SW did with TS6 deep and shallow PGD EFW without a lag time included (Table 3, Table 4). Inclusion of lag times resulted in stronger correlations between TS6 SW and TS6 PGD EFW than observed at TS3 (Table 4). A lagged relationship between TS3 PGD EFW and TS6 PGD EFW did exist, but this relationship was very weak (Table 4). At both of the TS6 wells, PGD EFW had much stronger

correlations with all of the upstream SW stages than it had with TS6 SW stage and Florida Bay stage, especially without a lag time included (Table 3, Table 4). An approximately 2 month lag time was occurred between both shallow and deep TS6 PGD EFW and Florida Bay stage, when much stronger correlations were revealed (Table 4). The same 2 month lag time existed between deep TS6 PGD EFW and TS6 SW (Table 4). The PGD EFW in both of the TS3 wells had much weaker correlations with all of the SW and GW stage measurements, even when lag times were considered (Table 3, Table 4).

Similar seasonality occurs in each of the upstream SW and GW stage measurements, but differs from the seasonal patterns observed in TS6 SW and GW stages and Florida Bay stage (Figure 17, Figure 18, Figure 19, Figure 20). Lows in upstream SW stages occur later in the year than the lows observed in TS6 and Florida Bay stage (Figure 17, Figure 18, Figure 19, Figure 20). The later lows in upstream SW stage correspond with the lows in PGD EFW at both TS6 wells much more so than Florida Bay SW lows do with the TS6 PGD EFW values (Figure 17, Figure 18, Figure 19, Figure 20). Two of the upstream SW stages (NP72, and P36) have much greater ranges than TS6 SW stage and Florida Bay stage, but the other three upstream SW stages (CP, OL, TS3) have lesser ranges than TS6 SW stage and Florida Bay stage (Figure 17, Figure 18, Figure 19, Figure 20). At TS3, clear and consistent relationships are not present between shallow and deep PGD EFW and any of the regional SW stages, with the exception of shallow TS3 PGD EFW from 2012 onwards (Figure 19 & Figure 20). From 2012 onwards, shallow TS3 PGD EFW displayed some degree of periodicity that appears loosely related to upstream SW stages (Figure 19). As upstream SW stages rapidly rose each year, shallow TS3 PGD EFW also rose to a seasonal high and declined with a general similarity to upstream SW stages (Figure 19). The relationship between TS3 PGD EFW and upstream SW stage is very weak though; and much weaker than the relationships between both shallow and deep PGD EFW at TS6 and upstream SW stages (Figure 16, Table 3).

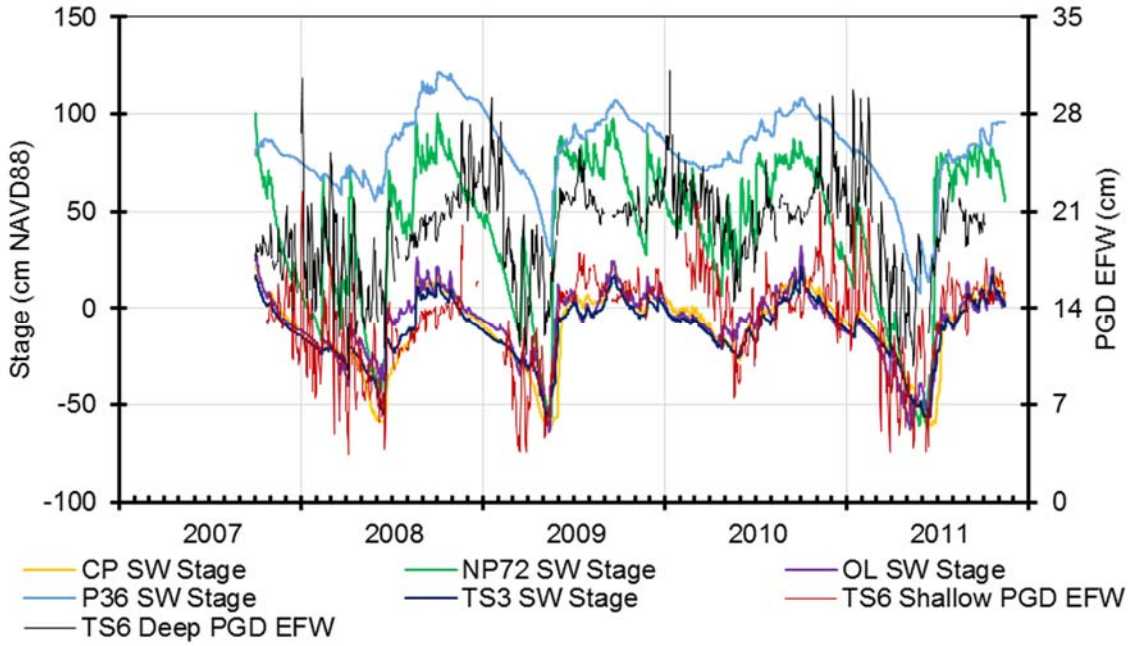

Figure 17: Daily density corrected groundwater discharge potential (PGD EFW) at TS6 and upstream SW stages (CP, NP72, OL, P36, TS3) over time.

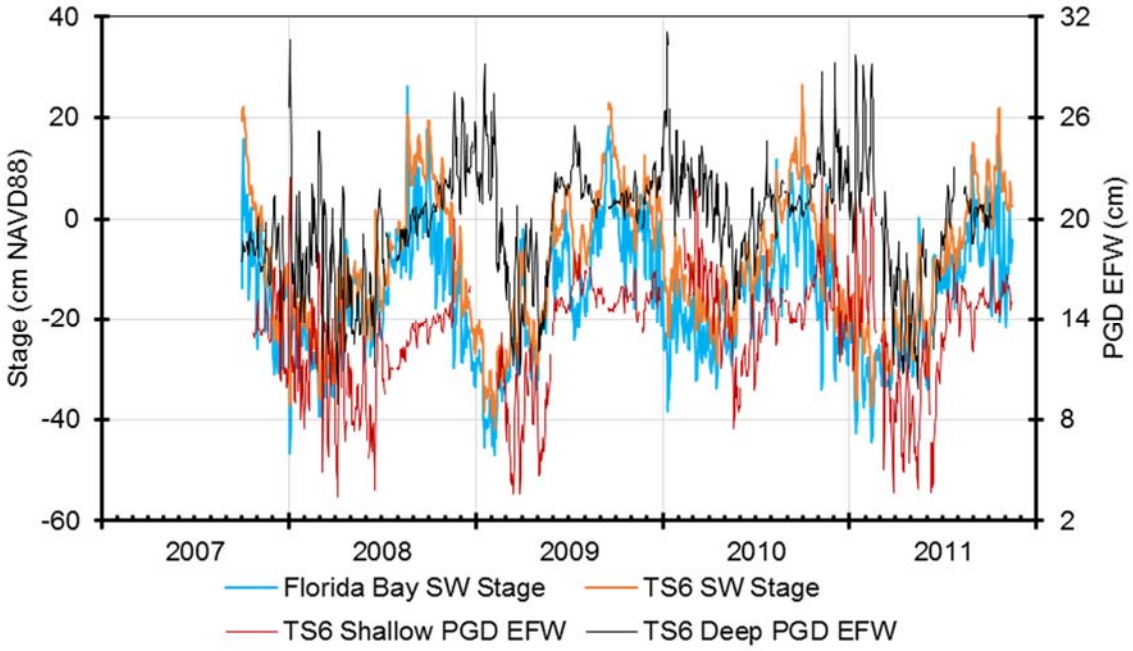

Figure 18: Daily density corrected groundwater discharge potential (PGD EFW) at TS6 and downstream SW stages (TS6, Florida Bay) over time.

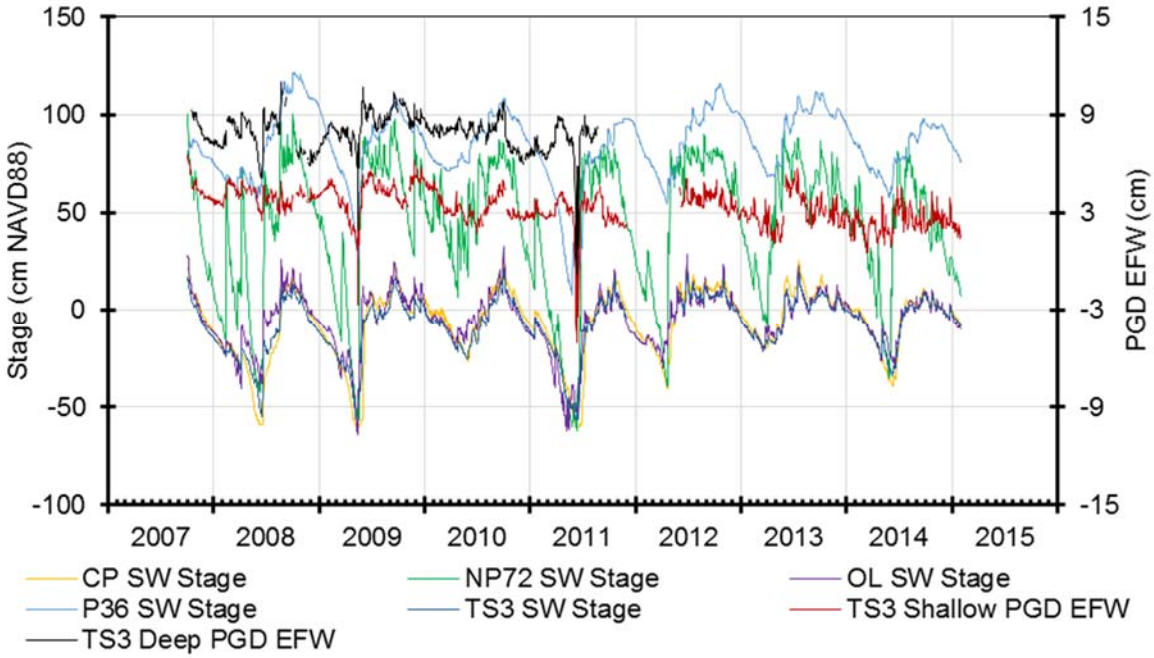

Figure 19: Daily density corrected groundwater discharge potential (PGD EFW) at TS3 and upstream SW stages (CP, NP72, OL, P36, TS3) over time.

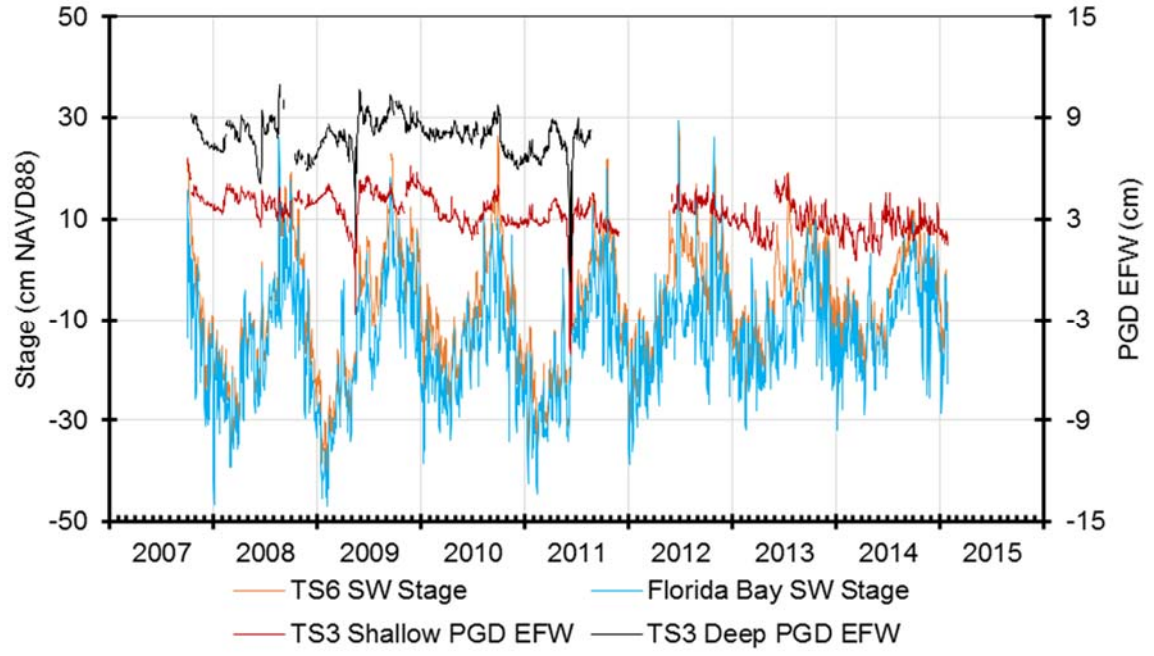

Figure 20: Daily density corrected groundwater discharge potential (PGD EFW) at TS6 and downstream SW stages (TS6, Florida Bay) over time.

Table 3: Correlation matrix for density corrected deep and shallow groundwater discharge potential (PGDEFW) at TS6 & TS3; surface water (SW) stage at TS3 & TS6; uncorrected deep and shallow groundwater (GW) stages at TS3 & TS6; and regional SW stages over 4-7 years. 4-year corrleations have n≤1506, 7-year correlations have n>1507.

Pearson r 2-Tail Sig. n	TS6 Shallow GW	TS6 Deep GW	TS6 SW	TS6 Shal-low PGD EFW	TS6 Deep PGD EFW	TS3 Shal-low GW	TS3 Deep GW	TS3 SW	TS3 Shal-low PGD EFW	TS3 Deep PGD EFW	CP SW	NP72 SW	OL SW	P36 SW
TS6 Deep GW	.998 .000 1330	1 1400												
TS6 SW	.982 .000 1401	.976 .000 1384	1 2635											
TS6 Shallow PGDEFW	.439 .000 1306	.452 .000 1225	.278 .000 1306	1 1306										
TS6 Deep PGDEFW	.317 .000 1273	.278 .000 1341	.067 .014 1341	.952 .000 1192	1 1341									
TS3 Shallow GW	.790 .000 1406	.778 .000 1389	.732 .000 2447	.692 .000 1297	.589 .000 1331	1 2479								
TS3 Deep GW	.793 .000 1366	.790 .000 1382	.701 .000 1420	.685 .000 1258	.575 .000 1324	.999 .000 1451	1 1452							
TS3 SW	.800 .000 1406	.791 .000 1391	.745 .000 2455	.688 .000 1297	.583 .000 1332	.996 .000 2470	.997 .000 1443	1 2488						
TS3 Shallow PGDEFW	.262 .000 1367	.266 .000 1351	.173 .000 2393	.174 .000 1262	.161 .000 1295	.349 .000 2425	.467 .000 1415	.253 .000 2416	1 2425					
TS3 Deep PGDEFW	.453 .000 1242	.418 .000 1263	.416 .000 1295	.215 .000 1151	.028 .328 1206	.465 .000 1327	.492 .000 1327	.412 .000 1318	.714 .000 1315	1 1327				
CP SW	.720 .000 1415	.706 .000 1400	.671 .000 2635	.689 .000 1306	.582 .000 1341	.969 .000 2479	.957 .000 1452	.970 .000 2488	.267 .000 2425	.357 .000 1327	1 2680			
NP72 SW	.798 .000 1415	.785 .000 1400	.687 .000 2635	.656 .000 1306	.566 .000 1341	.861 .000 2479	.892 .000 1452	.846 .000 2488	.354 .000 2425	.476 .000 1327	.808 .000 2680	1 2680		
OL SW	.838 .000 1415	.825 .000 1400	.767 .000 2635	.653 .000 1306	.558 .000 1341	.947 .000 2479	.944 .000 1452	.942 .000 2488	.336 .000 2425	.472 .000 1327	.876 .000 2680	.871 .000 2680	1 2680	
P36 SW	.680 .000 1415	.635 .000 1400	.576 .000 2635	.557 .000 1306	.563 .000 1341	.862 0.000 2479	.849 .000 1452	.853 .000 2488	.281 .000 2425	.292 .000 1327	.823 .000 2680	.773 .000 2680	.855 .000 2680	1 2680
FL Bay SW	.874 .000 1415	.876 .000 1400	.912 .000 2635	.084 .002 1306	-.119 .000 1341	.532 .000 2479	.530 .000 1452	.547 .000 2488	.071 .001 2425	.385 .000 1327	.469 .000 2680	.522 .000 2680	.591 .000 2680	.424 .000 2680

Table 4: Cross-correlation matrix showing lag times of greatest correlation between surface water (SW) stages, groundwater (GW) stages, and density corrected groundwater discharge potential (PGD EFW) at TS6 and TS3. Lag times tested were +/- 100 days. Lag units are days. Positive lags indicate that the variable in the leftmost column tends to change before the variable in the top row. Negative lags indicate that the variable in the leftmost column tends to change after the variable in the top row. Lagged variables are highlighted in bold. Numbers of observations correspond with Table 3.

Max Corr / Lag	TS6 Shallow GW	TS6 Deep GW	TS6 SW	TS6 Shallow PGD EFW	TS6 Deep PGD EFW	TS3 Shallow GW	TS3 Deep GW	TS3 SW	TS3 Shallow PGD EFW	TS3 Deep PGD EFW	CP SW	NP72 SW	OL SW	P36 SW
TS6 Deep GW	.998 / 0	1												
TS6 SW	.981 / 0	.975 / 0	1											
TS6 Shallow PGD EFW	**.527 / -17**	**.537 / -17**	**.458 / -18 & -19**	1										
TS6 Deep PGD EFW	**.472 / -17**	**.494 / -5 & -4**	**.444 / -62**	.955 / 0	1									
TS3 Shallow GW	.760 / 0	.770 / 0	.681 / 0	.698 / 0	.658 / 0	1								
TS3 Deep GW	.770 / 0	.779 / 0	.692 / 0	.695 / 0	.652 / 0	.999 / 0	1							
TS3 SW	.762 / 0	.772 / 0	.681 / 0	.706 / 0	.668 / 0	.998 / 0	.998 / 0	1						
TS3 Shallow PGD EFW	.311 / 0	.302 / 0	.308 / 0	**-.236 / -95 & -94**	**-0.240 / -98 & -97**	.409 / 0	.397 / 0	.358 / 0	1					
TS3 Deep PGD EFW	.441 / 0	.426 / 0	.441 / 0	**.223 / -100**	**.212 / -100**	.393 / 0	.421 / 0	.363 / 0	.653 / 0	1				
CP SW	.671 / 0	.681 / 0	.594 / 0	.685 / 0	.639 / 0	.955 / 0	.951 / 0	.957 / 0	.318 / 0	.300 / 0	1			
NP72 SW	.775 / 0	.786 / 0	.699 / 0	.646 / 0	.619 / 0	.863 / 0	.871 / 0	.863 / 0	.333 / 0	.434 / 0	.768 / 0	1		
OL SW	.822 / 0	.833 / 0	.750 / 0	.658 / 0	.622 / 0	.928 / 0	.933 / 0	.928 / 0	.367 / 0	.411 / 0	.831 / 0	.898 / 0	1	
P36 SW	.666 / 0	.685 / 0	.607 / 0	.563 / 0	.571 / 0	.875 / 0	.874 / 0	.878 / 0	.274 / 0	**.323 / -100**	.816 / 0	.811 / 0	.898 / 0	1
FL Bay SW	.882 / 0	.870 / 0	.932 / 0	**.425 / 62**	**.419 / 62**	.494 / 0	.507 / 0	.493 / 0	**.232 / 1** & 0	.407 / 0	**.474 / 64**	.558 / 0	.595 / 0	**.476 / 61 & 54**

Table 5: Mean, minimum, and maximum values for regional surface water (SW) stages around Taylor Slough over 4 years.

SW Stage (cm NAVD88)	Mean	Minimum	Maximum	# of Observations
TS3 SW	-10.87	-56.48	21.64	1497
CP SW	-9.91	-60.66	27.13	1506
NP72 SW	40.61	-62.18	100.58	1506
OL SW	-7.49	-64.01	32.61	1506
P36 SW	81.42	7.92	121.62	1506
TS6 SW	-9.25	-41.87	26.49	1473
Florida Bay SW	-15.63	-47.00	26.15	1506

Table 6: Mean, minimum, and maximum values for regional surface water (SW) stages around Taylor Slough over 7 years.

SW Stage (cm NAVD88)	Mean	Minimum	Maximum	# of Observations
TS3 SW	-7.34	-56.48	21.64	2488
CP SW	-6.53	-60.66	27.13	2680
NP72 SW	43.18	-62.18	100.57	2680
OL SW	-5.54	-64.01	32.61	2680
P36 SW	84.44	7.92	121.62	2680
TS6 SW	-7.19	-41.87	29.31	2635
Florida Bay SW	-13.77	-47.00	29.50	2680

Surface Water Discharge

Upstream SW discharge into Taylor Slough, measured at TSB, occurs seasonally and reached daily average flows of over 15 m^3/s during two of the wet seasons, but fell to zero during each of the dry seasons (Figure 21). Upstream SW discharge into Taylor Slough at TSB demonstrates very similar seasonal patterns to upstream SW stages (Figure 22). Seasonal highs in upstream SW discharge and upstream SW stage were coincident throughout the study period, while troughs in upstream SW stage lagged behing flow stoppages by a few months each year (Figure 21).

The general trends of SW discharge at TS6 and SW discharge upstream were similar, with a few notable differences (Figure 21). Flow reversal never occurred in upstream SW discharge and tended to be much greater in magnitude than TS6 SW discharge, when upstream SW discharge was occurring (Figure 21). There was not a consistent relationship between the timing of peaks between these two series of SW discharge observations, beyond the overall wet/dry season pattern; peak upstream SW discharges sometimes lagged behind peak TS6 SW discharges, but at other times peak upstream SW discharges preceeded peak TS6 SW discharges (Figure 21).

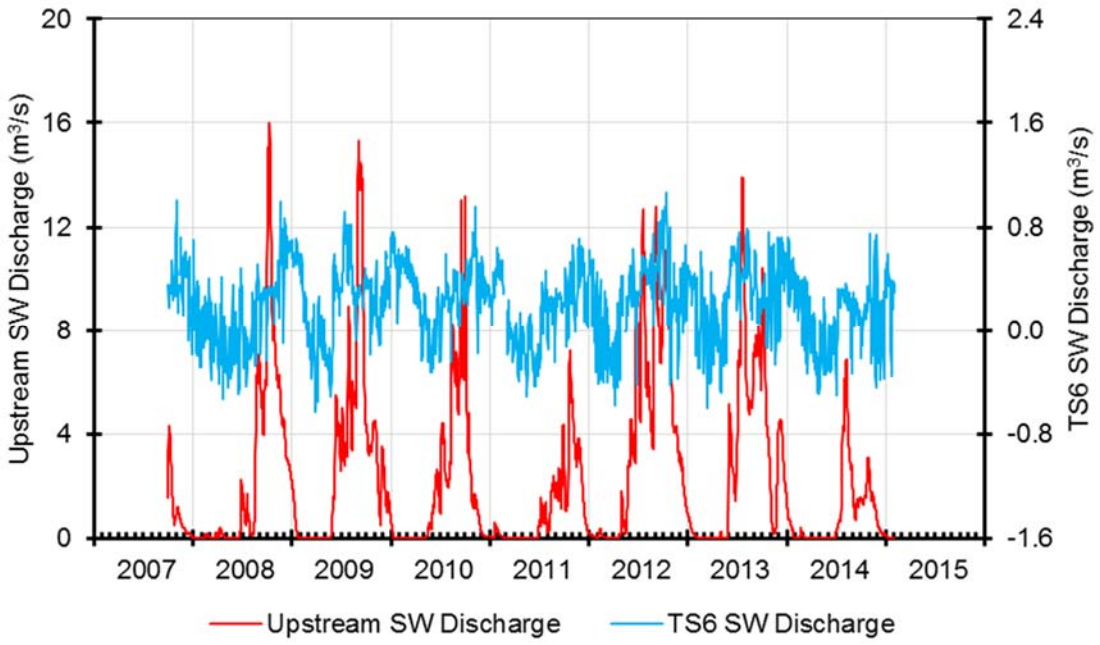

Figure 21: Surface water (SW) discharge over time at TS6 and upstream (TSB).

Peaks in upstream SW discharge generally occurred 0-1 months before peaks in upstream SW stage, with the exception of upstream SW discharge peaks at the end of 2014, which preceeded upstream SW stage peaks by 3 months (Figure 22). The lowest upstream SW stages occurred at the end of the zero-flow periods observed in upstream SW discharge (Figure 21). The greatest SW discharges occured at TS6 when upstream SW stages were highest (Figure 23). Negative discharge, or flow reversal, occured when upstream SW stages were lowest and Florida Bay SW stage was higher than some of the upstream SW stages (Figure 23). Discharge of SW at TS6 had significant, positive relationships with upstream stages (Figure 24). When upstream stages were higher (CP, NP72, OL, P36, TSB, TS3 SW), TS6 SW discharge was greater (Figure 24). When downstream stage in Florida Bay was higher, TS6 SW discharge was somewhat lower and often reversed, flowing upstream towards TS6 and into the mangrove ecotone, from Florida Bay (Figure 23, Figure 24). Stage of SW at TS6 and SW discharge at TS6 were not correlated (Figure 24).

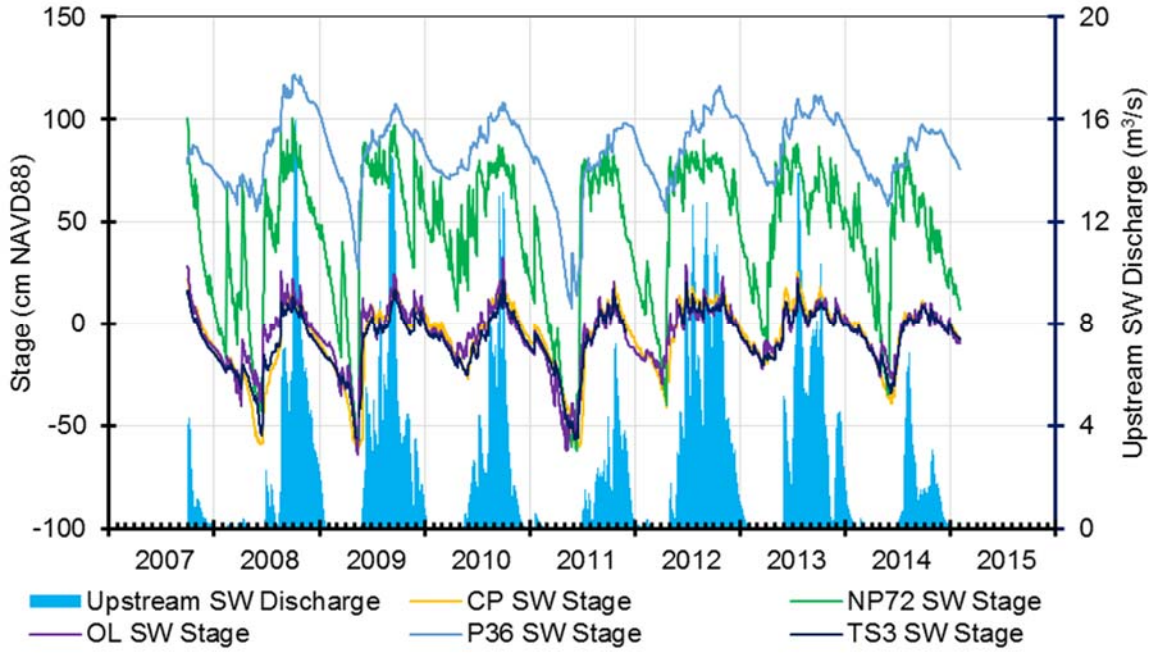

Figure 22: Upstream surface water (SW) discharge and upstream SW stages (CP, NP72, OL, P36, TS3) over time.

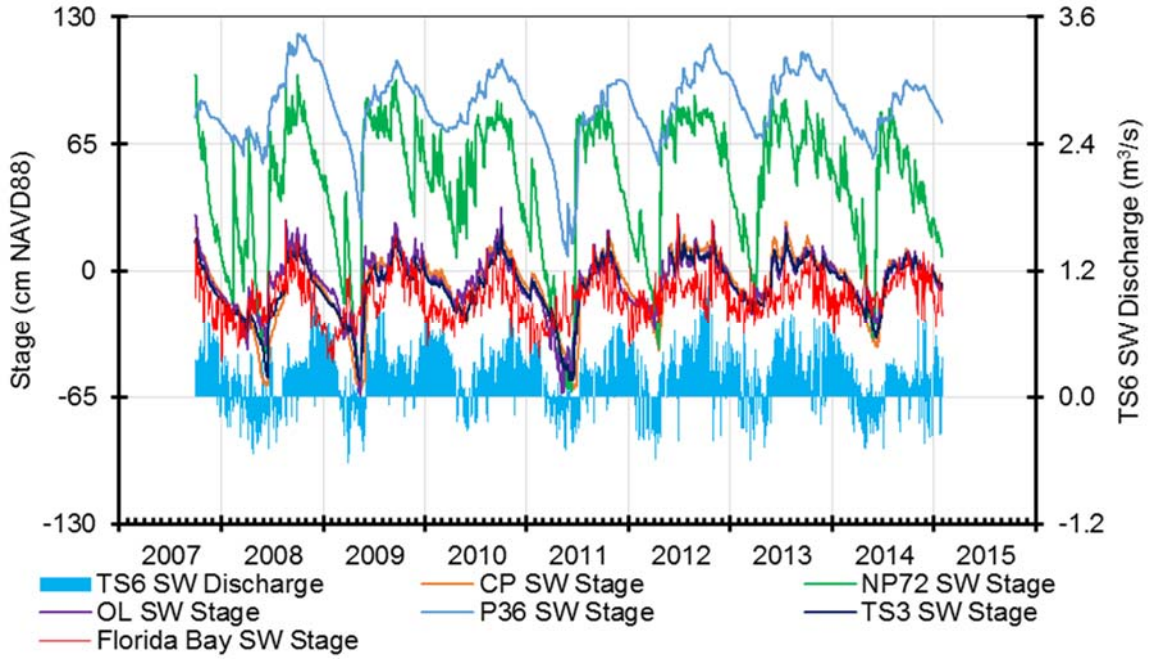

Figure 23: Surface water (SW) discharge at TS6, Florida Bay stage (LM), and upstream SW stages (CP, NP72, OL, P36, TS3) over time.

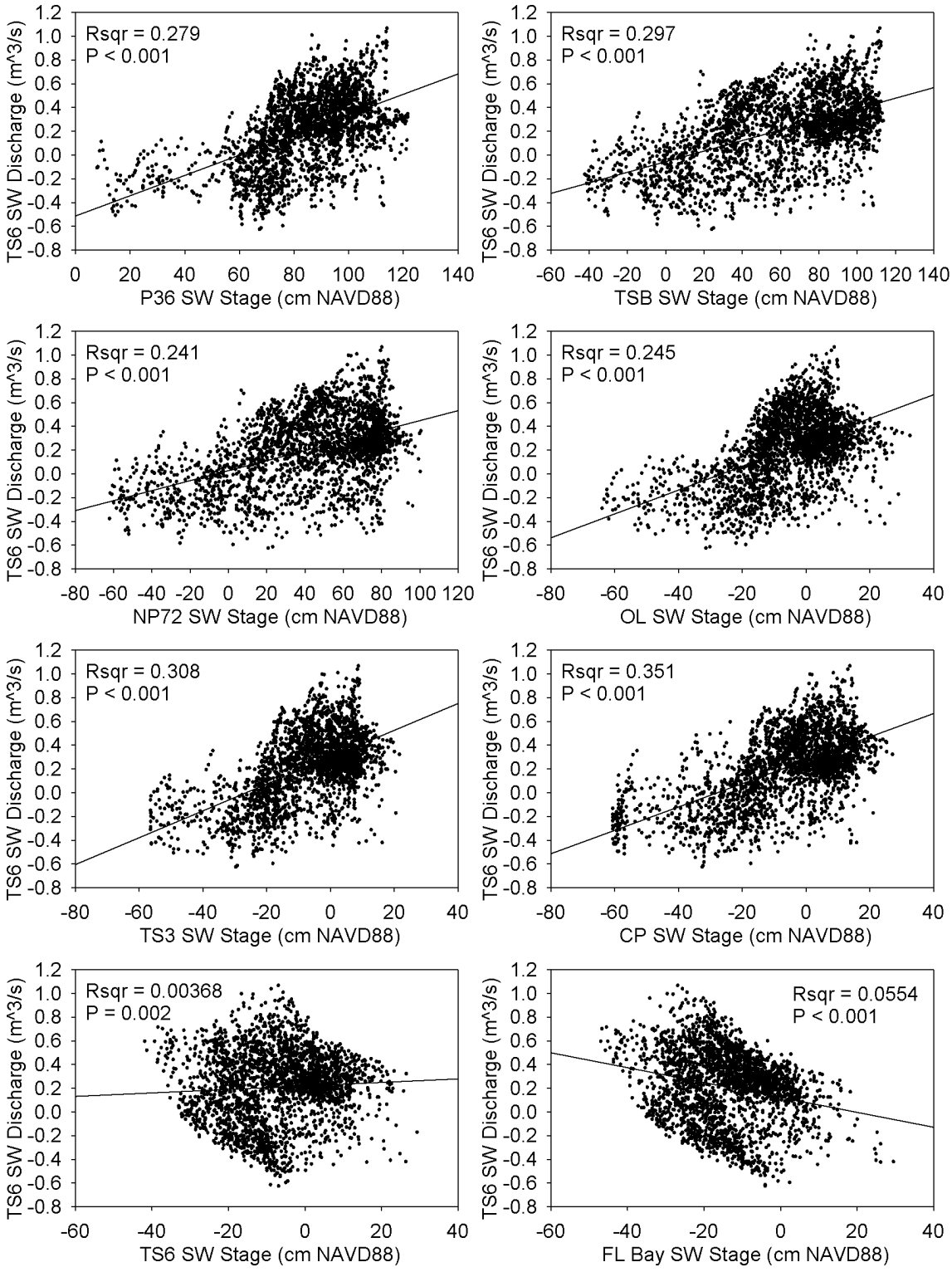

Figure 24: Average daily surface water (SW) discharge at TS6 vs regional SW stages in and around Taylor Slough over 7 years, as depicted in Figure 2.

At TS6, PGD EFW of both GW wells did not correlate with upstream SW discharge (Shallow: R^2=0.0931, p<0.001; Deep: R^2=0.0636, p<0.001) (Figure 25). When upstream SW flows ceased each year, PGD EFW at TS6 continued to exhibit variation (Figure 25). The same non-correlative relationship with upstream SW discharge exists for both of the TS3 PGD EFW, with the TS3 PGD EFW values varying independently of variations in upstream SW discharge (Shallow: R^2=0.0972, p<0.001; Deep: R^2=0.0959, p<0.001) (Figure 26). Although there was not a strong statistical relationship between upstream SW discharge and TS6 PGD EFW, there was a regular pattern observed between upstream SW discharge and TS6 PGD EFW (Figure 25). The greatest upstream SW discharges occurred a few months before the periods of highest TS6 PGD EFW and the lowest SW discharges occurred during the periods of lowest PGD EFW at TS6 (Figure 25). The same pattern does not hold for TS3 PGD EFW from October 2007 through November 2011, where the irregular time series do not compare well with the strong seasonality in upstream SW discharge (Figure 26). In 2012 and 2013, and to lesser extent in 2014, PGD EFW at shallow TS3 was generally higher when upstream SW discharge was higher, and gradually decreased until around the resumption of upstream (TSB) SW flows (Figure 26).

At both TS6 wells, PGD EFW and TS6 SW discharge were very closely related, exhibiting coincident peaks, coincident lows, and similar variability throughout the period of study (Figure 27). At TS6, PGD EFW at both of the wells was highly correlated with SW discharge (Figure 27, Figure 28, Figure 29). The relationship between deep and shallow TS3 PGD EFW and TS6 SW discharge, though significant in both cases, was very weak, with each PGD EFW varying independently of TS6 SW discharge (Figure 30).

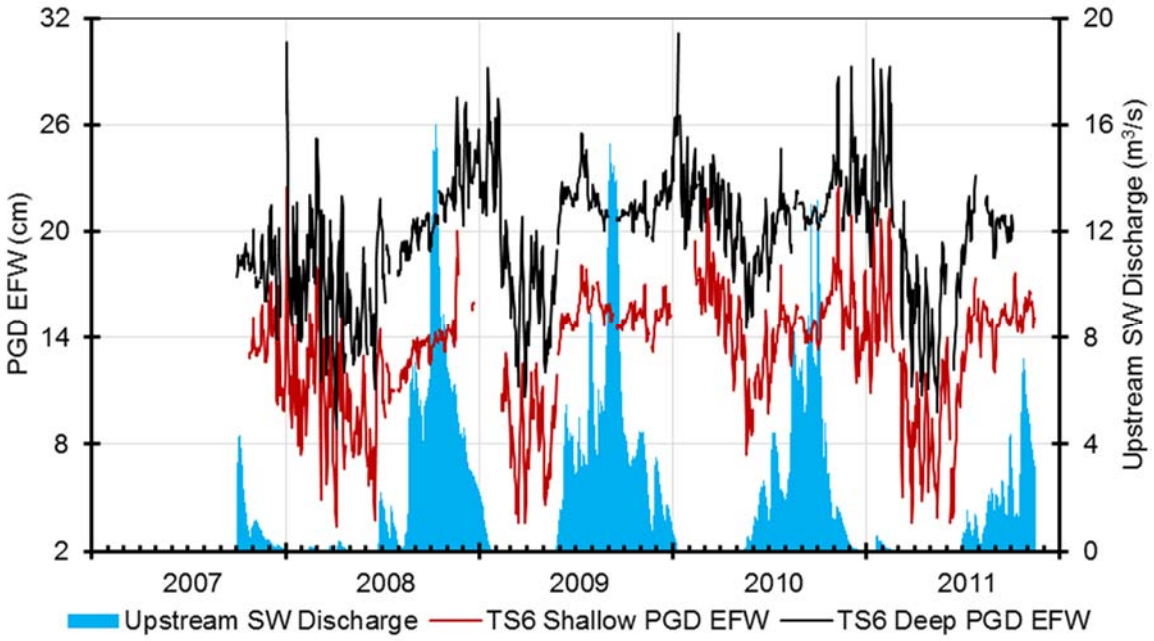

Figure 25: Density corrected groundwater discharge potential (PGD EFW) at TS6 and upstream (TSB) surface water (SW) discharge over time.

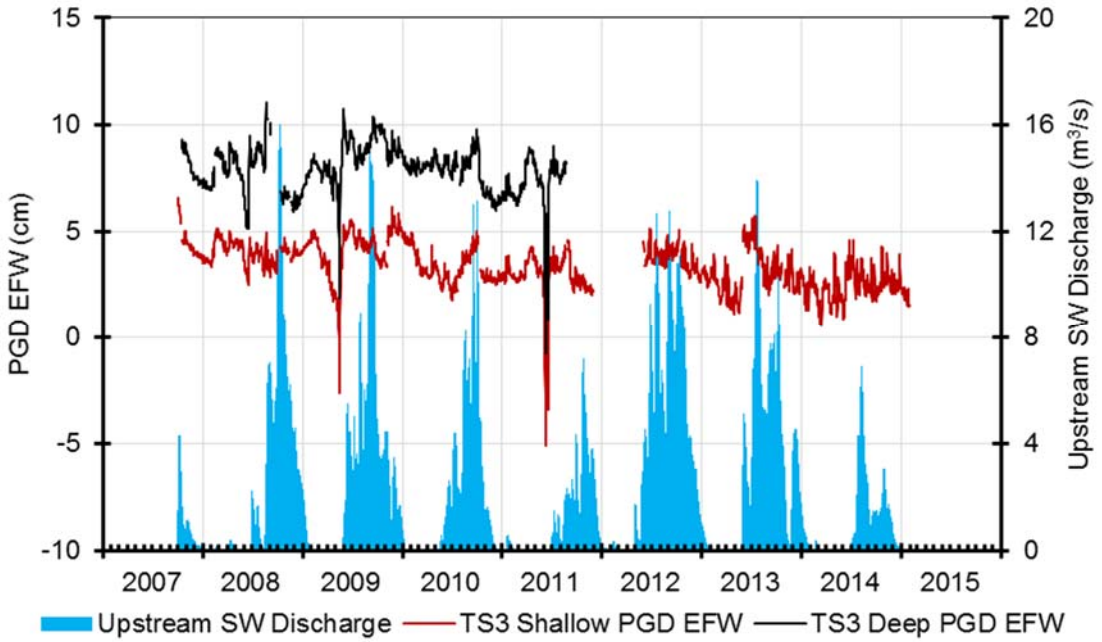

Figure 26: Density corrected groundwater discharge potential (PGD EFW) at TS3 and upstream (TSB) surface water (SW) discharge over time.

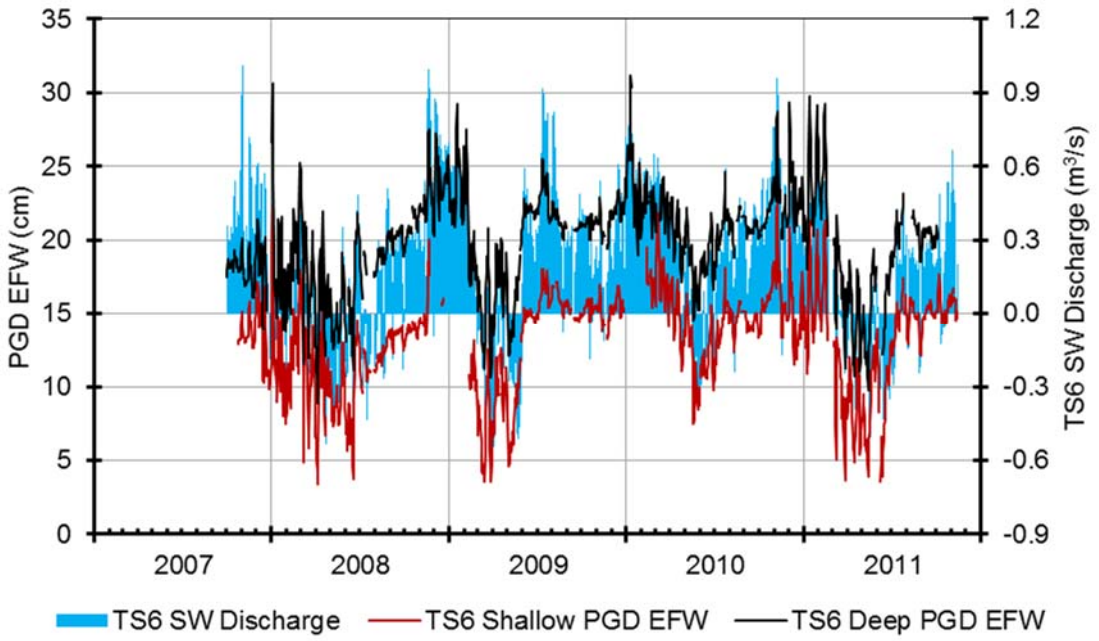

Figure 27: Shallow and deep density corrected groundwater discharge potential (PGD EFW) and surface water (SW) discharge at TS6 over time.

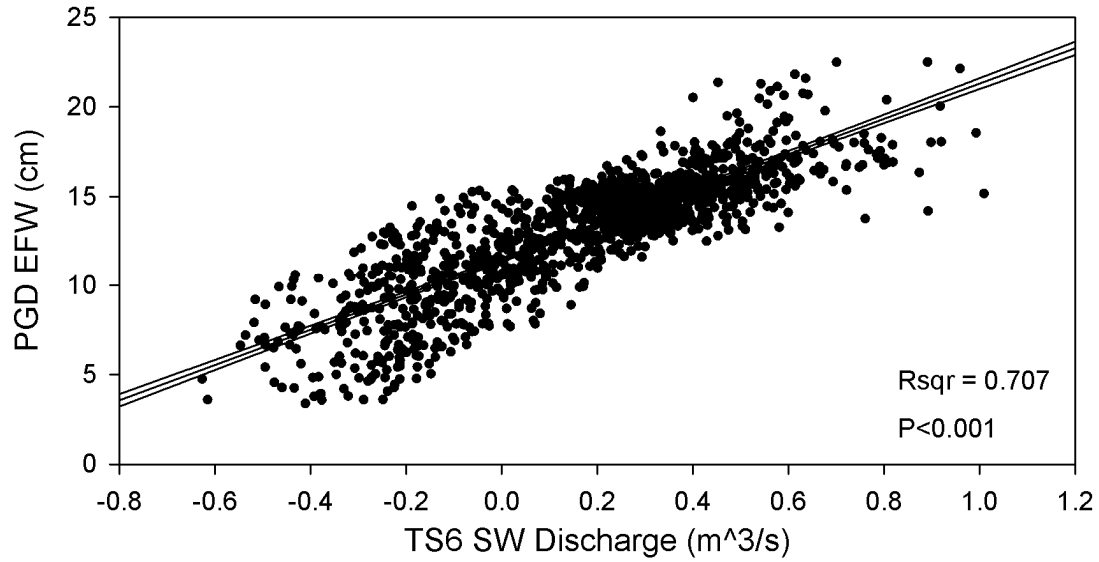

Figure 28: Surface water (SW) discharge at and shallow density corrected groundwater discharge potential (PGD EFW) over time at TS6. 95% confidence interval shown.

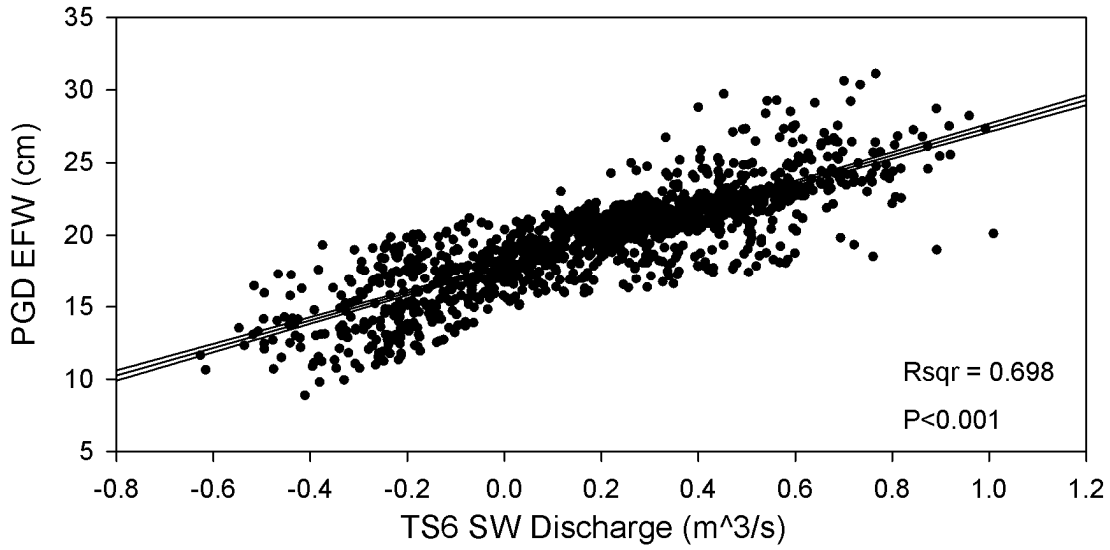

Figure 29: Surface water (SW) discharge at and deep density corrected groundwater discharge potential (PGD EFW) over time at TS6. 95% confidence interval shown.

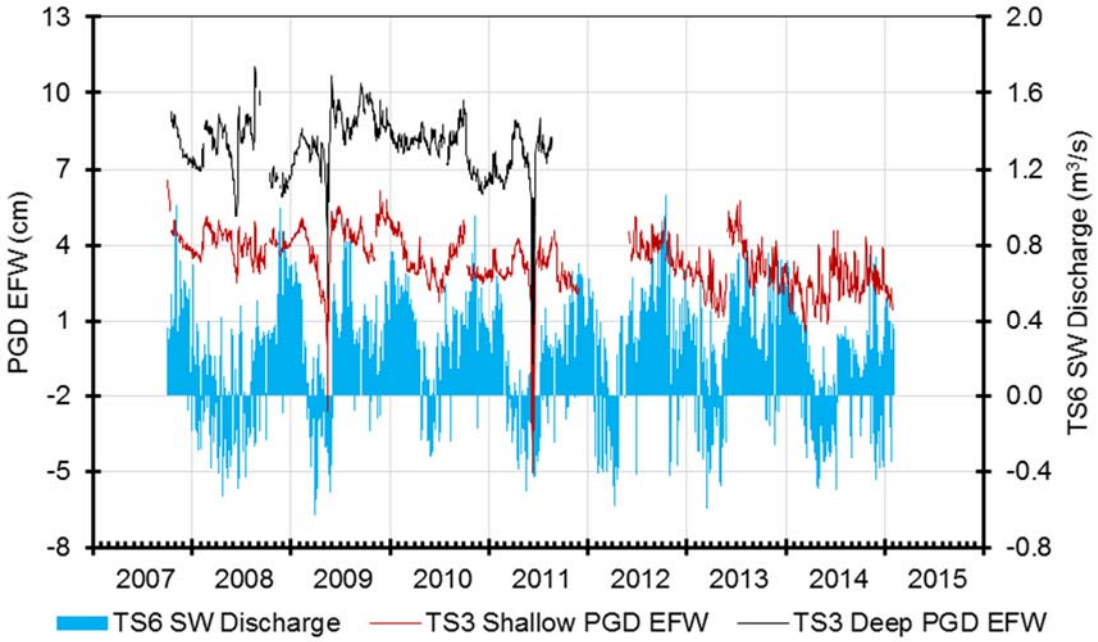

Figure 30: Shallow and deep density corrected groundwater discharge potential (PGD EFW) and surface water (SW) discharge over time at TS3.

Evapotranspiration and Rainfall

Strong and recurrent seasonality occurred in ET at both TS6 and TS3 (Figure 31, Figure 32). The highest ET values occurred from May through August and the lowest ET values occurred from November through January (Figure 31, Figure 32). At TS6, ET had a moderate to weak, inverse correlation with the PGD EFW series at TS6, but ET at TS3 did not correlate with shallow or deep TS3 PGD EFW (Table 7, Table 8).

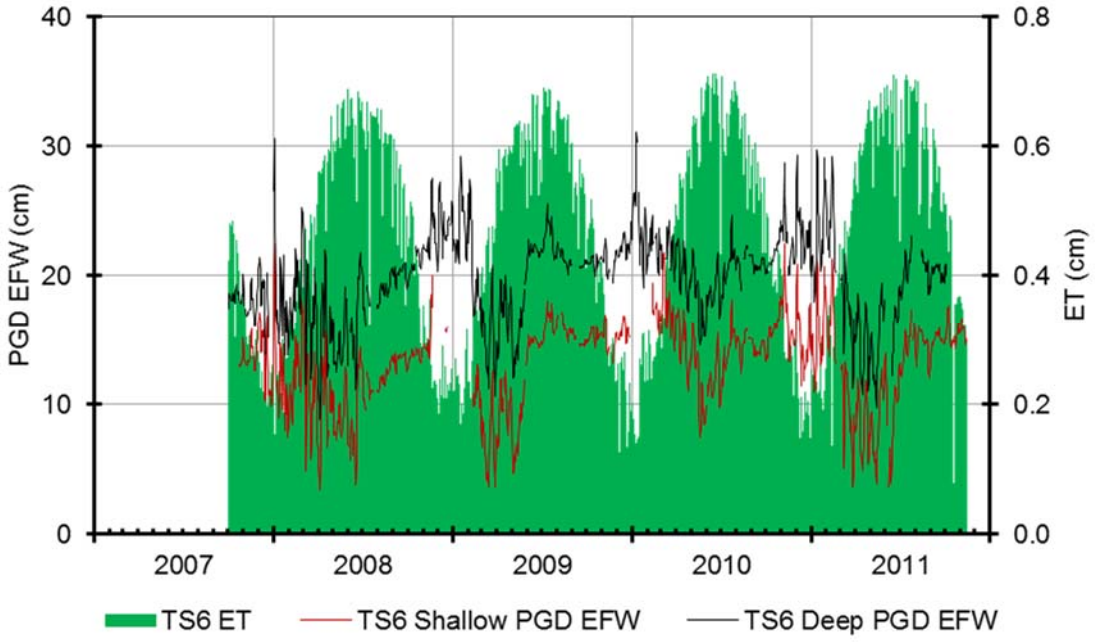

Figure 31: Shallow and deep density corrected groundwater discharge potential (PGD EFW) at TS6 and evapotranspiration (ET) at TS6 over time.

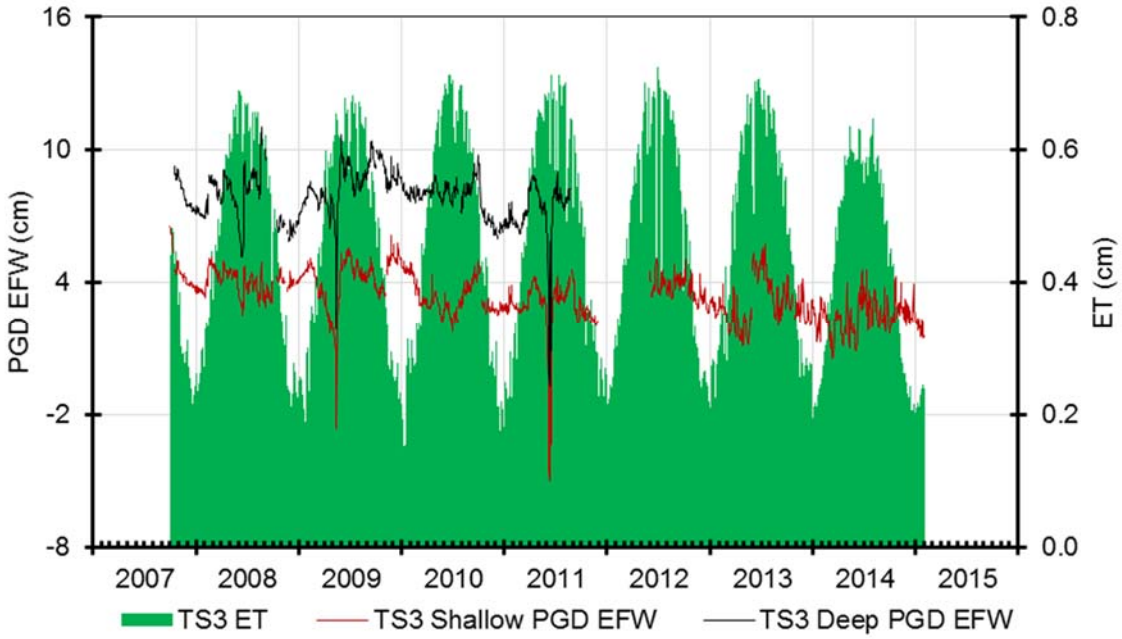

Figure 32: Shallow and deep density corrected groundwater discharge potential (PGD EFW) at TS6 and evapotranspiration (ET) at TS3 over time.

Table 7: Correlation matrix comparing deep and shallow density corrected groundwater discharge potential (PGD EFW), evapotranspiration (ET), and rainfall at TS6 over time.

		TS6 Deep PGD EFW (cm)	TS6 Shallow PGD EFW (cm)	TS6 ET (cm)	TS6 Rain (cm)	TS6 3-Day Cum Ant Rain (cm)	TS6 7-Day Cum Ant Rain (cm)
TS6 Shallow PGD EFW (cm)	Pearson Corr.	.952	1				
	Sig. (2-tailed)	0.000					
	N	1192	1306				
TS6 ET (cm)	Pearson Corr.	-.408	-.322	1			
	Sig. (2-tailed)	.000	.000				
	N	1341	1306	1506			
TS6 Rain (cm)	Pearson Corr.	-.016	.026	-.131	1		
	Sig. (2-tailed)	.570	.348	.000			
	N	1341	1306	1506	1506		
TS6 3-Day Cum Ant Rain (cm)	Pearson Corr.	.024	.081	-.021	.643	1	
	Sig. (2-tailed)	.386	.004	.419	.000		
	N	1341	1306	1506	1506	1506	
TS6 7-Day Cum Ant Rain (cm)	Pearson Corr.	.085	.166	.115	.430	.701	1
	Sig. (2-tailed)	.002	.000	.000	.000	.000	
	N	1341	1306	1506	1506	1506	1506
TS6 14-Day Cum Ant Rain (cm)	Pearson Corr.	.146	.277	.189	.340	.544	.777
	Sig. (2-tailed)	.000	.000	.000	.000	.000	.000
	N	1341	1306	1506	1506	1506	1506

Table 8: Correlation matrix comparing deep and shallow density corrected groundwater discharge potential (PGD EFW), evapotranspiration (ET), and rainfall at TS3 over 4-7 years. 4-year correlations have n≤1506, 7-year correlations have n>1507.

		TS3 Deep PGD EFW (cm)	TS3 Shallow PGD EFW (cm)	TS3 ET (cm)	TS3 Rain (cm)	TS3 3-Day Cum Ant Rain (cm)	TS3 7-Day Cum Ant Rain (cm)
TS3 Shallow PGD EFW (cm)	Pearson Corr.	.714	1				
	Sig. (2-tailed)	.000					
	N	1315	2425				
TS3 ET (cm)	Pearson Corr.	.138	-.064	1			
	Sig. (2-tailed)	.000	.002				
	N	1327	2425	2680			
TS3 Rain (cm)	Pearson Corr.	.146	.126	-.111	1		
	Sig. (2-tailed)	.000	.000	.000			
	N	1327	2425	2680	2680		
TS3 3-Day Rain (cm)	Pearson Corr.	.293	.230	.015	.630	1	
	Sig. (2-tailed)	.000	.000	.427	.000		
	N	1327	2425	2680	2680	2680	
TS3 7-Day Rain (cm)	Pearson Corr.	.405	.274	.152	.440	.710	1
	Sig. (2-tailed)	.000	.000	.000	.000	.000	
	N	1327	2425	2680	2680	2680	2680
TS3 14-Day Rain (cm)	Pearson Corr.	.467	.306	.250	.337	.544	.782
	Sig. (2-tailed)	.000	.000	.000	.000	.000	.000
	N	1327	2425	2680	2680	2680	2680

Rainfall exhibited high interday variability at TS6 and TS3, with 80% and 77% of the rainfall arriving during the wet season at each site, respectively (Figure 33; Figure 34). The magnitude of rainfall contributions, when rainfall did occur, were often much greater than ET on a specific day or month. During drier months, ET removals exceeded rainfall contributions. No correlative relationship between daily TS6 rainfall and TS6 PGD EFW was observed (Table 7). Similarly, no correlative relationship between TS3 PGD EFW and daily TS3 rainfall was observed either (Table 8). The sporadic and highly event-based measurements of rainfall and upstream SW discharges were difficult to compare to continuous times series like those of PGD EFW because the measurements fall to or approach zero at both the daily and monthly time scale multiple times each year. In an attempt to consider antecedent conditions of rainfall, 3, 7, and 14-day windows that accumulated prior rainfall amounts into single day values were utilized for comparisons, in addition to the original daily totals (Figure 33, Figure 34). This exercise resulted in stronger correlations between PGD EFW at TS6 and TS3, with correlations consistently increasing as antecedent cumulative window size was increased at both sites, although none of the correlations were particularly strong with the exception of deep TS3 PGD EFW (Table 7,Table 8). Deep TS3 PGD EFW had a moderate correlation with the 7 and 14-day rainfall time series when compared over a daily time-step (Table 8).

Monthly shallow and deep PGD EFW at TS6 lagged behind basinwide and local rainfall by three months (Figure 35, Figure 36). Monthly shallow PGD EFW at TS3 did not have a strong correlation with basinwide or local precipitation at any lag time (Figure 37). Monthly deep PGD EFW at TS3 lagged one month behind both basinwide and local rainfall (Figure 37). Monthly local rainfall at TS6 lagged one month behind TS6 ET (Figure 31, Figure 35). Similarly, local rainfall at TS3 lagged one month behind TS3 ET (Figure 32, Figure 37).

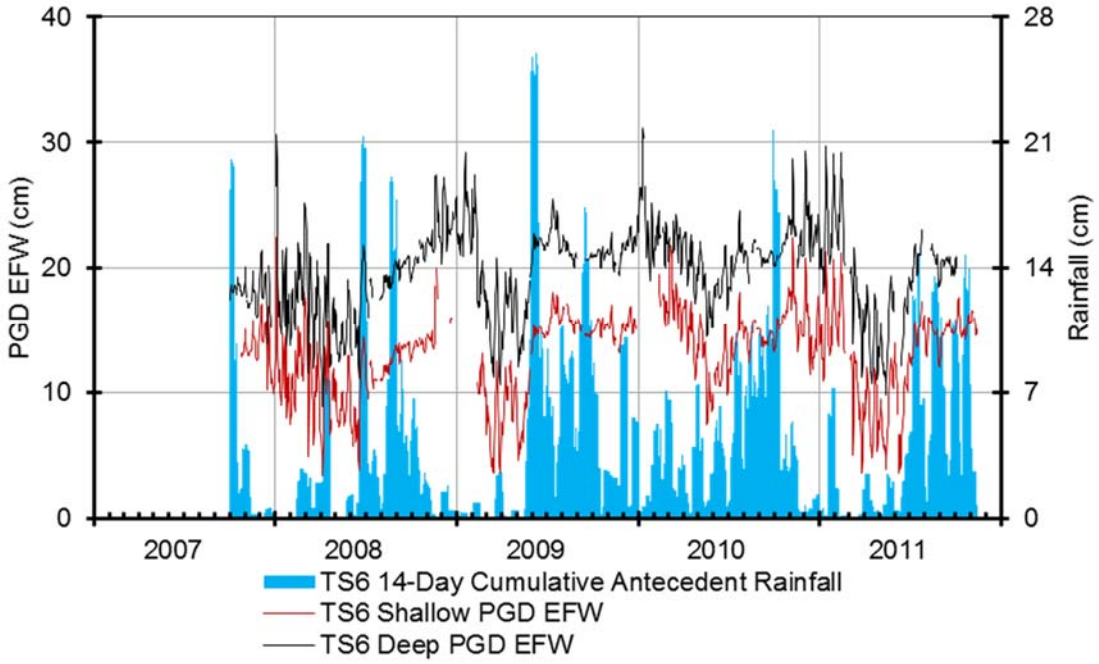

Figure 33: Deep and shallow density corrected groundwater discharge potential (PGD EFW) and TS6 14-day Antecedent Cumulative Rainfall over time.

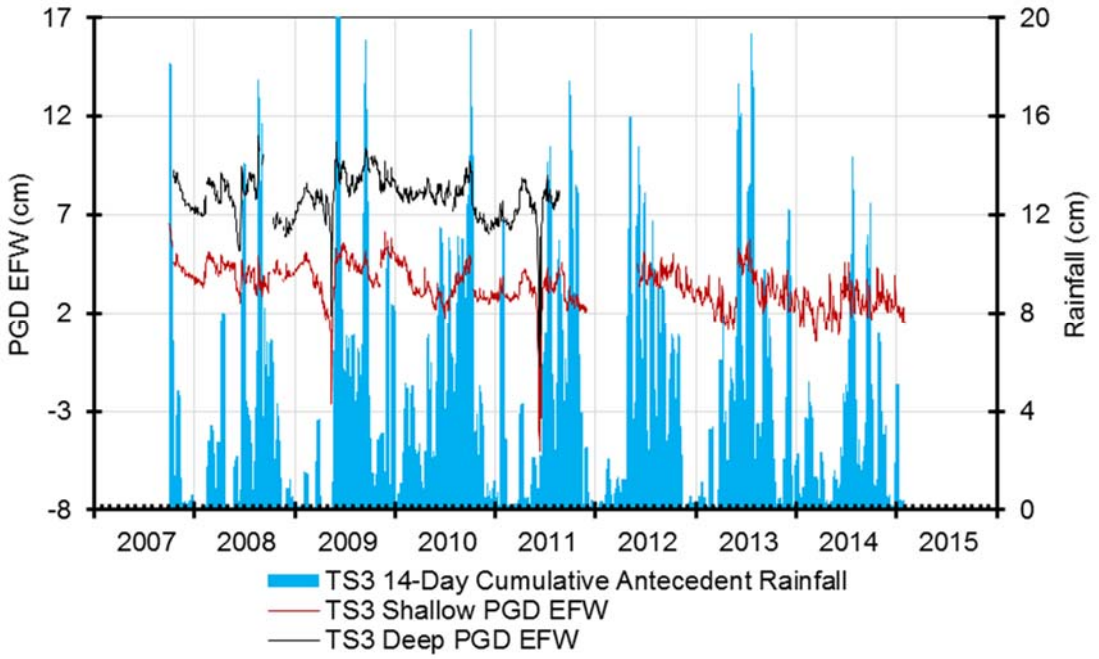

Figure 34: Deep and shallow density corrected groundwater discharge potential (PGD EFW) and TS3 14-day Antecedent Cumulative Rainfall over time.

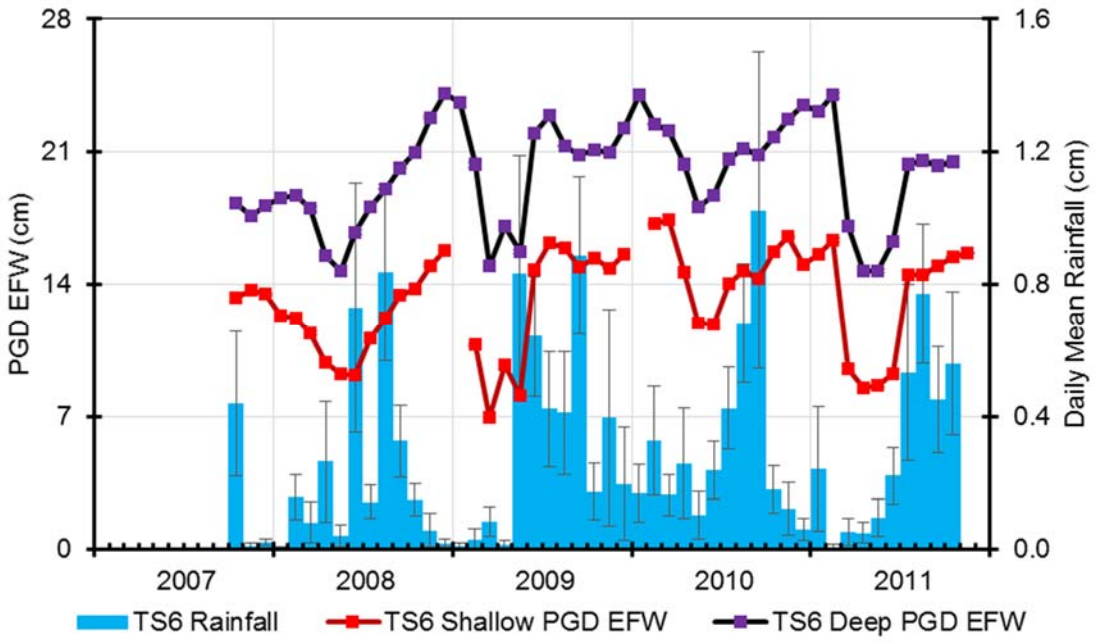

Figure 35: Monthly rainfall at TS6 with deep and shallow groundwater discharge potential (PGD EFW) over time at TS6 time with standard errors shown.

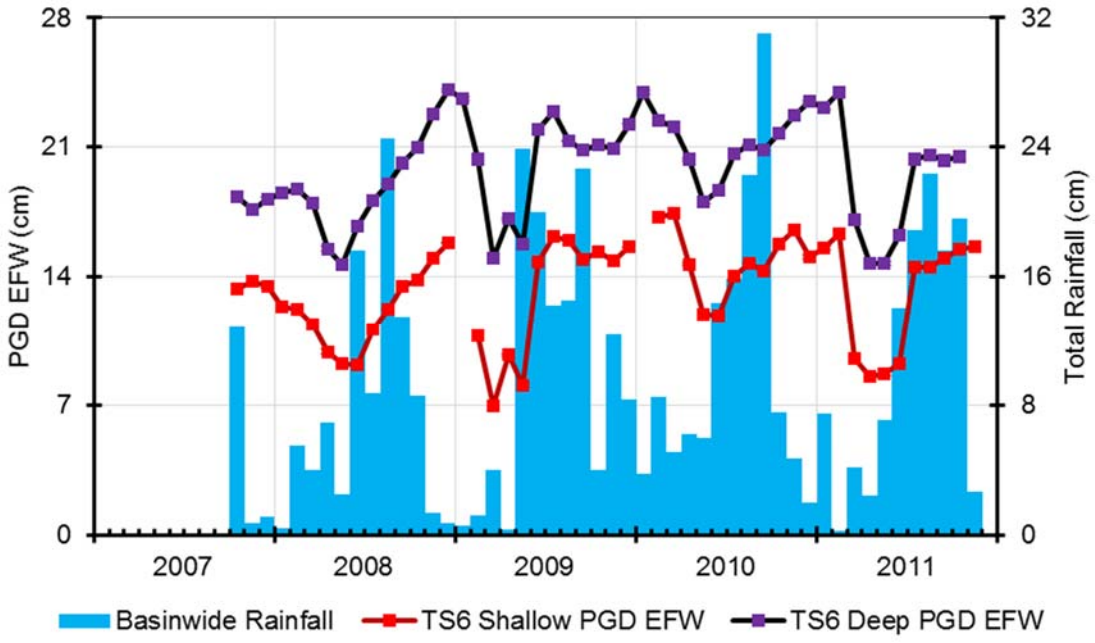

Figure 36: Monthly basinwide rainfall from Sandoval (2013), compared with deep and shallow groundwater discharge potential (PGD EFW) over time at TS6 with standard errors shown. Standard errors are not available for basinwide rainfall values.

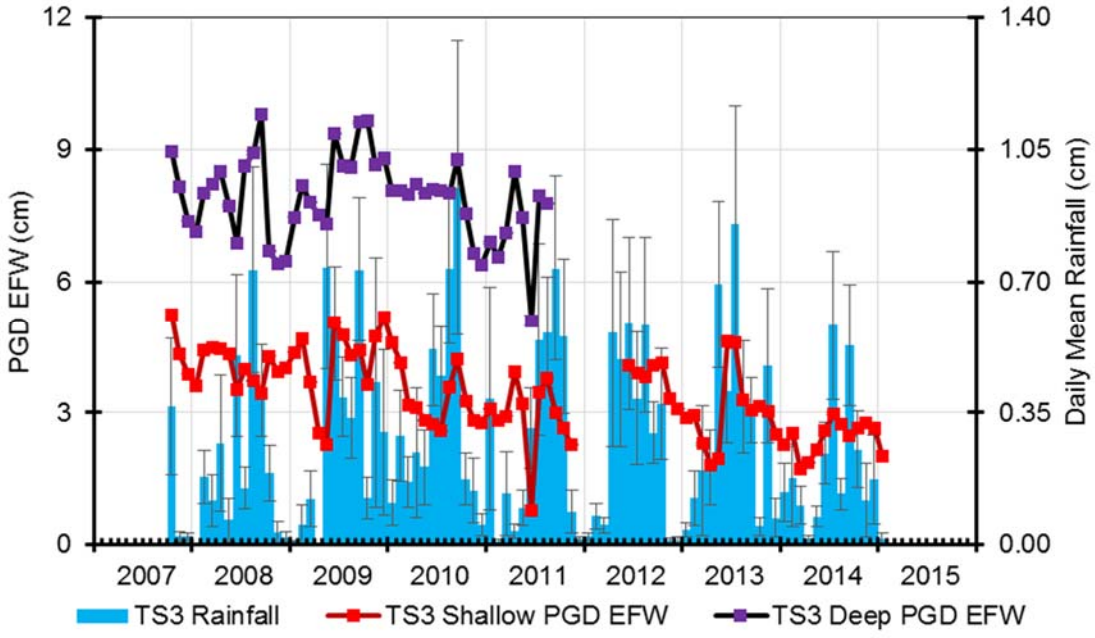

Figure 37: Monthly rainfall at TS3 with deep and shallow groundwater discharge potential (PGD EFW) over time at TS3 with standard errors shown.

CONTROLS OF SURFACE WATER CHEMISTRY

Salinity in shallow GW at TS6 exhibited strong seasonality with greater variation occurring during periods of low PGD EFW, compared to the relatively constant salinity that occurred during periods of higher PGD EFW (Figure 38). The periods of less variable shallow GW salinity generally plateaued at salinities of approximately 29 psu (Figure 38). Shallow GW salinity at TS6 was highest when shallow GW stage was highest (Figure 39). As shallow GW salinity decreased from the 29 psu plateau, variability in shallow GW salinity was much higher (Figure 38). The shallow GW salinity decrease appears to be somewhat coincident with the decrease in shallow GW stage and PGD EFW (Figure 38, Figure 39). Increases in shallow GW salinity were preceded by increases in shallow PGD EFW each year, but the timing was not consistent from year to year (Figure 38). Salinity in deep GW at TS6 was comparatively more stable throughout the study period, relative to shallow GW salinity at TS6, with a similar plateau of approximately 29 psu (Figure 40). Deep GW salinity at TS6 was highest as deep GW stage was rising (Figure 40). The 29 psu plateau salinity reached in both TS6 GW wells was more clearly defined and lasted longer each season in the deeper well (Figure 38, Figure 40). The shallower GW did not maintain the plateau salinity as consistently as the deeper well (Figure 38, Figure 40). The deeper GW well's salinity at TS6 remained at the plateau salinity for the majority of the study period (Figure 40). When TS6's deeper well's salinity did deviate from the plateau salinity, deep GW salinity exhibited higher peaks that coincided with increasing deep PGD EFW and deep GW stage, following lows in seasonal deep PGD EFW and deep GW stage (Figure 40, Figure 41). The highest salinity observed in the deeper well was 32.30 psu and the highest salinity observed in the shallower well was 29.27 psu (Figure 42, Table 9). Salinity in the shallower GW well at TS6 was always lower than that of TS6's deeper GW well by a mean of 3.53 psu, with the exception of a 6-day period during the dry season of 2011, from January 23 (Figure 42). During that brief period, salinity in TS6's shallower well was higher by a mean of 0.11 psu than in TS6's deeper well (Figure 42). Salinity differences between the deeper and shallower wells ranged from 0.15

psu to -18.56 psu, with negative values indicative of higher salinities in the deeper well than in the shallower well (Figure 42, Table 9).

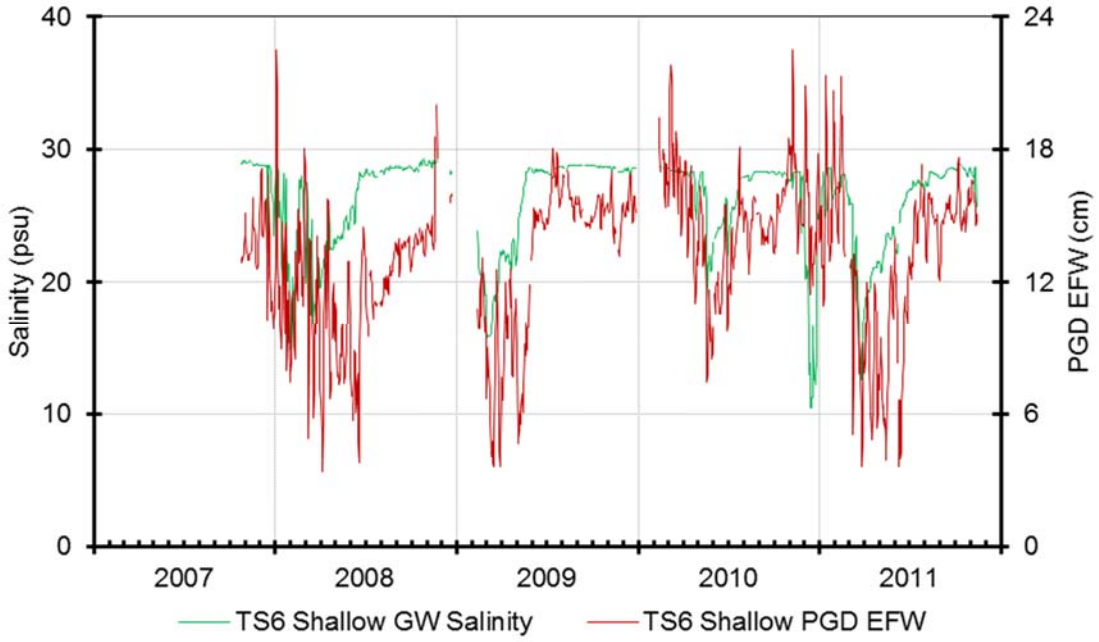

Figure 38: Daily density corrected shallow groundwater discharge potential (PGD EFW) and shallow groundwater (GW) salinity over time at TS6.

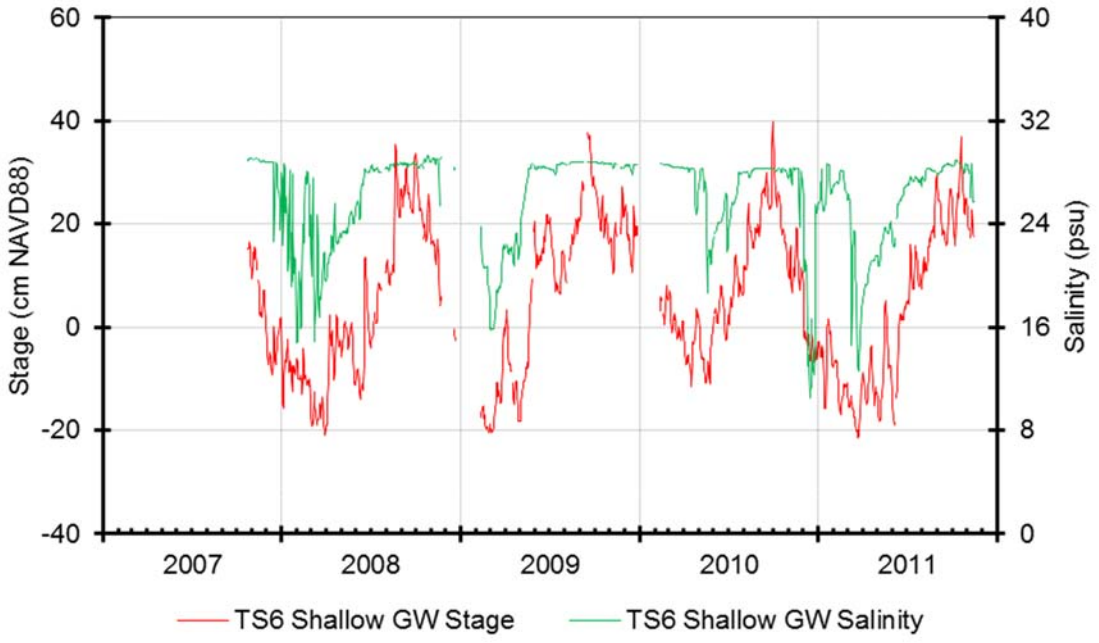

Figure 39: Daily salinity and stage of shallow groundwater (GW) over time at TS6.

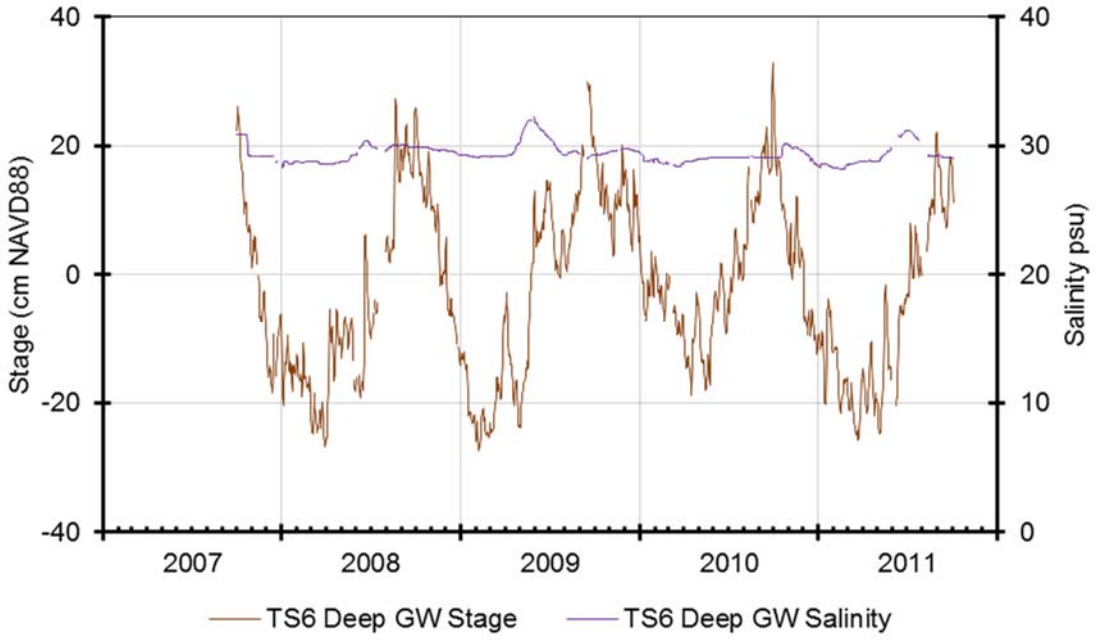

Figure 40: Daily salinity and stage of deep groundwater (GW) over time at TS6.

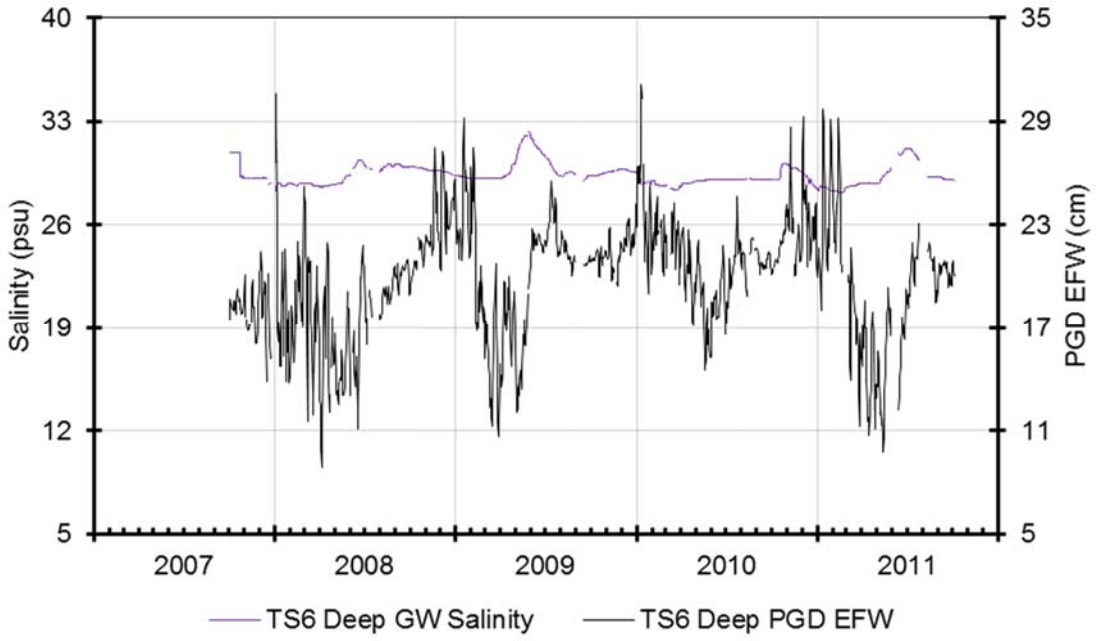

Figure 41: Daily density corrected deep groundwater discharge potential (PGD EFW) and deep groundwater (GW) salinity over time at TS6.

Table 9: Daily mean, minimum, maximum, and number of observations for surface water (SW) and groundwater (GW) stage.

Salinity (psu)	Mean	Minimum	Maximum	# of Observations
TS6 SW	11.46	0.40	44.47	1468
TS6 Shallow GW	25.97	10.47	29.27	1322
TS6 Deep GW	29.39	28.20	32.30	1357
TS6 Deep GW – Shallow GW	-3.53	-18.56	0.15	1208
TS3Shallow GW	4.45	3.20	6.20	2598
TS3 Deep GW	13.63	12.78	14.10	1328
TS3 Deep GW – Shallow GW	9.39	8.02	10.30	1316

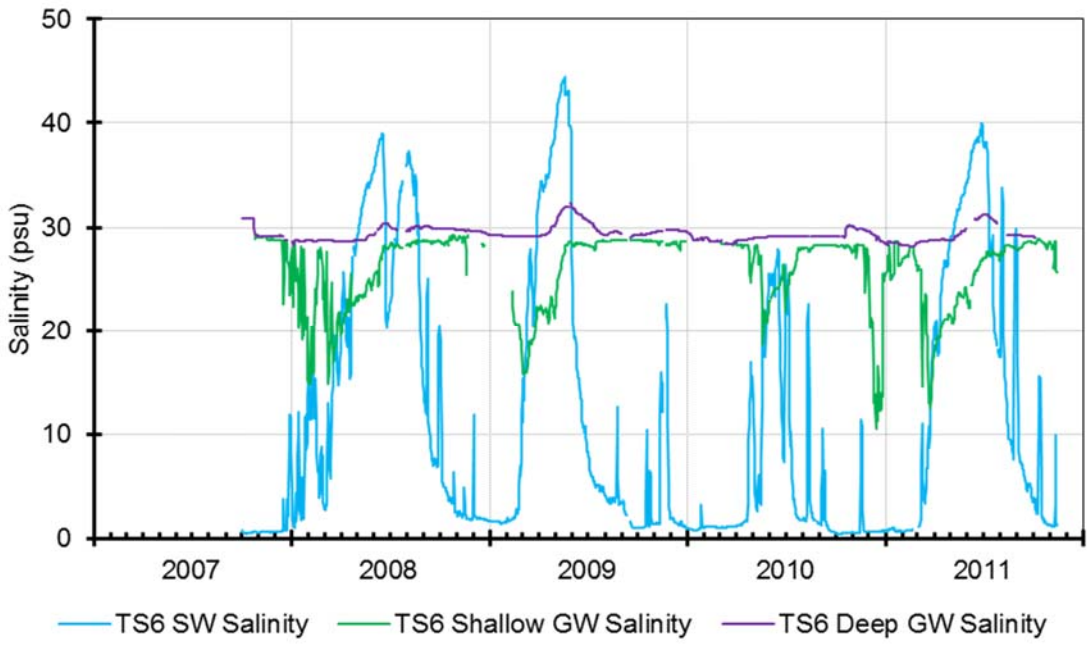

Figure 42: Daily salinity of deep groundwater (GW), shallow GW, and surface water (SW) over time at TS6.

Salinity gradually increased over time at TS3 in both shallow GW and deep GW (Figure 43, Figure 44, Figure 45, Figure 46). Neither of the PGD EFW series at TS3 were related to their corresponding shallow and deep salinity measurements (Figure 43, Figure 44). Strong seasonality occured in TS3's shallow GW salinity, with salinity generally varying inversely with local water levels, albeit with a lagged response (Figure 47, Figure 48). With lags considered, TS3 shallow GW correlated much better to TS3 shallow GW salinity with a 40 or 41 day lag than without a lag (Figure 47, Figure 48). At TS3, deep GW stage and deep GW salinity did not correlate well at any lag time (Figure 49). Deep GW salinity was always higher than shallow GW

salinity at TS3, but TS3's deeper GW had a smaller salinity range than TS3's shallow GW did (Figure 43, Figure 44).

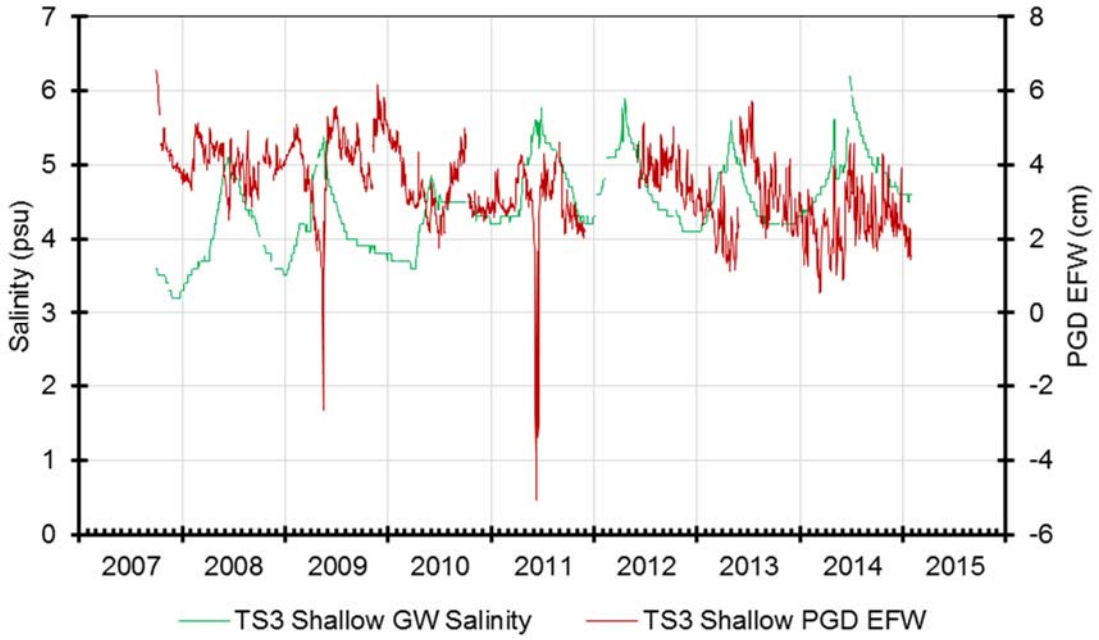

Figure 43: Daily shallow density corrected groundwater discharge potential (PGD EFW) and shallow GW salinity over time at TS3.

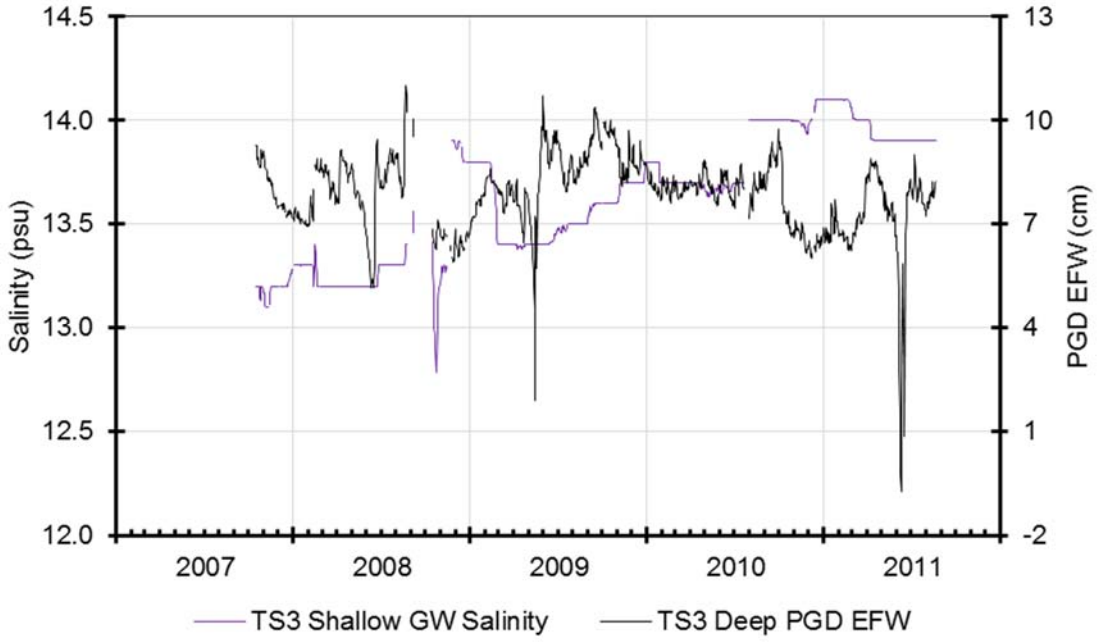

Figure 44: Daily deep density corrected groundwater discharge potential (PGD EFW) and deep groundwater (GW) salinity over time at TS3.

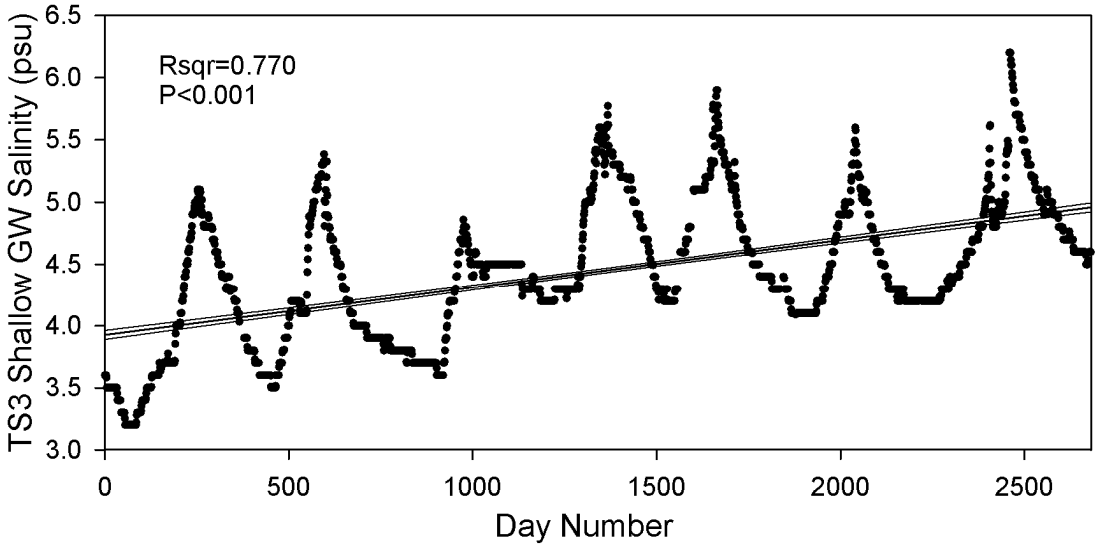

Figure 45: Linear regression between daily shallow groundwater (GW) salinity at TS3 and day number over time. 95% confidence interval shown.

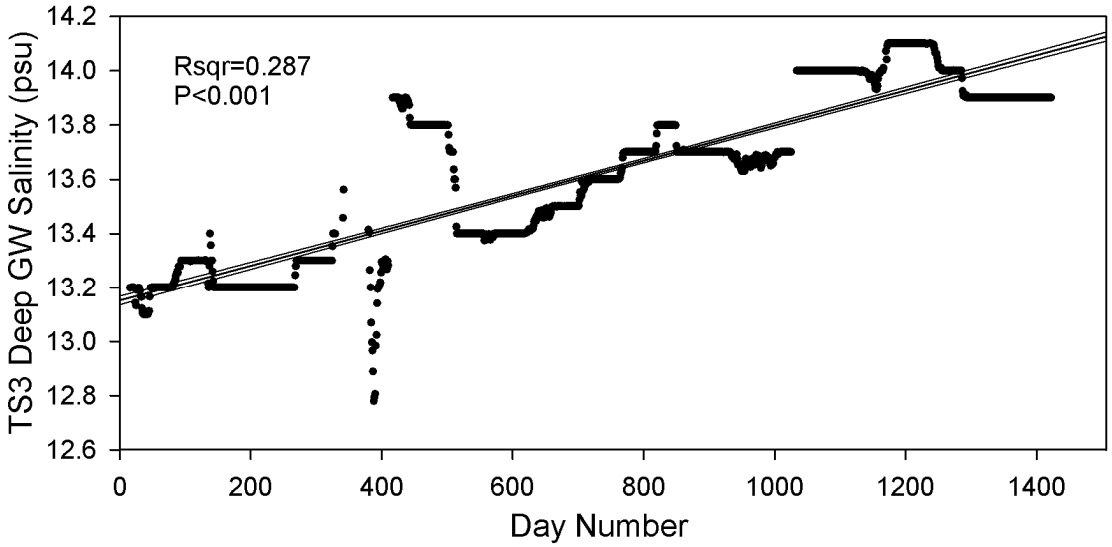

Figure 46: Linear regression between daily deep groundwater (GW) salinity at TS3 and day number over time. 95% confidence interval shown.

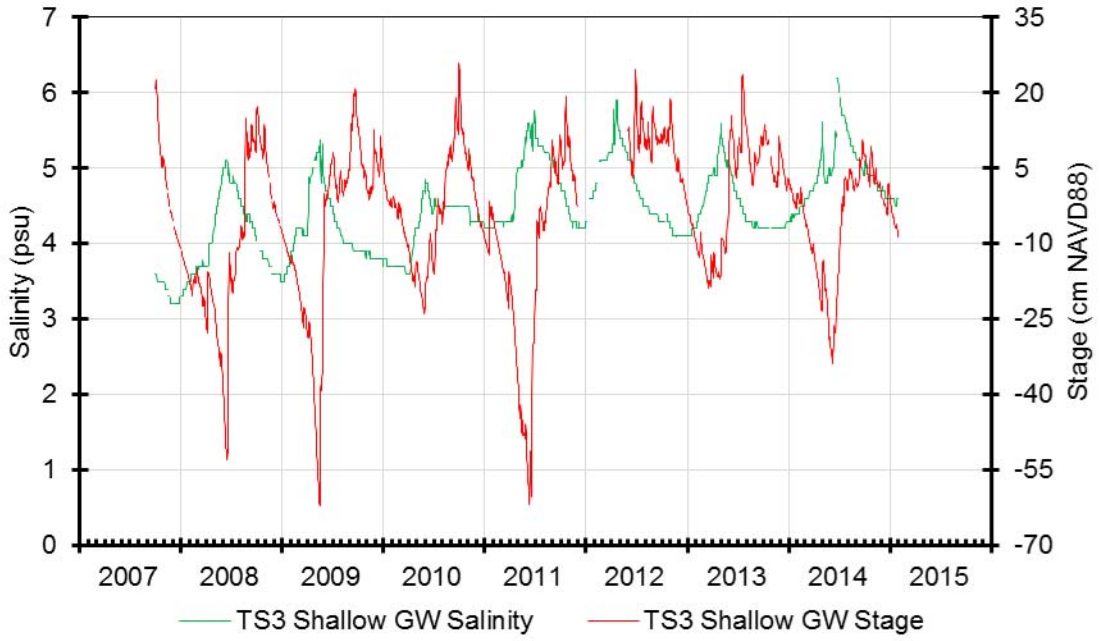

Figure 47: Daily salinity and stage of shallow groundwater (GW) over time at TS3.

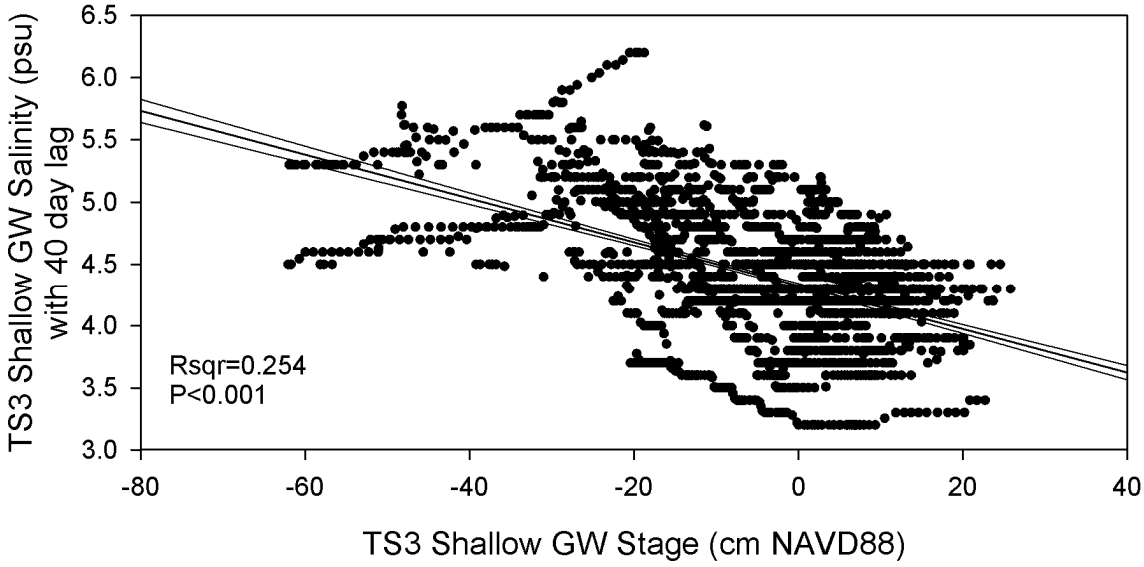

Figure 48: Linear regression between daily shallow groundwater (GW) stage and shallow GW salinity over time at TS3, with salinity lagged backwards by 40 days. 95% confidence intervals shown.

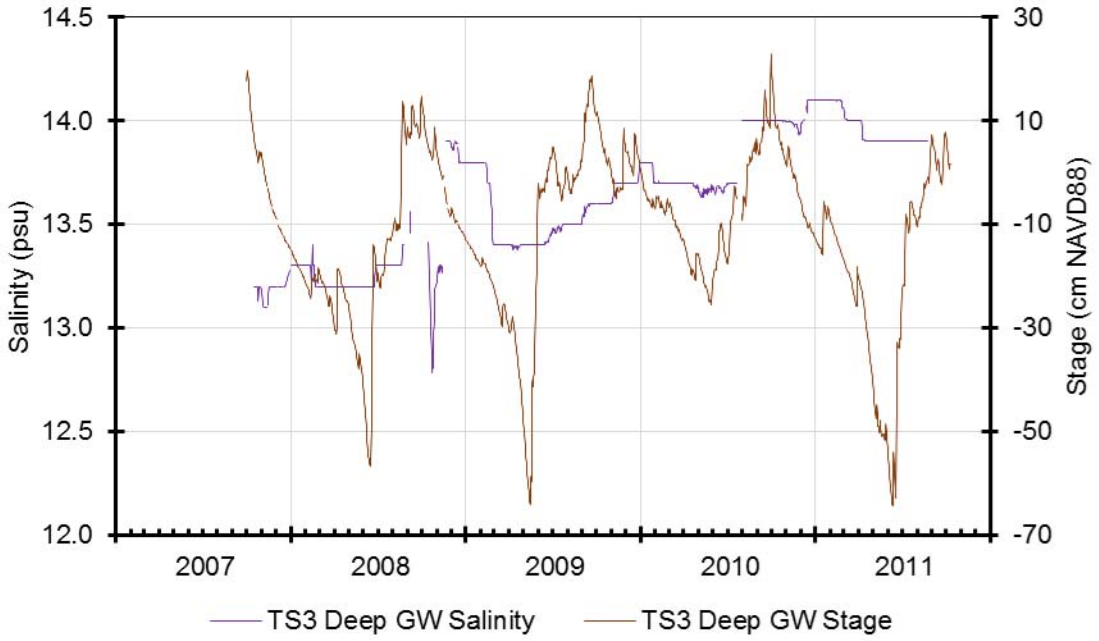

Figure 49: Daily salinity and stage of deep groundwater (GW) over time at TS3.

Salinity of SW at TS6 had a greater range and greater variability than both deep and shallow GW salinities at TS6 (Figure 50, Table 9). Seasonal lows and highs at TS6 in SW salinity exceeded those of both GW well's salinity each year, with the exception of SW salinity failing to exceed the salinity of deep GW in 2010 (Figure 50). Broad peaks in SW salinity are seasonally recurrent and coincide with dry season SW flow reversals at TS6 (Figure 50). The SW repeatedly underwent sudden peaks in salinity that were much higher than the preceding and suceeding measurements (Figure 50). Many of these brief peaks lasted for only a few days or less and are coincident with flow reversals recorded in TS6 SW discharge (Figure 50). Salinity of SW at TS6 had a strong, negative relationship with TS6 SW discharge (Figure 50, Figure 51). At TS6, the relationship between SW salinity and SW discharge is not deterministic when salinity is near zero, but showed much more linearity when discharge approached zero and reversed, coincident with increases in SW salinity (Figure 51). Lower shallow GW salinities occurred when SW discharge was reversed (Figure 50). During the initial few months of shallow GW freshening, SW salinity was often higher than shallow GW salinity each year (Figure 50). As SW salinity increased each year, coincident with TS6 SW flow reversal, shallow GW salinity remained at a lower salinity than

the overlying SW, making shallow GW salinity the freshest of the three TS6 salinity measurements during the later portions of the TS6 SW flow reversal periods (Figure 50). The peaks in deep TS6 GW salinity occur approximately one to two months after the peaks in TS6 SW salinity and SW flow reversal (Figure 50).

Seasonal peaks in shallow GW salinity at TS3 occur at or close to the end of each zero-flow period in upstream (TSB) SW discharge (Figure 52). Seasonal lows in TS3 shallow GW salinity are reached 7 of the 8 dry seasons, near the end of the seasonal upstream SW flow period (Figure 52). The seasonal low in shallow GW salinity was perturbed to the middle of the no-flow period in 2010, the exception to the other 7 dry seasons (Figure 52). No relationsip with deep GW salinity at TS3 was observed (Figure 52).

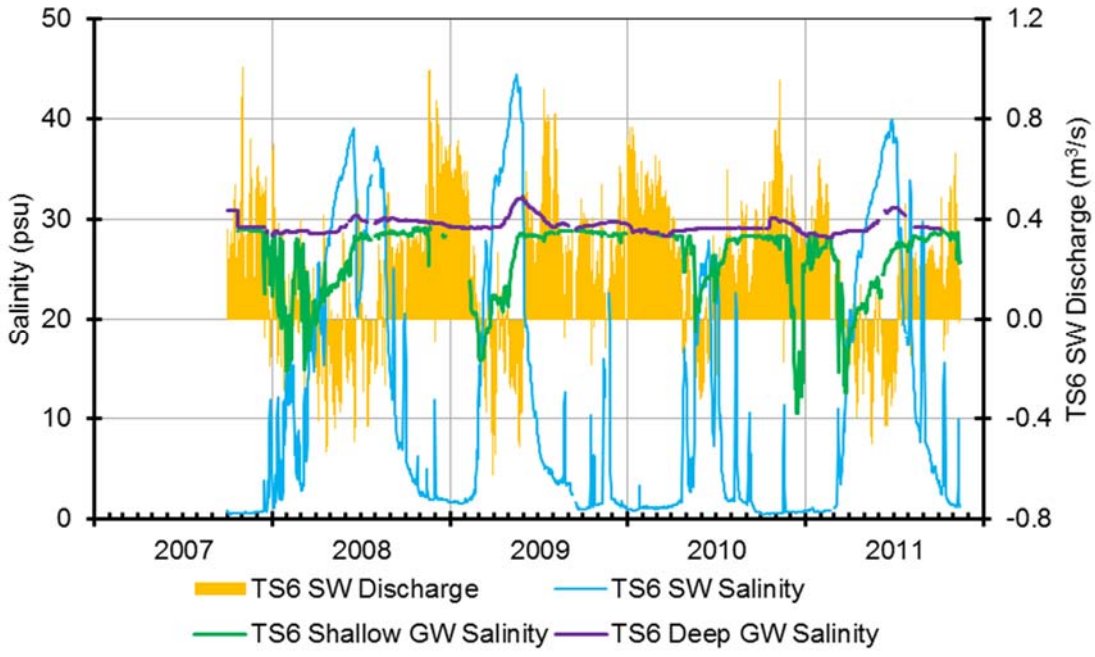

Figure 50: Daily surface water (SW) discharge and salinity of deep groundwater (GW), shallow GW, and SW over time at TS6.

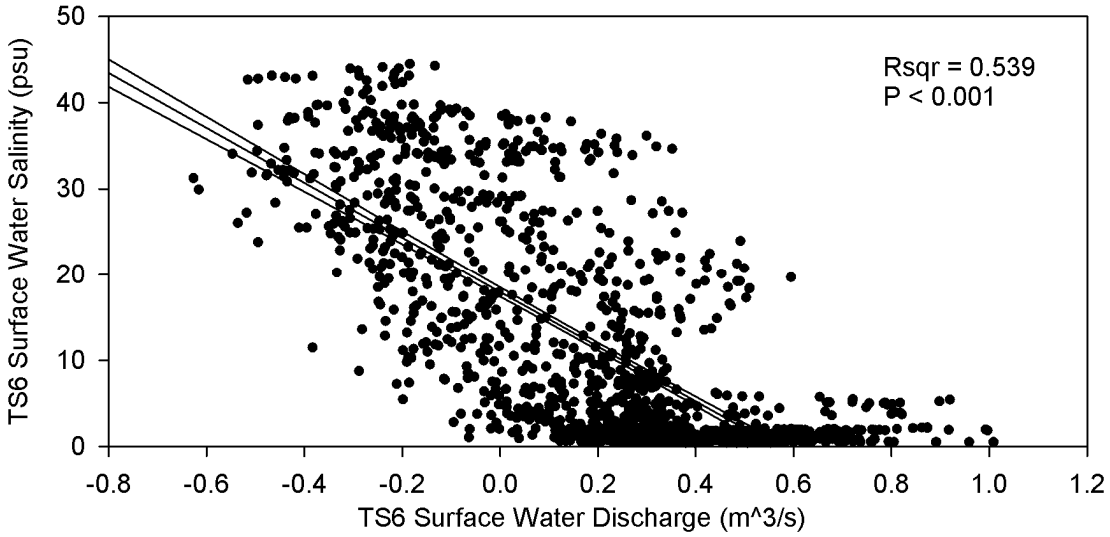

Figure 51: Linear regression with daily surface water discharge and surface water salinity over time at TS6. 95% confidence interval shown.

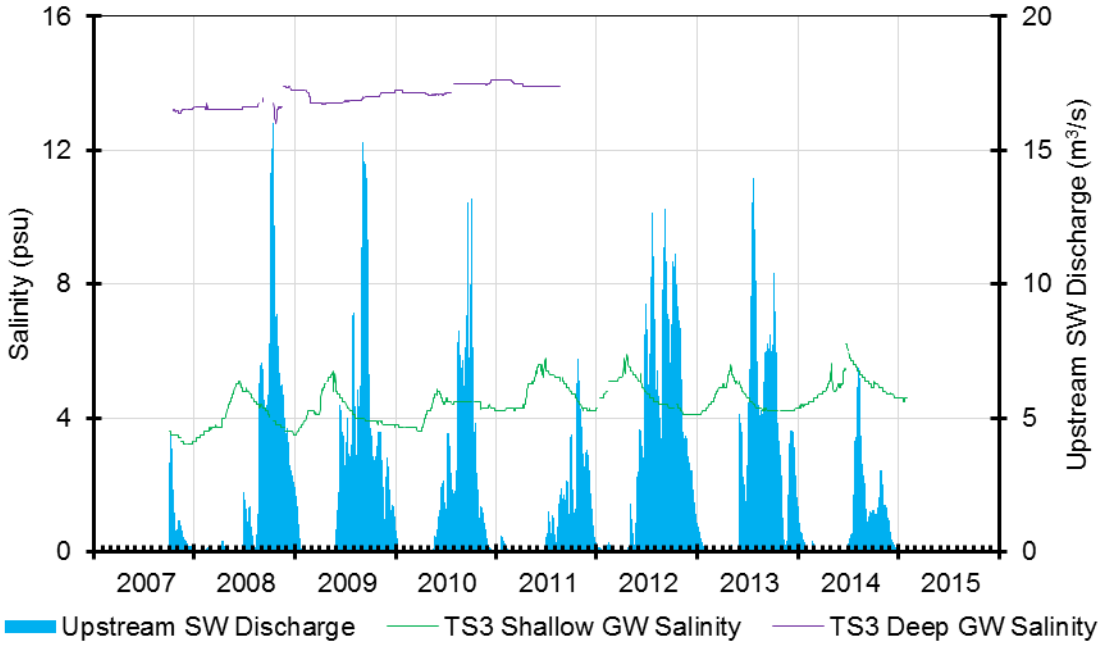

Figure 52: Daily upstream surface water (SW) discharge and salinity of shallow and deep groundwater (GW) over time at TS3.

The SW Ca/Cl ratio at TS6 and TS3 were regressed against each other, yielding a significant, but weak relationship between the two (R^2=0.152, P=0.015). Accordingly, Ca/Cl ratios in the two site's SW tended to increase and decrease at similar times (Figure 53). In SW at TS3,

Ca/Cl ratios were always higher than in SW at TS6, by a factor of at least 5.5 and up to 45.2 (Figure 53). At TS6, Ca/Cl ratios in SW did not have a consistent relationship with stages of SW or GW at TS6, with lows and highs in Ca/Cl ratios occurring both before and after lows and highs in the water stages. At TS6, SW Ca/Cl ratios had significant and positive relationships with both shallow and deep TS6 PGD EFW (Figure 54, Figure 55, Figure 56). Flow of SW at TS6 also had a significant and positive relationship with TS6 SW Ca/Cl ratios (Figure 57, Figure 58). The lowest Ca/Cl ratios occurred at times of TS6 SW flow reversal during each of the three years containing Ca/Cl ratio data that coincided with each flow reversal (Figure 57). The Ca/Cl ratios in SW at TS6 did not have a consistent relationship with either local or basinwide rainfall.

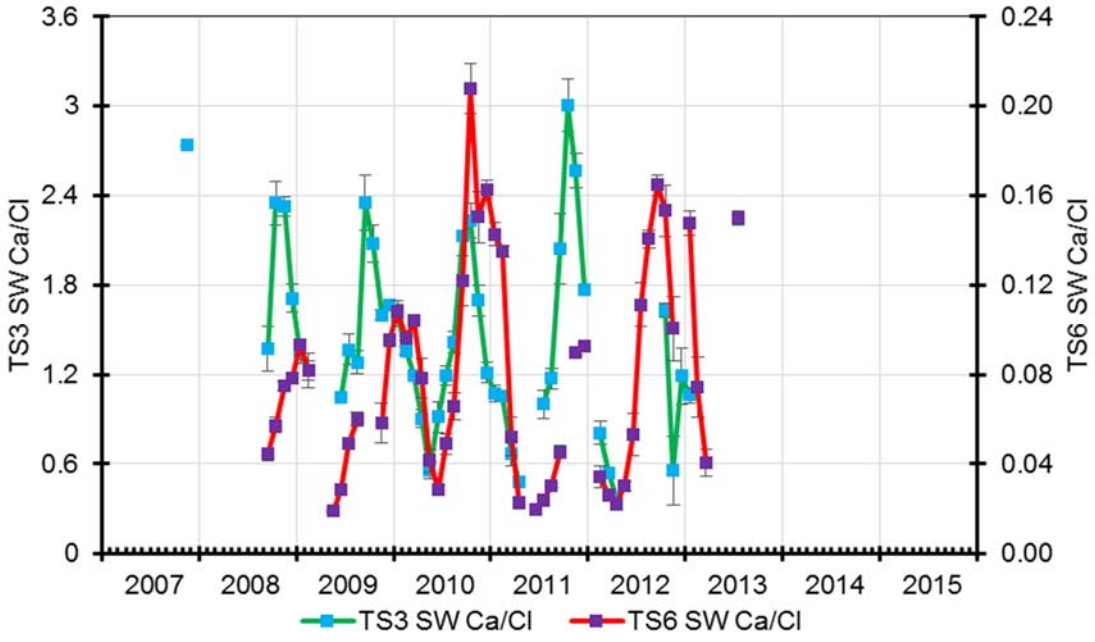

Figure 53: Monthly mean surface water (SW) Ca/Cl ratio at TS6 and TS3 over time with standard errors.

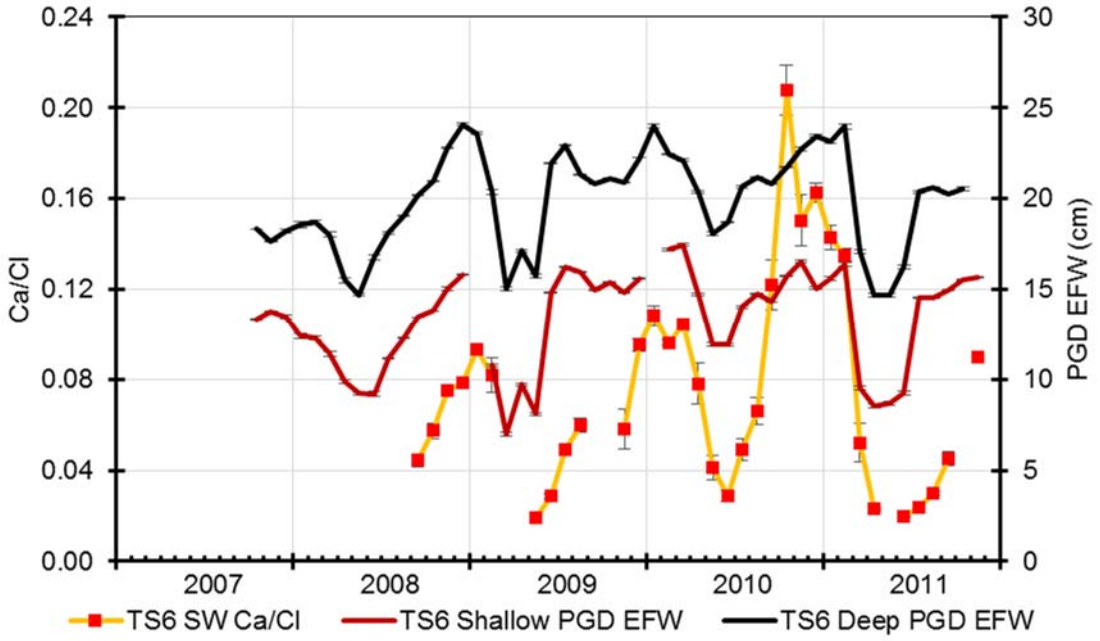

Figure 54: Monthly mean density corrected groundwater discharge potential (PGD EFW) and surface water (SW) Ca/Cl ratio over time at TS6 with standard errors.

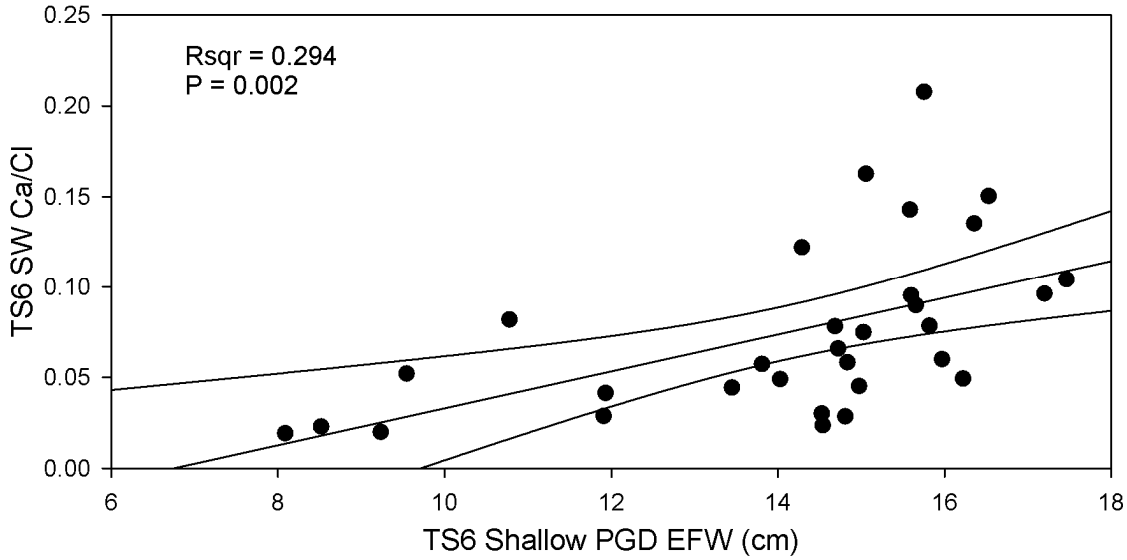

Figure 55: Linear regression with monthly mean density corrected shallow groundwater discharge potential (PGD EFW) and surface water (SW) Ca/Cl ratio over time at TS6. 95% confidence interval shown.

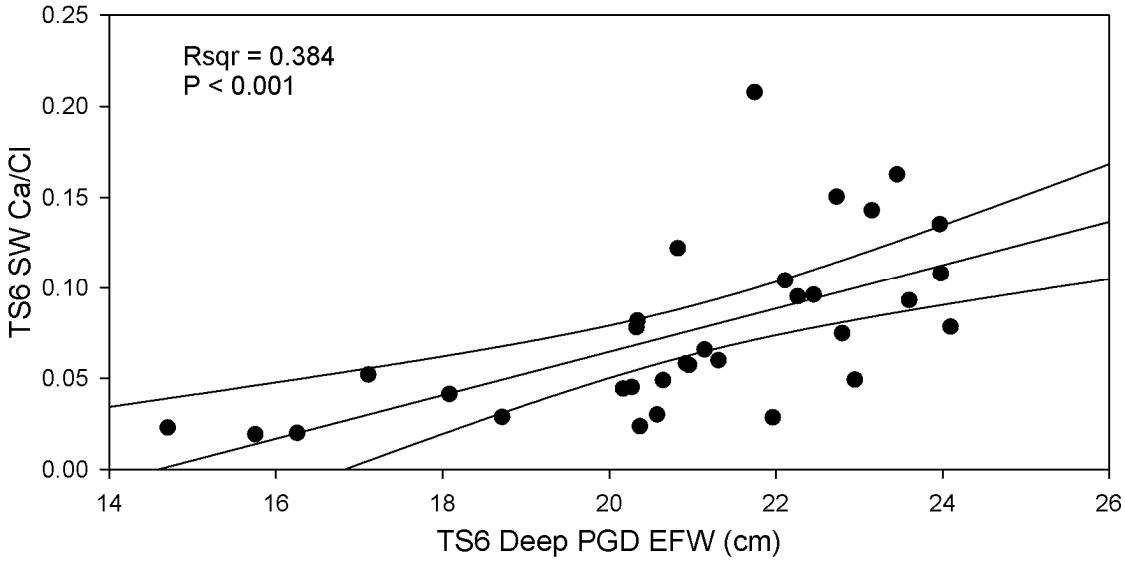

Figure 56: Linear regression with monthly mean density corrected deep groundwater discharge potential (PGD EFW) and surface water (SW) Ca/Cl ratio over time at TS6. 95% confidence interval shown.

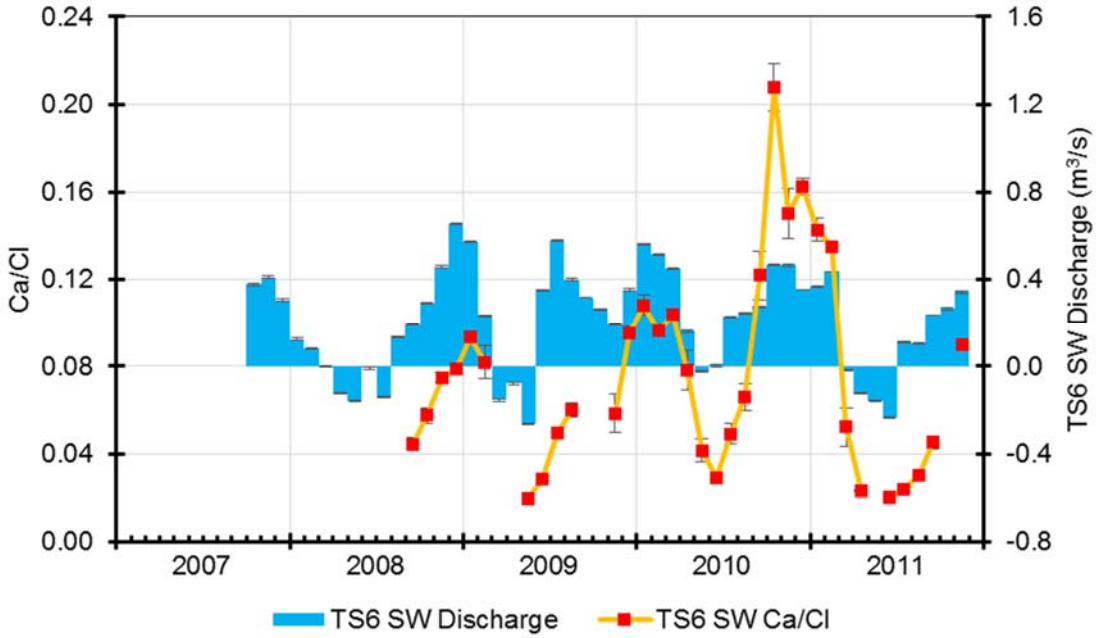

Figure 57: Monthly mean surface water (SW) discharge and SW Ca/Cl ratio over time at TS6 with standard errors.

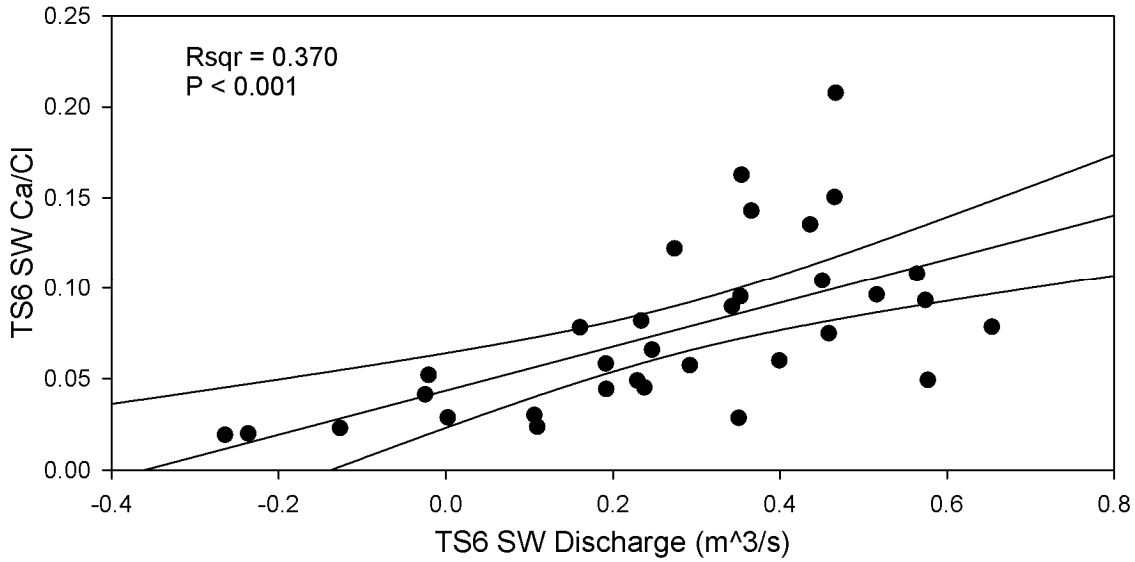

Figure 58: Linear regression with monthly mean surface water (SW) discharge and SW Ca/Cl ratio over time at TS6. 95% confidence interval shown.

Significant, positive relationships existed between SW Ca/Cl ratios and each of the SW and GW stages at TS3 (Figure 59, Figure 60, Figure 61, Figure 62). Neither shallow PGD EFW, nor deep PGD EFW exhibited a significant linear relationship with SW Ca/Cl ratios at TS3 (Shallow: R^2=0.015, P=0.456; Deep: R^2<0.001, P=0.884). Upstream SW discharge had a significant and positive relationship with SW Ca/Cl ratios at TS3 (R^2=0.270, P<0.001), but this relationship was much weaker than the relationships between TS3 SW Ca/Cl ratio and TS3 GW and SW stages (Figure 60, Figure 61, Figure 62, Figure 63).

Neither basinwide rainfall, nor TS3 rainfall exhibited a significant linear relationship with Ca/Cl ratios in TS3 SW (Basinwide rain: R^2=0.00791, P=0.606; TS3 rain: R^2=0.0185, P=0.384). Seasonal peaks in TS3 SW Ca/Cl ratios lagged behind those of both local and basinwide rainfall by 0-1 months (Figure 64, Figure 65). The overall trends of rainfall at both TS3 as well as that of basinwide rainfall were similar to that of TS3 SW Ca/Cl ratios (Figure 64, Figure 65).

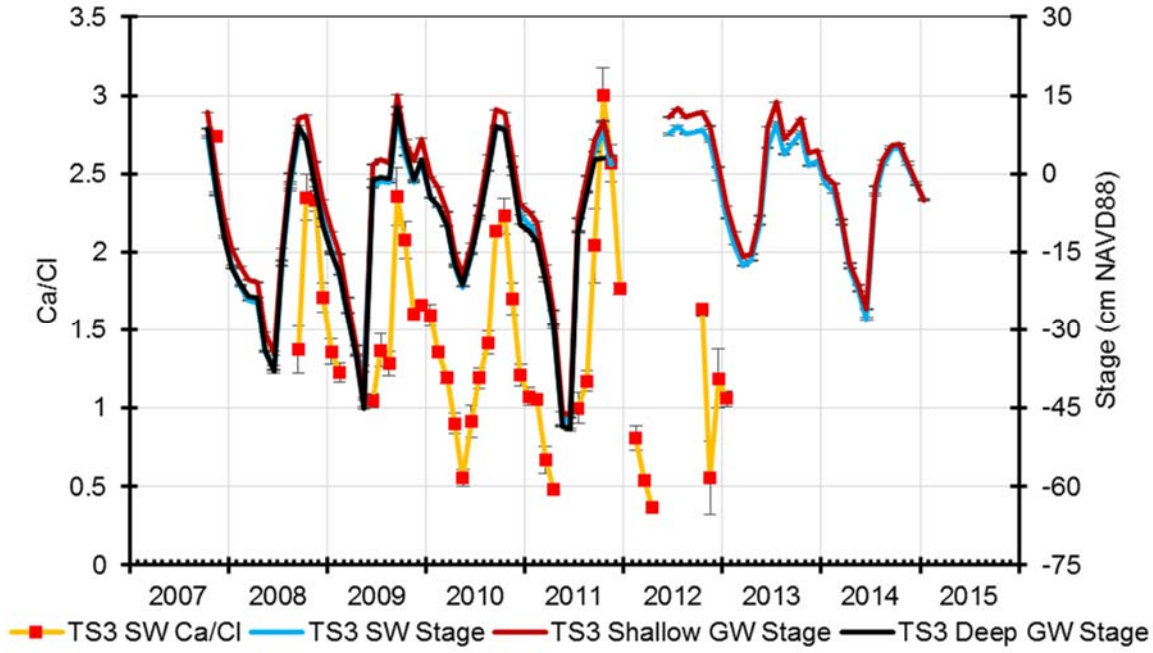

Figure 59: Monthly mean surface water (SW) stage, groundwater (GW) stages, and SW Ca/Cl ratio over time at TS3 with standard errors.

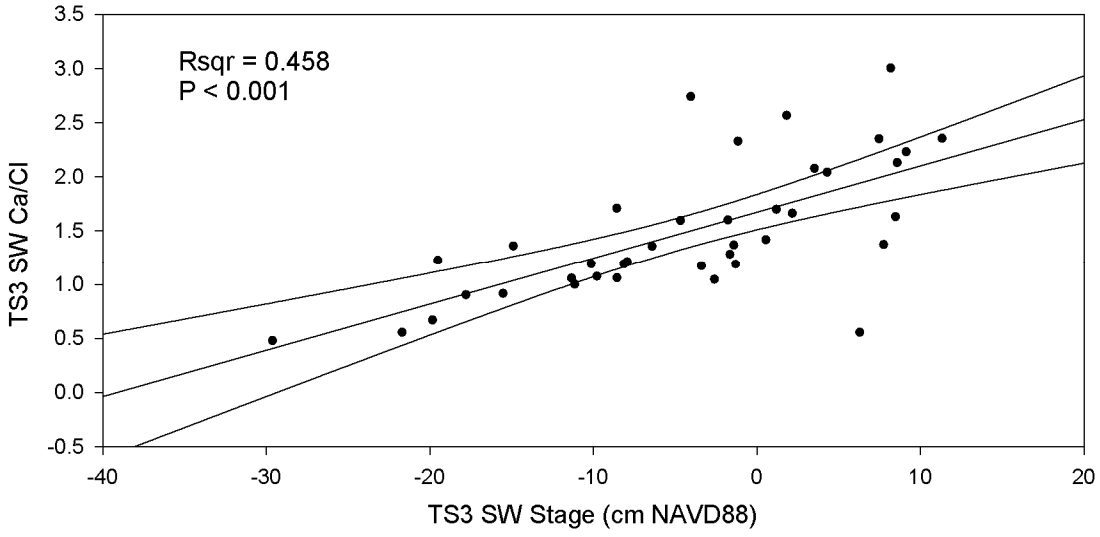

Figure 60: Linear regression with monthly mean surface water (SW) stage and SW Ca/Cl ratio over time at TS3. 95% confidence interval shown.

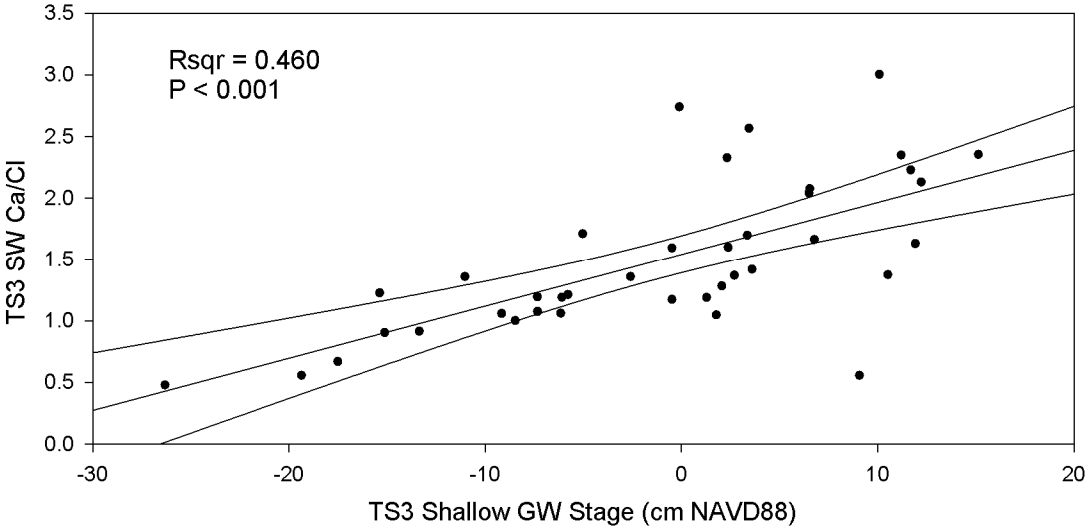

Figure 61: Linear regression with monthly mean shallow groundwater (GW) stage and surface water (SW) Ca/Cl ratio over time at TS3. 95% confidence interval shown.

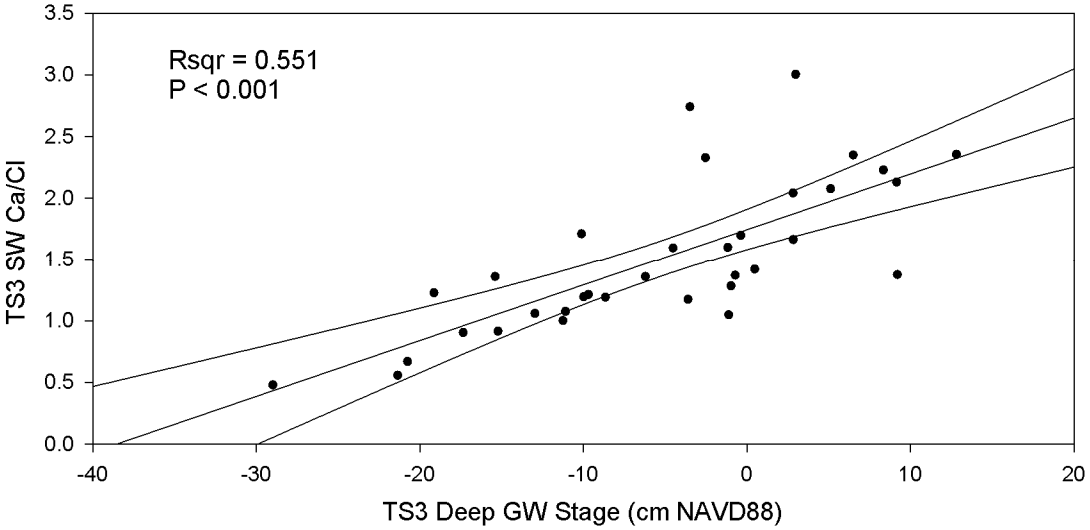

Figure 62: Linear regression with monthly mean deep groundwater (GW) stage and surface water (SW) Ca/Cl ratio over time at TS3. 95% confidence interval shown.

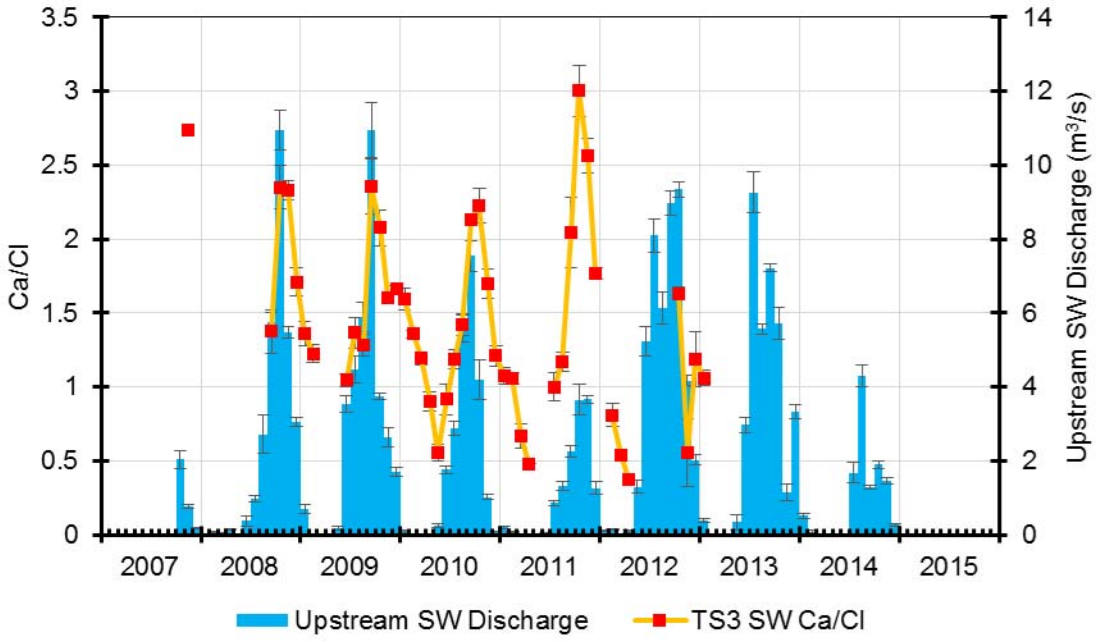

Figure 63: Monthly mean upstream surface water (SW) discharge and SW Ca/Cl ratio over time at TS3 with standard errors.

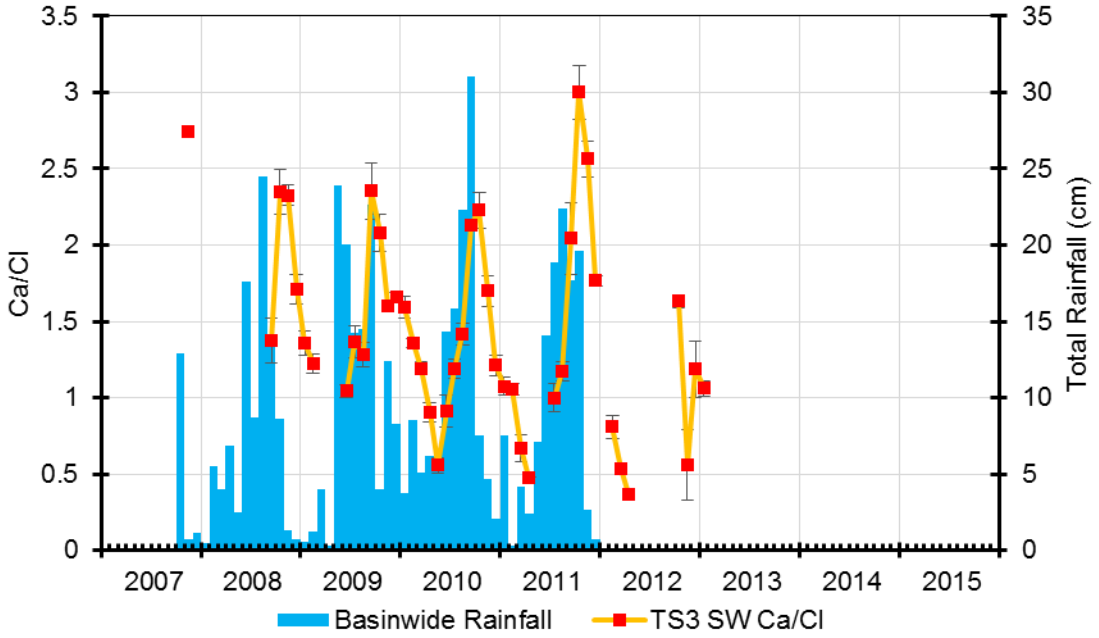

Figure 64: Monthly mean basinwide rainfall and surface water (SW) Ca/Cl ratio over time at TS3 with standard errors. Standard errors are not available for basinwide rainfall.

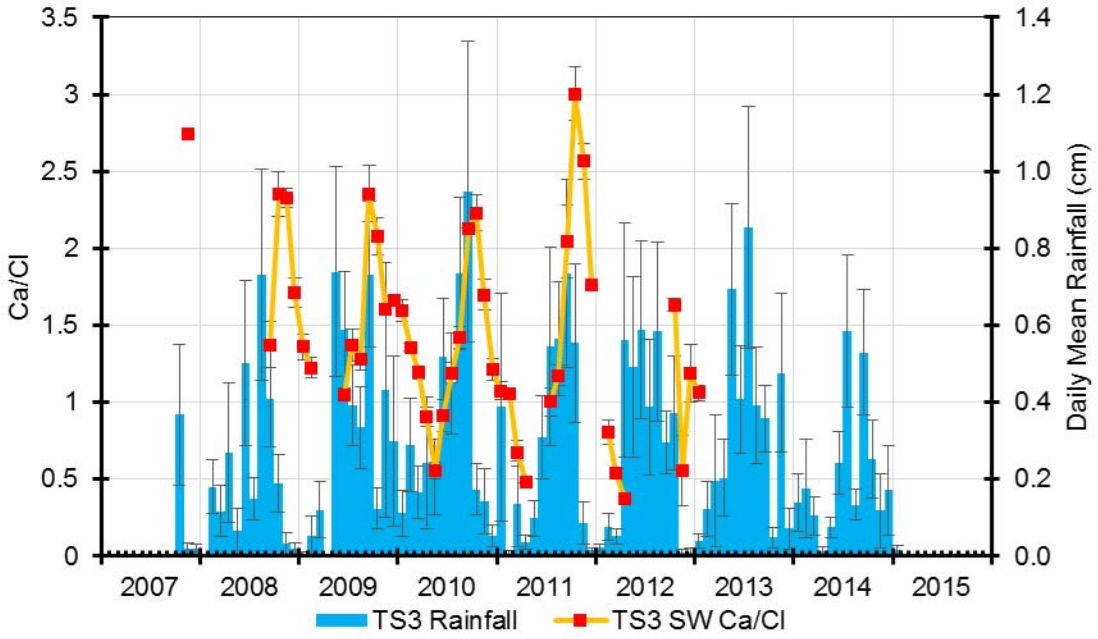

Figure 65: Monthly mean rainfall and surface water (SW) Ca/Cl ratio over time at TS3 with standard errors.

The monthly mean autosampler Ca/Cl ratios of TS6 SW dropped to the mean Ca/Cl ratio of Florida Bay (TS-Bay S) and approached those of upstream waters (TSB SW) throughout the study period (Figure 66). When increased SW discharge at TS6 occurred, Ca/Cl ratio in TS6 SW approached the upstream water Ca/Cl ratios (Figure 66). When SW flow reversals occurred at TS6, TS6 SW Ca/Cl ratios reached seasonal lows for each of the 5 years of dry season Ca/Cl ratio data, approaching the TS-Bay S Ca/Cl ratios (Figure 66). The seasonal peaks in TS6 SW Ca/Cl ratio always lagged behind upstream SW discharge peaks by 1-3 months, with seasonal Ca/Cl ratio lows occurring close to the seasonal inception of upstream SW flows (Figure 66).

The Ca/Cl ratios in TS3 SW ranged around the means of upstream SW (TSB SW) (Figure 67). Lows in Ca/Cl ratios in TS3 SW approached downstream SW (TS-Bay S), but never reached the lower values (Figure 67). Seasonal highs in TS3 SW Ca/Cl ratios did not fluctuate greatly, remaining close to that of TSB SW (Figure 67). Seasonal lows in TS3 SW Ca/Cl ratio decreased from 2009 through 2012, but increased slightly in 2013, relative to 2012 (Figure 67). Seasonal highs in TS3 SW Ca/Cl ratio coincided with highs in upstream SW discharge and TS3

GW and SW stages (Figure 59, Figure 67), when TS3 SW Ca/Cl ratios were most similar to the mean Ca/Cl ratio of TSB SW (Figure 67). Seasonal lows in TS3 SW Ca/Cl ratio were reached at the end of upstream SW discharge stoppages, with the exception of the low in TS3 SW Ca/Cl ratios in November 2012 (Figure 67).

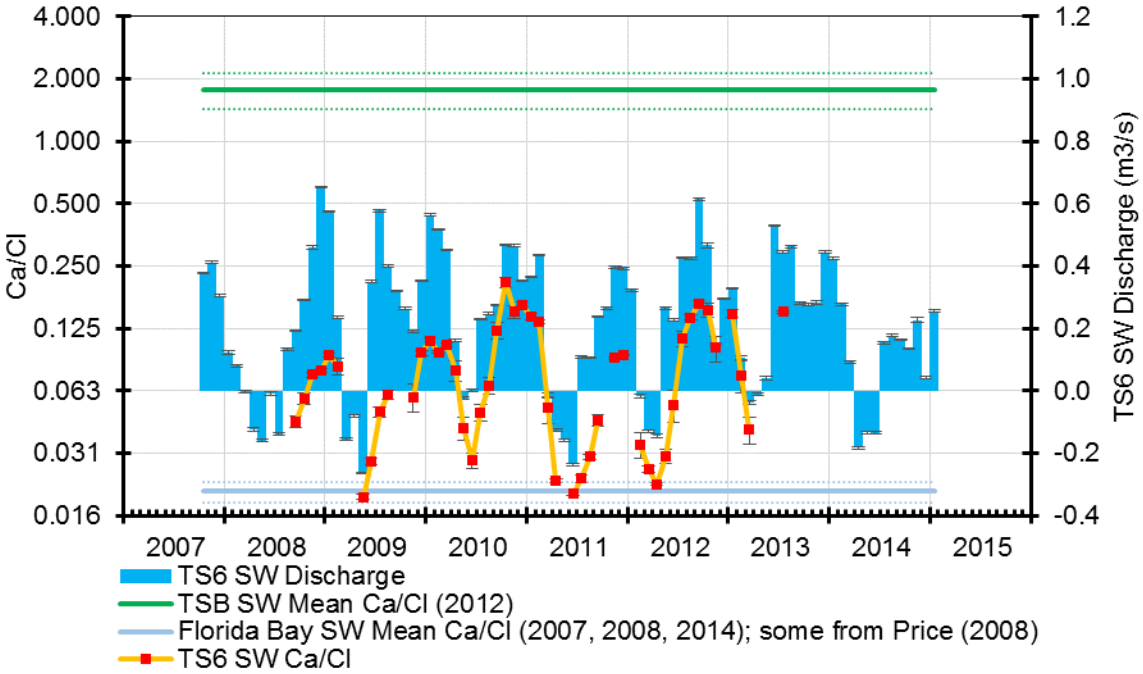

Figure 66: Surface water (SW) Ca/Cl ratio and SW discharge over time at TS6 with standard errors. Mean Ca/Cl ratios from manually collected, charge balanced samples from TSB SW and Florida Bay (TS-Bay s), with standard errors surrounding mean values.

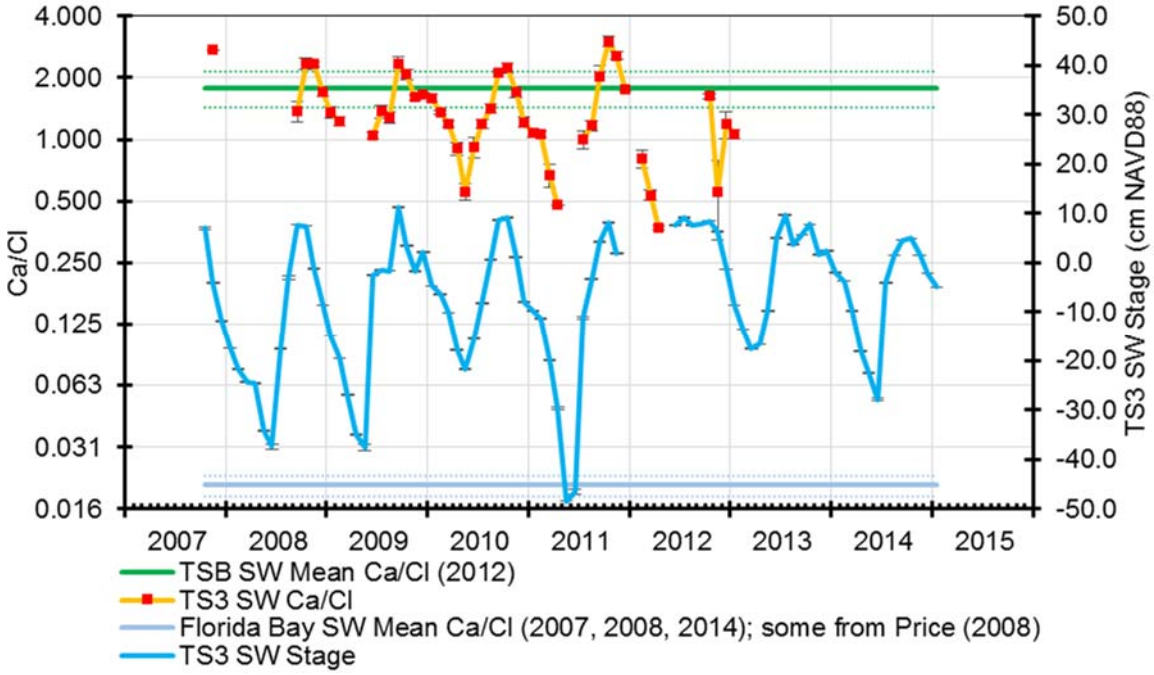

Figure 67: Surface water (SW) Ca/Cl ratio at TS3 and upstream SW discharge over time with standard errors. Mean Ca/Cl ratios from manually collected, charge balanced samples from TSB SW and Florida Bay (TS-Bay S), with standard errors surrounding mean values.

The TP concentrations in TS6 SW were mostly higher than those of TS3 SW (Figure 68). When SW TP at TS6 and TS3 were regressed against each other, a significant, but very weak linear relationship was found (R^2=0.00825, P=0.010). Peaks in TS6 SW TP decreased over the study period, whereas TS3 SW TP variability generally remained relatively constant (Figure 68).

At TS6, the first three SW TP peaks that occurred in 2008, 2009, and 2010 lagged behind water level lows by 1-2 months (Figure 69). Lower TP was generally present in TS6 SW when TS6 SW stages were higher (Figure 69). Concentrations of TP in TS6 SW had an inverse relationship with both shallow and deep TS6 PGD EFW (Figure 70, Figure 71, Figure 72). Similarly, TS6 SW TP also had an inverse relationship with TS6 SW discharge, with the highest seasonal TP concentrations occurring during the dry season, when SW flow reversal at TS6 occurs each season (Figure 73, Figure 74). An exception to this pattern occurred in October and November of 2010, when a two month spike in TS6 TP occurred (Figure 73). A consistent relationship between TS6 SW TP concentrations and rainfall at both the local and monthly scale

did not exist, though the dry season TP peaks in TS6 SW tended to precede higher wet-season rainfall by 2-3 months.

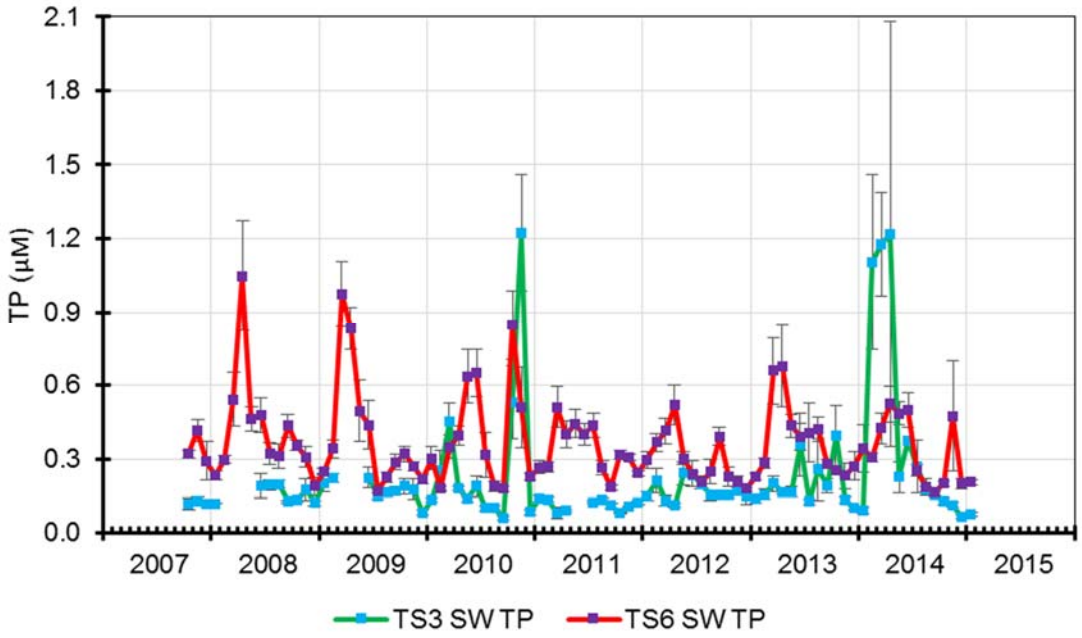

Figure 68: Monthly mean surface water (SW) total phosphorus (TP) concentration over time at TS6 and TS3 with standard errors.

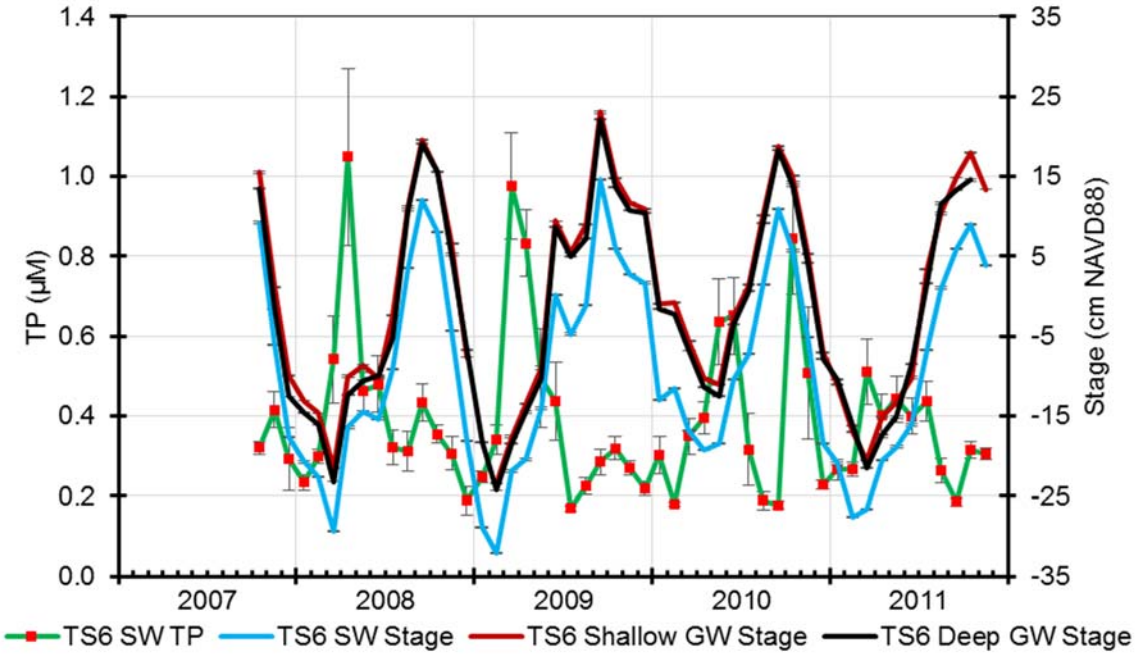

Figure 69: Monthly mean surface water (SW) stage, groundwater (GW) stages, and SW total phosphorus (TP) concentration over time at TS6 with standard errors.

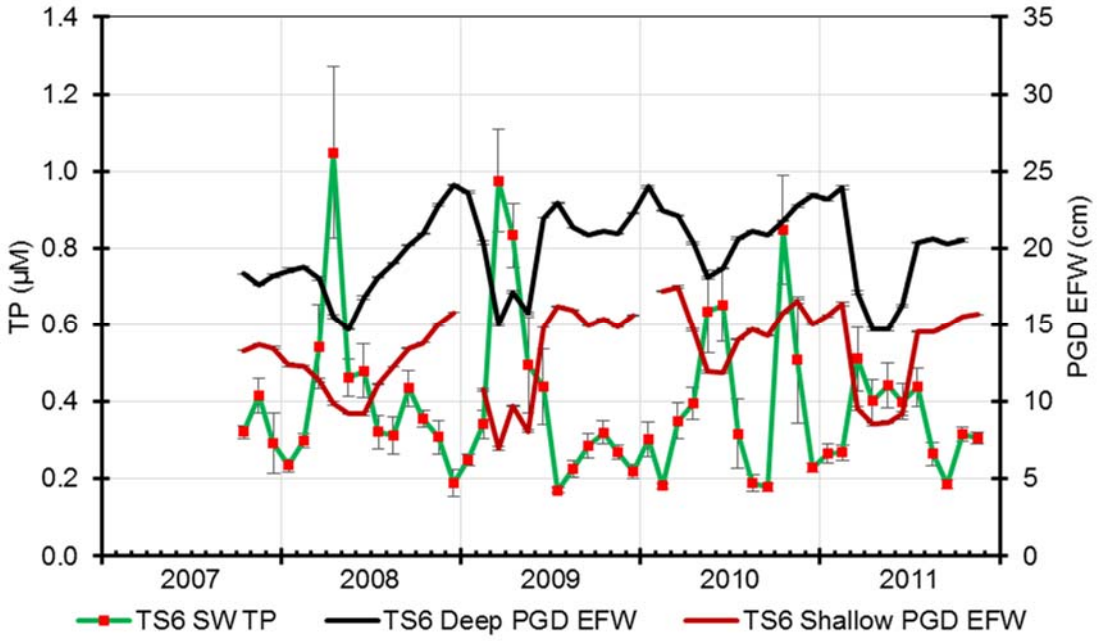

Figure 70: Monthly mean density corrected groundwater discharge potential (PGD EFW) and surface water (SW) total phosphorus (TP) concentration over time at TS6 with standard errors.

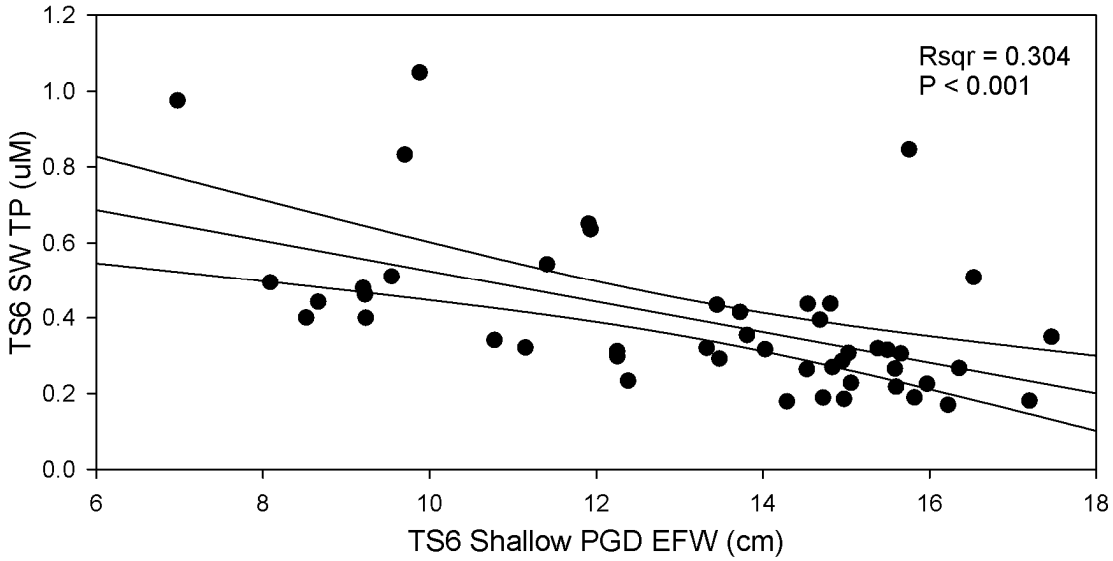

Figure 71: Linear regression with monthly mean density corrected shallow groundwater discharge potential (PGD EFW) and surface water (SW) total phosphorus (TP) concentration over time at TS6. 95% confidence interval shown.

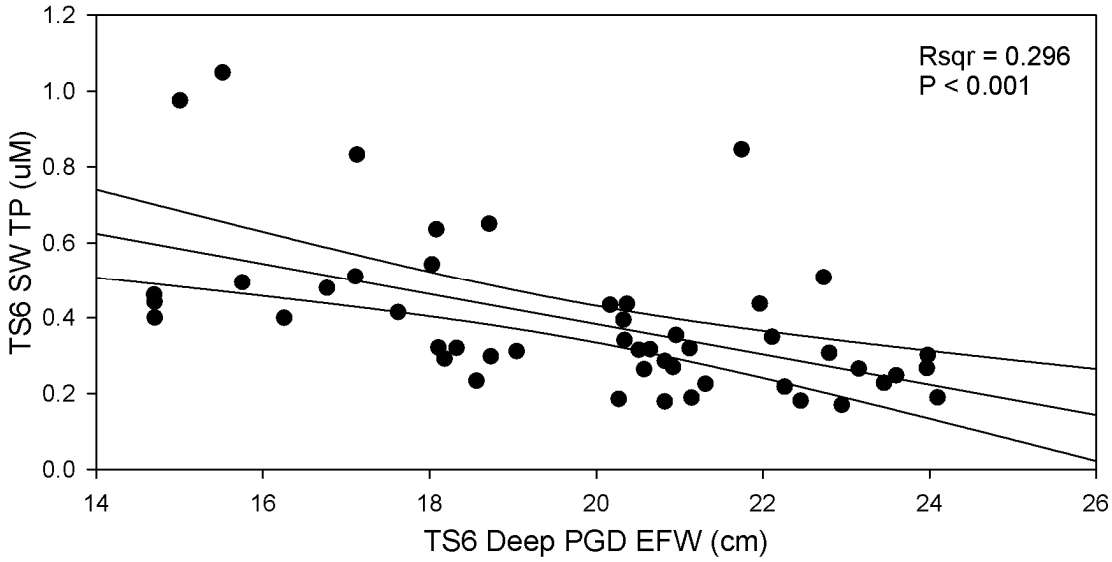

Figure 72: Linear regression with monthly mean density corrected deep groundwater discharge potential (PGD EFW) and surface water (SW) total phosphorus (TP) concentration over time at TS6. 95% confidence interval shown.

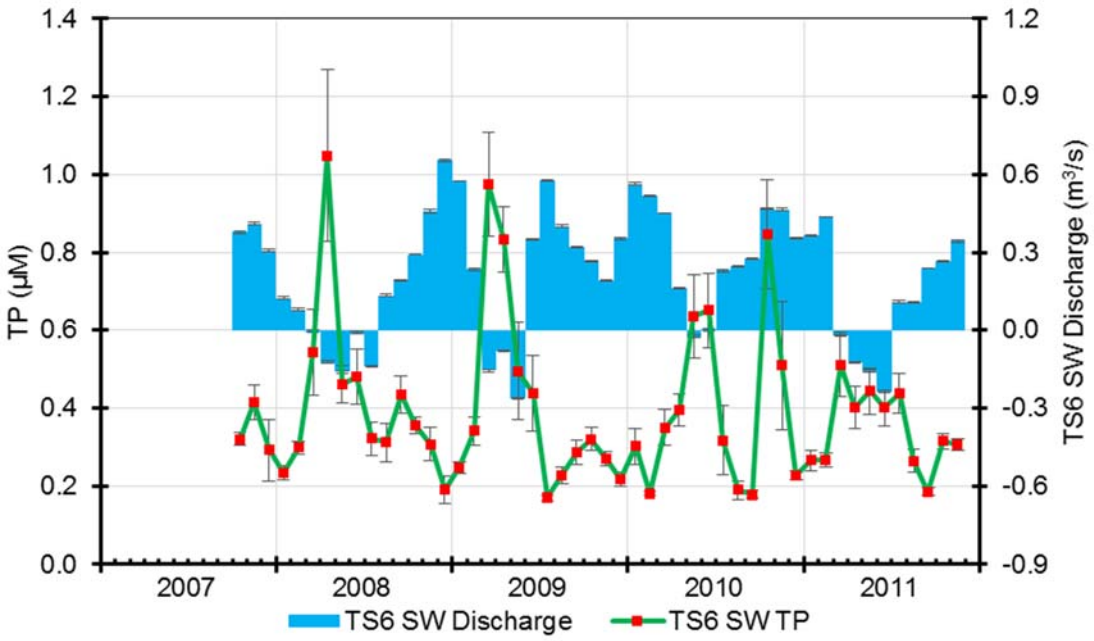

Figure 73: Monthly mean surface water (SW) discharge and SW total phosphorus (TP) concentration over time at TS6 with standard errors.

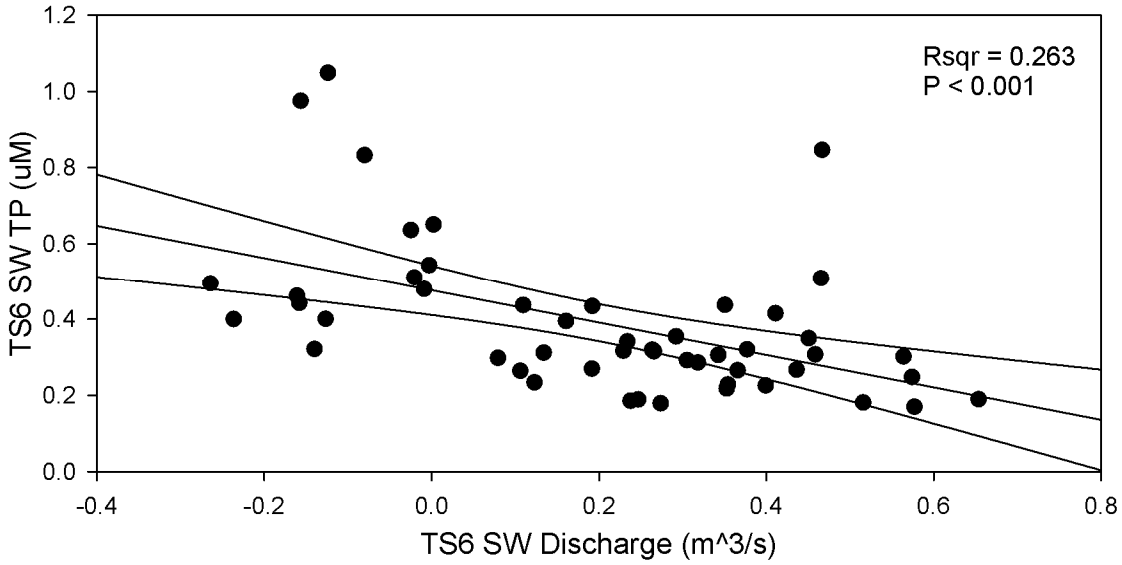

Figure 74: Linear regression with monthly mean surface water (SW) discharge and SW total phosphorus (TP) concentration over time at TS6. 95% confidence interval shown.

Water stages at TS3 varied independently of TS3 SW TP concentrations. Shallow PGD EFW at TS3 had a significant linear relationship with SW TP, but the relationship was very weak (R^2=0.0813, P=0.014). Deep PGD EFW did not have a significant linear relationship with SW TP at TS3 (R^2=0.0359, P=0.255). Upstream SW discharge also did not have a significant linear relationship with SW TP at TS3 (R^2=0.0227, P=0.185). Basinwide and local rainfall at well as local evapotranspiration varied independently of TP in TS3 SW.

The mixing model developed for TS6 SW monthly average TP concentrations demonstrated clear endmember separation between the manually collected sample averages from TSB SW, TS6 Bedrock GW, and Florida Bay SW (Figure 75). Very low TP concentrations were present in TSB SW and Florida Bay SW, in contrast to those of TS6 Bedrock GW and TS/Ph-6b Peat GW, which had elevated TP concentrations (Figure 75). Many of the autosampler monthly averages plot within the triangular mixing model bounds (Figure 75). The mean TP concentration of TS/Ph-6b Peat GW plotted almost directly on the line connecting TSB SW and TS6 Bedrock SW (Figure 75).

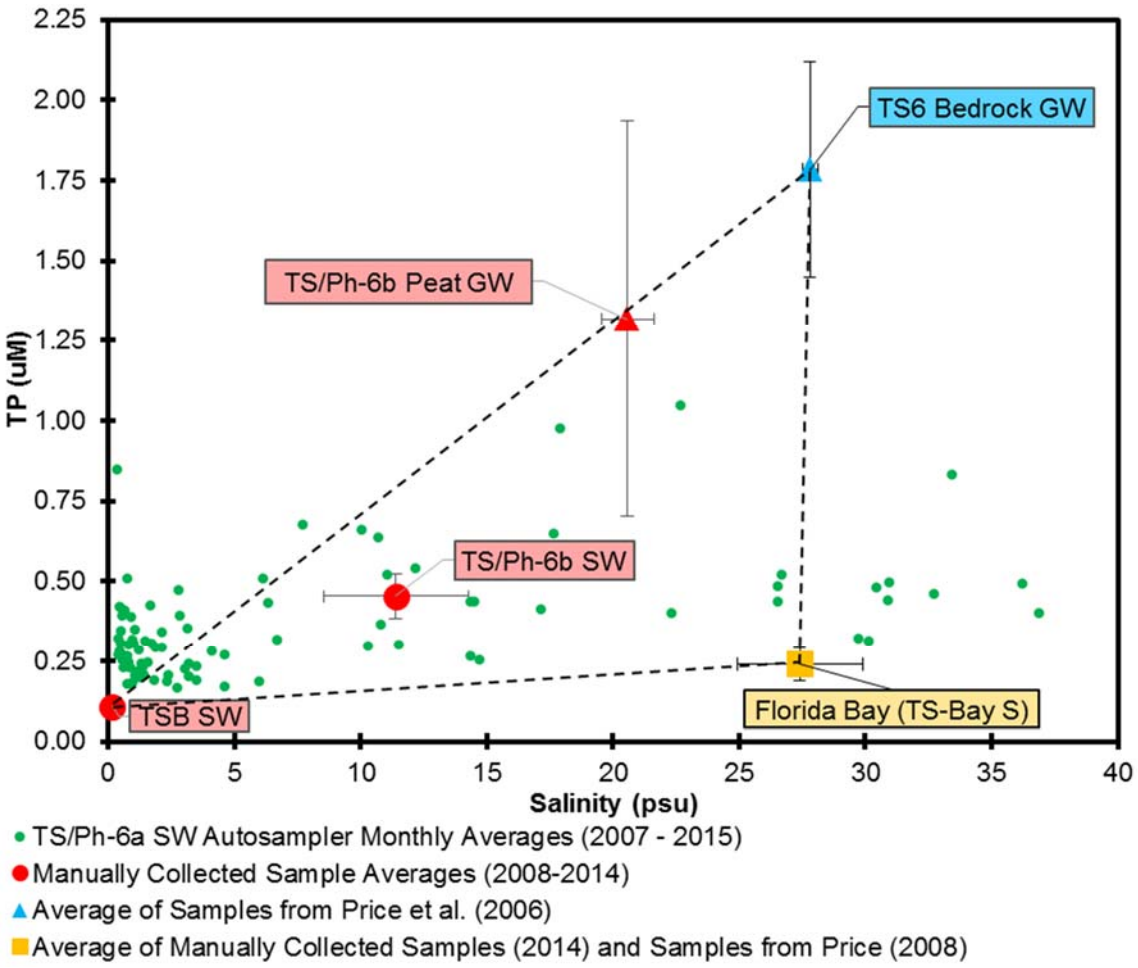

Figure 75: TP vs. salinity mixing diagram for TS/Ph-6a surface water (SW) autosampler monthly averages (smaller circles), between SW and groundwater (GW) endmembers (larger symbols).

DISCUSSION

CONTROLS OF GROUNDWATER DISCHARGE

Strong seasonality between wet and dry season water levels, SW flows, rainfall, and ET was observed at all of the sites examined in this study, similar to those of Koch et al. (2012), Kotun & Renshaw (2014), Sandoval (2013), and (Michot et al. 2011). The stages of SW upstream of the Everglades' mangrove ecotone (CP, NP72, OL, P36, TSB) varied on a daily basis more similarly to each other than to downstream and ecotone stages (TS6 SW, TS-Bay S) and with zero lag time between stages on a daily time step (Table 4). Stages of SW and GW at TS6 in the Everglades' mangrove ecotone and Florida Bay stage (TS-Bay S) also co-varied with one another (Figure 16; Figure 18; Table 4). These findings suggest that upstream water levels generally rose and fell as one population while ecotone and downstream water levels behaved similarly, but as a separate and somewhat independent, ecotone/downstream population (Table 4). Lesser similarity between SW and GW downstream at TS6 and Florida Bay as well as with upstream SW levels (CP, NP72, OL, P36) was exhibited by SW and GW at TS3, which is located at the northern boundary of the Everglades' mangrove ecotone where the mangroves begin to transition to upstream marsh and SW salinities are low (Figure 2; Table 4). These two separate groups of highly correlated and co-varying sites suggest that there is some degree of isolation between water stages of the upstream and ecotone/downstream groupings, with the intermediate location of TS3 reflecting the influences of both upstream and downstream water levels.

The method used in this project for determining PGD EFW is similar to Darcy's Law in one dimension using vertical hydraulic gradient, but does not consider hydraulic conductivity or cross-sectional area (Brodie et al. 2007; Darcy 1856; Kalbus et al. 2006; Winter et al. 1998; Zapata-Rios & Price 2012). Therefore, the actual flux of GW at each site is unknown in these analyses as that would require the determination of hydraulic conductivity of aquifer material from each well site. However, assuming that the hydraulic conductivity of the material at each site did not vary with time, the flux of the GW at each site should be directly proportional to the calculated PGD EFW according to Darcy's Law. Zapata-Rios & Price (2012) reported GW discharge rates in

southern Taylor Slough of up to 14.82 mm/day from their water budget method and up to 63 mm/day for their hydraulic gradient method, which were calculated in the same areas as this project.

The similarity between upstream SW stages and TS6 PGD EFW, which had stronger relationship than between TS6 PGD EFW and both ecotone and downstream SW stages, suggests a linkage between the two. This linkage is supported by SW discharge at TS6, which is very closely related to both shallow and deep PGD EFW at TS6 (Figure 27, Figure 28, Figure 29). Increased SW discharge at TS6 cannot directly cause discharge of GW, as described by the Bernoulli principle, because the interface between SW and GW is not an open tube. Rather than a causal mechanism of PGD EFW, increased SW discharge at TS6 is directly indicative of upstream water levels. Higher upstream water levels result in greater SW discharge through Taylor Slough's mangrove ecotone at TS6 (Figure 23). Upstream water levels also result in a greater head difference between GW and SW downstream at TS6, which is why SW discharge and PGD EFW measurements are so similar; they share the same primary driver in upstream water levels. The effects of upstream SW stage changes on PGD EFW is likely subdued, with the aquifer damping the higher frequency pulses of SW fluctuations as differential pressures caused by upstream head variations propagate through the aquifer. Seasonally variable upstream head levels and recharge can drive downstream GW discharge in sand aquifers (Michael et al. 2005). The similar results presented here are derived from a karst aquifer and suggest that the influence of upstream water levels on downstream GW discharge may not be dependent upon aquifer type.

Stages at TS3, CP, NP72, and OL annually decrease far below that of Florida Bay SW stage three of the four years on record at TS6 (Figure 17, Figure 18). These decreases coincide with the SW flow reversals observed at TS6 and suggest that flow reversals may at least partially be driven by the horizontal gradient of SW, in addition to wind direction (Michot et al. 2011, Sutula 1999). Variations in SW discharge relative to upstream SW stage would be damped in a manner similar to that of GW discharge as a result of GW flow through the aquifer, but to a lesser degree. The damping effect on SW flow is a function of SW residence times in the watershed, which in

turn are influenced by volume, horizontal gradient, and resistances to flow such as vegetation and surface roughness, among other factors.

At TS3, PGD EFW was not strongly associated with any of the potential hydrologic drivers examined (Table 3, Table 4,Table 8). The strongest relationship observed at TS3 was between deep PGD EFW and 14-day antecedent cumulative rainfall, though the correlation was only moderate (Table 8). The lack of consistently strong associations between TS3 PGD EFW with water levels, precipitation, and ET is probably a result of the intermediate and transitional location of the site, between the fresh upstream and ecotone regions. Additionally, seasonal dry-down occurs at TS3, when SW levels descend below the surrounding bedrock, effectively becoming GW measurements (Figure 5). Water levels at TS3 are continuously measured despite the occurrence of dry-down because the measurement apparatus used is capable of measuring shallow water stages below surrounding bedrock. During the dry periods, PGD EFW was generally lowest, especially evident during the two dramatically lower negative spikes in stage that occurred in 2009 and 2011 (Figure 5, Figure 11).

The relationships between rainfall and water stages were expected to be stronger because rainfall and ET are the two primary components of Taylor Slough's water budget (Sandoval 2013, Zapata-Rios & Price 2012). Any correlations with rainfall and ET that were observed were probably because of the seasonal characteristics of ET and rainfall and their seasonal control on water stages, rather than on daily GW and SW stage difference fluctuations. Rapid dispersal and infiltration of rainfall upon falling to the ground during intense and sporadic rainfall events can explain the lack of an apparent influence of rainfall on GW and SW stage difference, especially when the overlying peat layer is dehydrated and rewetting (Michot et al. 2011). Broad seasonal changes in rainfall and ET are probably important components in the overall trends observed in the differences in stage between GW and SW in Taylor Slough, but their effects are not apparent in the day-to-day fluctuations of the GW and SW stage differences (Table 7, Table 8).

Zapata-Rios & Price (2012) used a multi-method approach to determine the timing of GW discharge in southern Taylor Slough with a water balance component whose scale was basin-wide and a hydraulic gradient technique that used multiple point based measurements of stage differences between SW and GW. The greatest monthly GW contribution to Taylor Slough's water budget, based on the water balance approach, occurred in April 2009 (Zapata-Rios & Price 2012). This April 2009 peak was linked to increased ecosystem productivity in southern Taylor Slough by Koch et al. (2012). The next largest GW input peaks from Zapata-Rios & Price's (2012) water balance calculations were in July and March of 2008. Brief peaks in shallow and deep PGD EFW at TS6 were apparent between March and May 2009, but these occurred in the midst of the dry season when PGD EFW and GW stages were both close to their seasonal lows (Figure 12, Figure 14).

A smaller head difference between GW and SW may be needed to produce GW discharge when regional water levels are lower. The smaller peaks in Zapata-Rios & Price's (2012) water balance results also occurred when GW stage and PGD EFW were near their seasonal lows. At TS6, PGD EFW exhibited the highest variability during these periods, with rapid fluctuations between higher and lower PGD EFW. The clearest similarity between TS6 PGD EFW and the monthly water budget results of Zapata-Rios & Price (2012) occurred in May 2008, when TS6 deep PGD EFW was at a seasonal low and TS6 shallow PGD EFW was very close its seasonal low, which occurred in June (Figure 10). Despite the similarity between these seasonal lows, the value for May 2008 from Zapata-Rios & Price (2012) was negative, whereas all of the monthly PGD EFW values at TS6 were positive (Figure 10). Although the overall trends of the GW discharge and PGD EFW evaluation techniques shared some similarity, they did not agree well when compared on a monthly basis.

The monthly PGD EFW results at TS3 shared even less similarity with the results from Zapata-Rios & Price (2012) than the TS6 PGD EFW results did. The April 2009 peak did not agree with either the shallow or deep TS3 PGD EFW calculations (Figure 11). Instead of a positive peak, a negative peak occurred in both shallow and deep PGD EFW at TS3 in April 2009

(Figure 11). The same is true of the peaks in July and March of 2008 from Zapata-Rios & Price (2012); they did not agree well with this study's PGD EFW results at TS3 (Figure 11). The TS6 PGD EFW peaks occurred in December and January, with the exception a peak in July 2009 (Figure 10). The discrepancy between Zapata-Rios & Price's (2012) GW discharge calculations and the PGD EFW results from this project may be a result of differences in scale; this study used single well points whereas Zapata-Rios & Price's (2012) water balance calculations were basinwide in scale.

The vertical hydraulic gradient timing results of Zapata-Rios & Price's (2012) study similarly did not agree with the results from PGD EFW analyses made at TS6 or at TS3 (Figure 10, Figure 11), despite being of a similar method to those of this study. The vertical hydraulic gradient comparison made by Zapata-Rios & Price (2012) considered peat GW for the GW component, rather than bedrock GW. Furthermore, equivalent freshwater heads were not considered for the stage difference calculations; only measured stages were considered in their study (Zapata-Rios & Price 2012).

The highest volumes of water in Taylor Slough occurred in October and September between 2001 and 2011 (Sandoval 2013). Seasonal highs for PGD EFW at TS6 and TS3 tended to occur at or close to October and September (Figure 10, Figure 11). The shortest flushing times and smallest in-basin volumes occurred in May (Sandoval 2013). May was also the month of lowest PGD EFW for TS6 shallow, TS6 deep, and TS3 shallow (Figure 10, Figure 11). December was the month of lowest PGD EFW for TS3 deep (Figure 11). These relationships, with the possible exception of TS3 deep PGD EFW, demonstrate the necessity of upstream heads to produce a vertical hydraulic gradient downstream.

Between 2001 and 2011, October had the lowest average contribution of GW to Taylor Slough's water budget, whereas May had the highest average GW contribution (Sandoval 2013). These results from Sandoval (2013) are the opposite of the results from the PGD EFW analyses, which were relatively high during October and relatively low during May, particularly at TS6 (Figure 10, Figure 11). The PGD EFW calculations consider vertical stage differences and

potential for vertical flow over time. Horizontal inflows and outflows of GW to and from the watershed could account for the discrepancies, especially if the aquifer matrix is anisotropic and there is less resistance to horizontal flow than to vertical flow. Furthermore, the scale of Sandoval's (2013) study was the entire watershed, versus the point observations made in this project.

Florida Bay waters tended to flow into Taylor Slough from March through May each year (Sandoval 2013), which agrees with the timing of recurrent salinity spikes observed in TS6 SW (Figure 50) and the findings of Michot et al. (2011) and Zapata-Rios & Price (2012). Sandoval's (2013) study did not investigate creeks that connect Taylor Slough to Florida Bay, other than Taylor River. If the flows in those creeks seasonally reverse as they do in Taylor River, neglecting to include the contributions of the other creeks to the water budget would have contributed to the residual GW term observed in the drier months. Relatively small contributions of water are more important to water budgets when the total volume of water in a basin is smaller, because small contributions become more significant as total volumes decrease and should therefore not be ignored. Michot et al. (2011) also suggested that during the wet season, the overland component of flow is important to consider because during the wet season, SW flow is not confined to the Taylor River channel. Unmonitored wet season SW outflows, both overland and through unmonitored creeks, would result in smaller apparent GW contributions to the Slough's water budget.

Results from Michot et al. (2011) demonstrated that rainfall and ET play only a minor role in the region of TS6 during the wet season. Michot et al. (2011) explain rainfall's minor influence through peat rewetting events. Michot et al. (2011) also found that GW flow near TS6 was predominantly upward, and similar to the rate of ET. The consistently positive daily PGD EFW values calculated at TS6 in this study agree with their GW flow result, which used data from the same shallow GW well at TS6 that this study used (Figure 10). Michot et al.'s (2011) study ended immediately before this study's timeframe, so their results do not temporally overlap with this study's results.

Upstream water levels are a function of multiple phenomena, predominantly precipitation and ET. Water management activities also affect the quantity of water in Taylor Slough (Zapata-Rios & Price 2012, Kotun & Renshaw 2014), providing another control on upstream SW stages. The high correlation and lack of a lag time between upstream water stages examined in this study suggests that inputs of water to Taylor Slough will result in higher water stages throughout the basin. Higher upstream SW stages are associated with both increased PGD EFW in the ecotone and higher SW flows past TS6 and into Florida Bay. Greater flows of fresh SW through the ecotone retard the surficial inflow of saline estuarine inflows from Florida Bay, which can be expected to increase as Florida Bay stage rises with global sea levels.

CONTROLS OF SURFACE WATER CHEMISTRY

The high salinities observed in TS6 SW cannot be explained by GW discharge, even from deep GW at TS6, because they repeatedly exceed those of underlying GW (Figure 42). Increased SW salinities occur at TS6 when SW discharge is negative, typically between March and August (Figure 50). Alternative sources of high salinity SW are inflows from Florida Bay and ET; the most likely explanation for the presence of high salinity SW at TS6 is a combination of hypersaline Florida Bay inflows and ET. The highest ET totals occur at approximately the same time that the SW salinities are elevated in 2008, 2010, and 2011, but not in 2009 (Figure 31, Figure 50). Inflows from Florida Bay are probably the primary mechanism for elevated salinity because the periods of elevated SW salinity at TS6 are closely related to inflows from Florida Bay and pronounced daily spikes in salinity are frequently related to rapid shifts in SW discharge, when flow shifts from positive to negative on a daily basis (Figure 50). Inflows from Florida Bay occur in conjunction with lower upstream stages (Figure 23), which in turn are controlled by seasonal rainfall, ET, and water management practices.

The brief diversion from the overall trend of stratified GW salinity at TS6 could signify a downward movement of higher salinity SW, whose greater density would propel a downward infiltration of SW, but that is probably not the case because PGD EFW values at TS6 are always

positive (Figure 10). The broad peaks observed in deep GW salinity at TS6 occur approximately one to two months after reversed SW flow and intrusion of high salinity SW (Figure 50). Salinity peaks observed in deep GW at TS6 cannot be caused by recharge from high salinity SW because the salinity of SW repeatedly exceeds that of deep GW by many psu during three of the four years of this study at TS6, while salinity in shallow GW remains intermediate to SW and deep GW, thus necessitating explanation by another source of high salinity GW.

The seasonal salinity peaks observed in deep GW and SW must be caused by seasonally variable saltwater intrusion, similar to results discussed by Michael et al. (2005), but the mechanisms of saltwater intrusion that affect GW and SW are different. Potential mechanisms for intrusion of saltwater into a similar aquifer along the southwestern edge of the Florida peninsula are discussed by Shoemaker & Edwards (2003). These potential mechanisms include horizontal motion of the interface between fresh and salty GW, upward movement of higher salinity GW, infiltration of saltier SW from channels on the surface, and motion of old seawater pockets within the aquifer. Shoemaker & Edwards (2003) further stated that upwards movement and lateral movement are the most likely of the possible saltwater intrusion processes.

Saltwater intrusion on the surface does not demonstrate a lag time with SW flows, based on the rapid response of SW salinity at TS6 to flow reversals, supporting a causal relationship between SW flow reversals and elevation SW salinity (Figure 50). Saltwater intrusion affects GW salinity at a lower rate, lagging behind the salinity response of SW to surficial saltwater intrusion. The lagged response of GW to the seasonally varying influence of saltwater intrusion, and the lack of influence on GW salinity by high salinity SW, suggest two things: 1) GW salinity is not controlled by saline SW inflows; and 2) salinity peaks in deep GW are caused by changes to the geometry and/or the location of the brackish mixing zone. The source of seasonally increased salinity in deep GW at TS6 must be either lateral or upward inflows from higher salinity GW, which is very likely to exist seaward and below the TS6 wells, further into the brackish mixing zone. The PGD EFW calculations at TS6 and the upstream stage measurements indicate that lower hydraulic gradients are present when the peaks in deep GW salinity occur at TS6 (Figure

17, Figure 41). As PGD EFW decreases at TS6, concurrent with decreasing upstream head, GW's brackish mixing zone changes in location and/or geometry, lagging behind high salinity SW inflows and producing the salinity peaks that are observed in deep GW (Figure 41). As PGD EFW at TS6 rises following the deep GW salinity peaks, the brackish mixing zone returns to its previous location and/or geometry and the 29 psu plateau salinity is reached again. The plateau salinity that TS6 GW salinity exhibits may represent a period of stability in the brackish mixing zone (Figure 42).

The lag times exhibited between GW and SW salinity peaks must be a result of the difference in flow velocities between GW and SW. Flow of GW typically occurs at a significantly lower rate than SW flow because GW flow occurs through aquifer materials, which present a much greater resistance to flow than that experienced by SW in a river channel. The SW salinity changes caused by intrusion of high salinity Florida Bay SW were thus produced more quickly than those observed in GW, in response to environmental drivers.

Shallow GW salinity at TS6 decreases seasonally, corresponding with seasonal decreases in PGD EFW and increases in PGD EFW variability at TS6 (Figure 38). If the high salinities observed in shallow GW are maintained by the upward, advective flow of saltier deep GW (Shoemaker & Edwards 2003), a decrease in PGD EFW would decrease the likelihood that higher salinity GW would flow upwards from deeper strata. The more variable and lower salinity periods observed in shallow PGD EFW at TS6 may reflect a spatially fluctuating brackish mixing zone (Figure 42). Fresher upstream GW flow towards the coast could explain the lower salinities observed in shallow GW at TS6 when PGD is lower. When less vertical forcing occurs, or lower PGD, impediment to horizontal flow may be decreased, allowing for fresher upstream GW to flow into the mangrove ecotone. Alternatively, lesser vertical forcing could result in shallower coastal GW circulation and lesser contributions of saltier, deep GW to the shallow portion of the aquifer underlying TS6. When the shallower portion of the mixing zone is subsequently stabilized by greater advection of deeper and saltier GW, the 29 psu plateau salinity is reached again. Another explanation for the reduced shallow GW salinities at TS6 is recharge of the shallow aquifer by the

low salinity SW that is present during the periods of reduced shallow GW salinity. This alternative explanation appears unlikely because PGD EFW at TS6 is always positive, although PGD EFW is generally lower and more variable during the periods of lower shallow GW salinity at TS6 (Figure 38).

An explanation for the seasonal freshening of GW in coastal aquifers affected by saltwater intrusion is discussed by Michael et al. (2005), but a different relationship between shallow GW salinity and stage is observed here (Figure 39). Shallow GW salinity is highest at TS6 when shallow GW stage is highest and deep GW salinity at TS6 peaks while deep GW stage is increasing, with the exception of two relatively small perturbations in deep GW salinity, as deep GW stage decreases at the end of 2009 and 2010 (Figure 40). These observations are different than the predictions made by Michael et al. (2005) that were based on the Ghyben-Herzberg approximation, in which they estimated that water table fluctuations could have up to a 40-fold greater effect on the depth of the saline/freshwater interface. According to Michael et al. (2005), lower water table elevations should result in a shallower brackish mixing zone, which in turn would result in higher salinities in shallow GW.

Michael et al.'s (2005) finding that slight variations in elevation of the water table overlying a brackish mixing zone could theoretically allow for a 40-fold amplified fluctuation in the depth of the saline/freshwater interface may not hold true for the coastal Everglades. With the extremely shallow horizontal gradients present in the Everglades, a very shallow mixing zone underlying the coast could exist. The consistently high salinities observed in the shallow GW well at TS6 suggest that the shallow well does indeed penetrate the brackish mixing zone. The seasonal freshening that occurs at TS6 appears to be a caused by fluctuations of the saline/fresh interface, with freshening occurring as shallow GW stage decreases, and increases in shallow GW salinity occurring when GW stage increases. As the brackish mixing zone seasonally changes in geometry and/or location, shallow GW salinities are lowered. A highly complex and dynamically circulating mixing zone may exist at depth along the southern coastal Everglades, and could account for the differences between these results and those of Michael et al. (2005).

In contrast to the results of this study, Michot et al. (2011) found that GW discharge is important to SW salinity in the mangrove ecotone. The TS6 SW salinity and SW discharge measurements as well as Ca/Cl ratios used in this study suggest that GW discharge is not an important control on SW salinity in the ecotone, at least where this study's continuous SW salinity measurement are made in Taylor River's main channel (Figure 2). Periods of voluminous and fresh SW discharges from upstream through the main channel of Taylor River could dilute high salinity, discharging GW. The effect of dilution would be particularly pronounced if actual GW discharge volumes were low compared to the volume of discharging SW. It is possible that a combination of GW discharge and saline SW inflows contributed to the salinity increases observed in the ecotone's SW, but SW inflows were probably the dominant mechanism of salinity increases in Taylor River's main channel (Figure 50), if not the entire ecotone. If the main channel's water is flushed with fresh water at a higher rate than the surrounding ecotone water, SW salinity in the main channel of Taylor River could be preferentially diluted and may not be representative of the rest of the ecotone.

In southern Shark Slough, GW discharge is an important contributor to the slough's water budget for at least part of the year, but is not of a magnitude to affect the salinity of SW (Saha et al. 2011). Although this is contrast to the findings of Michot et al. (2011) for Taylor Slough, a small amount of GW discharge could explain the lack of influence of GW discharge on Taylor Slough's salinity. There is the possibility that low rates of GW discharge are occurring throughout the ecotone and maintain the higher SW salinities previously observed outside of the main channel by Zapata-Rios & Price (2012).

Salinity of shallow GW at TS3 appears to be a function of water level, with higher water stages diluting the underlying GW (Figure 47), whereas deep GW salinity was dissimilar to water stage fluctuations at TS3 (Figure 49). The increasing GW salinities are indicative of an increasing salinization of the aquifer that is increasing a result of subsurface seawater intrusion. Price et al. (2006) suggested horizontal motion of the brackish mixing zone in an adjacent basin to the east (C-111), but their study also found that the salinity in Taylor Slough GW measured at TS3 did not

change notably. Price et al. (2006) interpreted their observed static salinities at TS3 as a relatively stable front of seawater intrusion. The increasing salinities at TS3 observed in this study suggest an advancing saltwater intrusion front (Figure 43, Figure 44, Figure 45, Figure 46), contrary to the findings of Price et al. (2006). There is clear seasonal variability in shallow GW salinity at TS3 (Figure 43), which also differs from the invariant salinities observed at TS3 by Price et al. (2006). The continuous and long term nature of the measurements used in this study allow for time series analyses that offer a much more complete depiction of water conditions than point measurements permit.

No evidence of flux between GW and SW at TS3 was found by Sandoval (2013), based on both isotopic and ionic data. The ionic data utilized in this study suggest a different interaction between GW and SW at TS3 (Figure 67). Although the PGD EFW calculations at TS3 were highly variable (Figure 11), the Ca/Cl ratios showed clear seasonal characteristics indicative of varying influences of GW and SW (Figure 67). Although SW salinities remained low at TS3, the Ca/Cl ratios repeatedly decreased and shifted toward saltwater intruded, lower Ca/Cl ratio chemistries when TS3 SW stage was low (Figure 67).

The ratio of Ca/Cl in SW at TS6 appears to be controlled by SW inflows from Florida Bay (Figure 66). When SW inflows seasonally reversed, TS6 SW became enriched in Cl^-, relative to Ca^{2+}, and approached the Ca/Cl ratios of Florida Bay. When SW flow at TS6 was directed towards Florida Bay, which generally coincided with higher upstream water stages, Ca/Cl ratios approached upstream TSB SW values, which are less influenced by seawater intrusion. At TS3, the ratio of Ca/Cl in SW appears to be controlled by water stage at TS3 (Figure 57). As water stages seasonally decreased, the Cl^- enriched GW at TS3 was able to increasingly influence the chemistry of the poorly isolated overlying SW, lowering the ratios of SW towards values indicative of saltwater intrusion (Figure 67). As water stages at TS3 rose, upstream SW inflows and rainfall brought Ca^{2+} enriched water from the surface to TS3. These inputs of Ca^{2+} enriched waters retained their high Ca/Cl ratios because they did not have a chance to interact with seawater

intruded SW or GW, thus increasing the Ca/Cl ratios of TS3 SW towards the upstream TSB SW ratio (Figure 67).

The spatially and temporally variable ratios of Ca/Cl in Taylor Slough are illustrative of the influence of saltwater intrusion in both GW and SW throughout the ecotone (Figure 66, Figure 67). In a carbonate aquifer dominated system, Ca/Cl ratios are expected to be highest when and where the influence of Cl^--rich seawater is lowest. If ET were responsible for the seasonal chemistry variations seen in TS6 SW and TS3 shallow GW, salinity would rise without significant changes to the Ca/Cl ratios in waters. Ratios of Ca/Cl in GW and SW increase as distance from Florida Bay increases (Figure 66, Figure 67). Saltwater in Florida Bay has much higher concentrations of Cl^-, relative to Ca^{2+}, and the intrusion of Florida Bay waters can explain the seasonal lowering of Ca/Cl ratios observed in TS6 SW and TS3 GW, through SW intrusion and GW intrusion, respectively.

The concentrations of TP were generally higher in TS6 SW than in TS3 SW, which agrees with previous findings and theoretical models of nutrient gradients (Childers 2006; Gaiser et al. 2012; Sutula et al. 2003) (Figure 68). The concentration of TP in TS6 SW over time had a generally inverse relationship with water stage at TS6 (Figure 69), and a more immediate, inverse relationship with both SW discharge and PGD EFW at TS6 (Figure 70, Figure 71, Figure 72, Figure 73). The data presented here agree with the mechanism previously described by Koch et al. (2012). In Koch et al.'s (2012) mechanism, when low-TP water was flushed through the ecotone from the upstream reaches of the basin, TP concentrations in the ecotone remained low (Figure 69). Furthermore, larger wet season volumes of upstream inflows diluted SW TP concentrations at TS6 and maintained low salinities in the ecotone, while contributing Ca^{2+} enriched SW (Figure 66). When lower and reversed flows occurred, TP concentrations in SW become elevated at TS6 (Figure 73) and GW discharge was able to make a volumetrically more significant contribution to SW, as suggested by Koch et al. (2012). Koch et al. (2012) linked the timing of GW discharge as described by Zapata-Rios & Price (2012) to pulses in ecosystem metabolism. The differing timings of PGD EFW and GW discharge between this study and

Zapata-Rios & Price (2012) may explain the difference in PGD EFW peaks and metabolic activity as described by Koch et al. (2012). The TP data used in this study are sourced from the same TP dataset utilized by Koch et al. (2012).

Based on the results from the previous section on controls of salinity and Ca/Cl ratios, the transfer of major ion constituents from GW to SW at TS6 was not as significant to SW chemistry as the effect of upstream inflows, but unlike salinity and Ca/Cl ratios, inflows of Florida Bay SW cannot explain the elevated TP concentrations that occur in the ecotone. Florida Bay SW has lower TP concentrations than ecotone SW and peat GW (Figure 75) (Price, 2008), so another source must have maintained the relatively high TP concentrations in the ecotone. A set of diagrams that synthesize the results from this study and depict the hydrologic forcing mechanisms and the resultant chemical changes that occur as a result of the hydrologic forcing mechanisms is presented in (Figure 76).

The salinities observed in TS6 GW (Figure 42) support the mobilization of P from carbonate bedrock as described by Price et al. (2010). Bedrock GW samples from both the TS6 GW wells (Price et al. 2006) and TS/Ph-6b Peat GW have elevated TP concentrations relative to Florida Bay SW and upstream TSB SW (Figure 75). The constantly positive PGD EFW values observed at TS6 suggests that there is always at least some GW contribution to SW chemistry (Figure 10). The contribution of P from GW to SW at TS6 may be far more significant to the SW concentrations of P than the GW discharge contribution of major ions to SW salinity and Ca/Cl ratios. Any GW discharge contributions to SW at TS6 that occurred when a smaller volume of water was present and lower flow rates occurred would be volumetrically more significant than during periods of higher stage and increased flows because there would be less water present to dilute the discharging GW's constituents, as described by Koch et al. (2012). Thus, the lower TP concentrations in TS6 SW can be explained by increased flow from upstream and higher stage at TS6 (Figure 69). Additionally, the salinity limited productivity mechanism in the ecotone described by Koch et al. (2012) would result in P not being as readily removed from the water column by metabolic activity when salinities are highest. The seasonally higher P concentrations in TS6 SW

are probably a result of GW discharge, while the seasonally higher salinities and lower Ca/Cl ratios are caused primarily by intrusion of high salinity, low Ca/Cl ratio SW from Florida Bay.

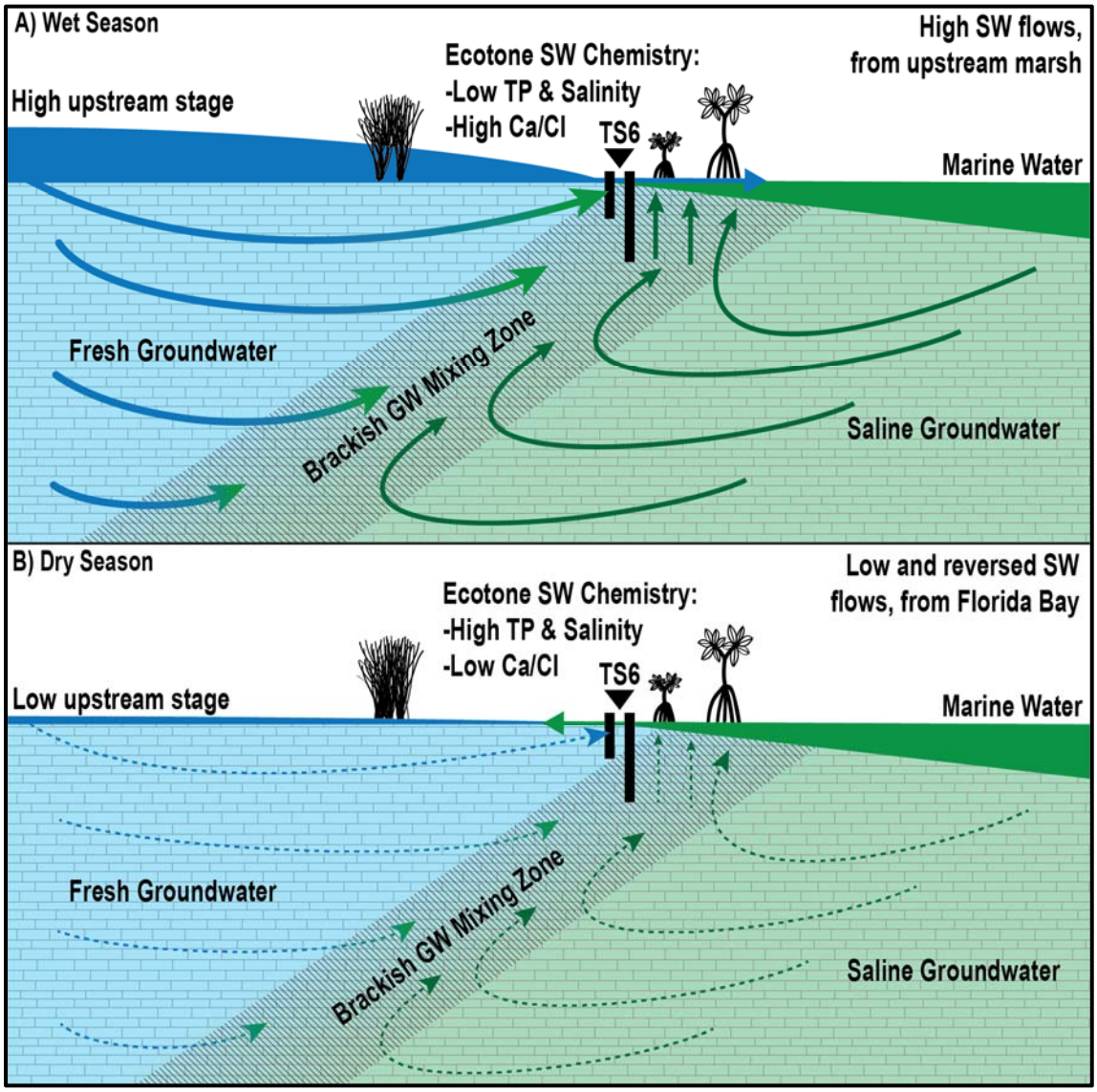

Figure 76: A) Higher upstream surface water (SW) stages during the wet season lead to a greater potential for groundwater (GW) discharge and greater flow from fresh sources (blue) through the ecotone, with lower TP, lower salinities, and higher Ca/Cl ratios in ecotone SW. B) Lower upstream SW stages during the dry season lead to a lesser potential for GW discharge and low to reversed SW saline flow from Florida Bay (green) into the ecotone, with higher TP, higher salinities, and lower Ca/Cl ratios in ecotone SW. GW wells at TS6 are denoted by black vertical lines. Fresh water observed in the shallow well at TS6 during the dry season may be related to the lower potential for upward movement of saltier water from deeper in the mixing zone, allowing fresh aquifer water to migrate to that well. Vertical dimensions are greatly exaggerated.

Sutula et al. (2001) found that atmospheric depositions was the most important contributor of P to Taylor Slough's nutrient budget throughout the year, with 50% more P being deposited during the wet season than during the dry season. The highest TP concentrations in TS3 SW (Sandoval 2013) occurred during the dry season (Figure 68) (Sandoval 2013). As described by Sandoval (2013), it is possible that higher rates of ET and lower water levels combine to produce the higher observed TP concentrations at TS3.

Significant heterogeneity in microtopography and landcover exist in Taylor Slough's mangrove ecotone, with some areas covered with mangroves and thick deposits of peat and marl, whereas other areas are barren of bedrock cover, particularly in sections of channels such as Taylor River's. Some other studies of GW discharge in other areas have been performed in saltmarshes with minimal relief and more homogeneous surface and landcovers (e.g. Michael et al, 2005, Tobias et al. 2001). The homogeneity of GW/SW interactions in regions like saltmarshes therefore makes estimates of regional phenomena more powerful because more homogeneous flow can be assumed. Results from studies like this one that use point observations in regions with dramatically variable surface features like those that exist in the southern Everglades should not be extrapolated over large areas unless appropriate assumptions are made.

The next step in this line of research should be an investigation of GW salinity and saltwater intrusion using a density dependent computer model of GW flow. Results from such a study would help in determining the drivers of GW salinity variations observed in shallow wells in the region, as well as the geometry and location of the brackish GW mixing zone. A GW modeling effort would assist in determining how variations in upstream stages due to either water management practices or climate change may influence hydrochemical conditions in the coastal Everglades.

CONCLUSIONS

Potential hydrologic drivers of GW discharge in the southern coastal Florida Everglades were investigated, along with potential hydrologic controls of SW chemistry. Strong seasonality was observed in all examined hydraulic parameters: water levels, precipitation and ET were all higher during the wet season and lower during the dry season. Similarly, SW flows were greater during the wet season and either ceased or reversed during the dry season.

A potential for upward flow from the Biscayne aquifer towards the surface, calculated as the density corrected equivalent freshwater head difference between GW and SW, was present for nearly the entire duration of this study at both southern Everglades study sites. Of the potential hydrologic drivers of GW discharge and SW chemistry examined in this study, water levels in the freshwater portion of Taylor Slough ultimately proved to be the most likely control of PGD EFW; SW and GW salinity; and Ca/Cl ratios at both TS6 and TS3. Concentration of TP in TS6 SW was probably controlled by upstream water levels, which in turn control SW flow through the ecotone and ecotone GW discharge. Lesser ecotone SW stages and SW flows allowed for volumetrically more significant contributions of P from underlying GW. Major ion chemistry of SW at TS6 and TS3 did not appear to be controlled by PGD EFW at either site.

Use of SW chemistry to discern the effects of GW discharge on ecotone SW is challenging because tracers such as salinity and Ca/Cl ratios are not unique to GW, and ecotone SW is strongly influenced by upstream SW. The ratios of Ca/Cl generally increased with distance from the coast, inland. As sea level rise progresses, decreases in Ca/Cl ratios can be expected to continue inland as the front of saltwater intrusion advances in both SW and GW. Maintenance of higher upstream water levels can be expected to retard the advance of saltwater intrusion in southern Taylor Slough and maintain lower TP concentrations in ecotone SW.

REFERENCES

Armentano, T, J Sah, M Ross, D Jones, H Cooley, and C Smith. 2006. Rapid responses of vegetation to hydrological changes in Taylor Slough, Everglades National Park, Florida, USA. *Hydrobiologia* 569, (1): 293-309.

Briceño, H, G Miller, and SE Davis. 2014. Relating freshwater flow with estuarine water quality in the southern everglades mangrove ecotone. *Wetlands* 34, (1): 101-11.

Brodie, R, B Sundaram, R Tottenham, S Hostetler, and T Ransley. 2007. *An overview of tools for assessing groundwater-surface water connectivity.* Canberra, Australia: Bureau of Rural Sciences.

Burnett, WC, PK Aggarwal, A Aureli, H Bokuniewicz, JE Cable, MA Charette, E Kontar, S Krupa, KM Kulkarni, and A Loveless. 2006. Quantifying submarine groundwater discharge in the coastal zone via multiple methods. *Science of the Total Environment* 367, (2): 498-543.

Burnett, WC, H Bokuniewicz, M Huettel, WS. Moore, and M Taniguchi. 2003. Groundwater and pore water inputs to the coastal zone. *Biogeochemistry* 66, (1-2): 3-33.

Childers, DL, 2006. A synthesis of long-term research by the Florida Coastal Everglades LTER program. *Hydrobiologia* 569, (1): 531-44.

Childers, DL, JN Boyer, SE Davis, CJ Madden, DT Rudnick, and FH Sklar. 2006. Relating precipitation and water management to nutrient concentrations in the oligotrophic "upside-down" estuaries of the Florida Everglades. *Limnology and Oceanography* 51, (1): 602-16.

Cooper, HH. 1959. A hypothesis concerning the dynamic balance of fresh water and salt water in a coastal aquifer. *Journal of Geophysical Research* 64, (4): 461-7.

Darcy, H. 1856. *Les fontaines publiques de la ville de Dijon*. Librairie des Corps Imperiaux des Ponts et Chaussees et des Mines, Paris.

Davis, SM, and JC Ogden. 1994. Introduction. In *Everglades: The ecosystem and its restoration*, eds. Steven M. Davis, John C. Ogden. 1st ed., 3-7. Delray Beach, FL: St. Lucie Press.

Davis, SE, DL Childers, JW Day, DT Rudnick, and FH Sklar. 2001. Wetland-water column exchanges of carbon, nitrogen, and phosphorus in a southern Everglades dwarf mangrove. *Estuaries* 24, (4): 610-22.

DeAngelis, DL, and PS White. 1994. Ecosystems as products of spatially and temporally varying driving forces, ecological processes, and landscapes: A theoretical perspective. In *Everglades: The ecosystem and its restoration.* eds. SM. Davis, JC. Ogden. 1st ed., 9-27. Delray Beach, FL: St. Lucie Press.

Duever, MJ, JF Meeder, LC Meeder, and JM McCollom. 1994. The climate of south Florida and its role in shaping the Everglades ecosystem. In *Everglades : The ecosystem and its restoration.*, eds. SM. Davis, JC. Ogden. 1st ed. Vol. 225, 225. Delray Beach, FL: St. Lucie Press.

Fennema, RJ, CJ Neidrauer, RA Johnson, TK MacVicar, and WA Perkins. 1994. A computer model to simulate natural everglades hydrology. In *Everglades: The ecosystem and its restoration*, eds. SM. Davis, JC. Ogden. 1st ed., 249-289. Delray Beach, FL: St. Lucie Press.

Fish, JE, and MT Stewart. 1991. *Hydrogeology of the surficial aquifer system, Dade County, Florida.* Tallahassee, Florida: U.S. Geological Survey, Water-Resources Investigations Report 90-4108.

Gaiser, EE, M Heithaus, R Jaffe, LA Ogden, and RM Price. 2012. *LTER: FCE III - coastal oligotrophic ecosystems research proposal*. Florida, USA.

Gaiser, EE, DL Childers, RD Jones, JH Richards, LJ Scinto, and JC Trexler. 2006. Periphyton responses to eutrophication in the Florida Everglades: Cross-system patterns of structural and compositional change. *Limnology and Oceanography* 51, (1/2): 617-30.

Harvey, JW, SL Krupa, and JM Krest. 2004. Ground water recharge and discharge in the central Everglades. *Ground Water* 42, (7): 1090-102.

Holmquist, JG., GVN Powell, and SM Sogard. 1989. Sediment, water level and water temperature characteristics of Florida Bay's grass-covered mud banks. *Bulletin of Marine Science* 44, (1): 348-64.

IBM Corp. 2013. *IMB SPSS Statistics for Windows*. Vol. 22.0. Armonk, NY.

Kalbus, E, F Reinstorf, and M Schirmer. 2006. Measuring methods for groundwater-surface water interactions: A review. *Hydrology & Earth System Sciences* 3, (4): 1809-50.

Koch, GR, DL Childers, PA Staehr, RM Price, SE Davis, and EE Gaiser. 2012. Hydrological conditions control P loading and aquatic metabolism in an oligotrophic, subtropical estuary. *Estuaries and Coasts* 25, (1): 292-307.

Kohout, FA. 1960. Cyclic flow of salt water in the Biscayne aquifer of southeastern Florida. *Journal of Geophysical Research* 65, (7): 2133-41.

Kotun, K, and A Renshaw. 2014. Taylor Slough hydrology. *Wetlands* 34, (1 Supplement): S9-S22.

Langevin, CD, DT Thorne Jr, AM Dausman, MC Sukop, and W Guo. 2008. *SEAWAT Version 4: A Computer Program for Simulation of Multi-Species Solute and Heat Transport*.

Li, L, DA Barry, F Stagnitti, and J-Y Parlange. 1999. Submarine groundwater discharge and associated chemical input to a coastal sea. *Water Resources Research* 35, (11): 3253-9.

Light, SS, and JW Dineen. 1994. Water control in the Everglades: A historical perspective. In *Everglades: The ecosystem and its restoration.*, eds. SM. Davis, JC. Ogden. 1st ed., 47-84. Delray Beach, FL: St. Lucie Press.

Maidment, DR. 1992. *Handbook of hydrology.* McGraw-Hill Inc.

Michael, HA, AE Mulligan, and CF Harvey. 2005. Seasonal oscillations in water exchange between aquifers and the coastal ocean. *Nature* 436, (7054): 1145-8.

Michot, B, EA Meselhe, VH Rivera-Monroy, C Coronado-Molina, and RR Twilley. 2011. A tidal creek water budget: Estimation of groundwater discharge and overland flow using hydrologic modeling in the southern Everglades. *Estuarine, Coastal and Shelf Science* 93, (4): 438-48.

Microsoft Corp. 2012. *Excel 2013*. Vol. 15.0. Redmond, WA.

Moore, WS. 2006. The role of submarine groundwater discharge in coastal biogeochemistry. *Journal of Geochemical Exploration* 88, (1): 389-93.

Moore, WS. 1999. The subterranean estuary: A reaction zone of ground water and sea water. *Marine Chemistry* 65, (1): 111-25.

Moore, WS, and AM Wilson. 2005. Advective flow through the upper continental shelf driven by storms, buoyancy, and submarine groundwater discharge. *Earth and Planetary Science Letters* 235, (3): 564-76.

Noe, GB, DL Childers, and RD Jones. 2001. Phosphorus biogeochemistry and the impact of phosphorus enrichment: Why is the everglades so unique? *Ecosystems* 4, (7): 603-24.

Price, RM. 2001. Geochemical determinations of groundwater flow in Everglades National Park. Ph.D., University of Miami.

Price, RM. 2008. Determining nutrient concentrations in groundwater beneath Florida Bay. Final report submitted to SFWMD on behalf of FIU, by, Dec.16 2008, 24pp.

Price, RM, MR Savabi, JL Jolicoeur, and S Roy. 2010. Adsorption and desorption of phosphate on limestone in experiments simulating seawater intrusion. Applied Geochemistry 25, (7): 1085-91.

Price, RM, and PK Swart. 2006. Geochemical indicators of groundwater recharge in the surficial aquifer system: Everglades National Park, Florida, USA. *Special Papers - Geological Society of America* 404: 251.

Price, RM, PK Swart, and JW Fourqurean. 2006. Coastal groundwater discharge – an additional source of phosphorus for the oligotrophic wetlands of the Everglades. *Hydrobiologia* 569, (1): 23-36.

Saha, AK, CS Moses, RM Price, V Engel, TJ Smith III, and G Anderson. 2012. A hydrological budget (2002–2008) for a large subtropical wetland ecosystem indicates marine groundwater discharge accompanies diminished freshwater flow. *Estuaries and Coasts* 35, (2): 459-74.

Sandoval, E. 2013. Ten year study on water flushing times and water quality in southern Taylor Slough, Everglades National Park, FL. Master of Science, FIU Electronic Theses and Dissertations.

SFNRC. South Florida Natural Resources Council. DataForEVER dataset. Public URL not available (accessed 2015).

SFWMD. South Florida Water Management District. Dbhydro. Available from http://www.sfwmd.gov/dbhydroplsqp/show_dbkey_info.main_menu. (accessed 2014)

Shoemaker, BW, and KM Edwards. 2003. *Potential for saltwater intrusion into the Lower Tamiami Aquifer near Bonita Springs, southwestern Florida.* US Department of the Interior, US Geological Survey, Tallahassee, FL.

Spence, V. 2011. Estimating groundwater discharge in the oligohaline ecotone of the everglades using temperature as a tracer and variable-density groundwater models.

Sullivan, PL, RM Price, JL Schedlbauer, A Saha, and EE Gaiser. 2014. The influence of hydrologic restoration on groundwater-surface water interactions in a karst wetland, the Everglades (FL, USA). *Wetlands* 34, (1): 23-35.

Sutula MA. 1999. Processes controlling nutrient transport in the southern Everglades Wetlands, Florida, U.S.A. PhD Dissertation, Louisiana State University, May 1999

Sutula, MA, JW Day, JE Cable, and DT Rudnick. 2001. Hydrological and nutrient budgets of freshwater and estuarine wetlands of Taylor Slough in southern Everglades, Florida (USA).*Biogeochemistry* 56, (3): 287-310.

Sutula, MA, BC Perez, E Reyes, DL Childers, S Davis, JW Day, D Rudnick, and F Sklar. 2003. Factors affecting spatial and temporal variability in material exchange between the southern Everglades wetlands and Florida Bay (USA). *Estuarine, Coastal and Shelf Science* 57, (5): 757-81.

Systat Software Inc. 2008. Vol. 11.0. San Jose, CA.

Tobias, CR, JW Harvey, and IC Anderson. 2001. Quantifying groundwater discharge through fringing wetlands to estuaries: Seasonal variability, methods comparison, and implications for wetland-estuary exchange. *Limnology and Oceanography* 46, (3): 604-15.

Tobler, WR 1970. A computer movie simulating urban growth in the Detroit region. *Economic Geography*: 234-40.

USGS a. United States Geologic Survey. Everglades depth estimation network. Available from http://sofia.usgs.gov/eden/index.php (accessed 2015).

USGS b. United States Geologic Survey. Everglades depth estimation network. Available from http://sofia.usgs.gov/eden/evapotrans.php (accessed 2015).

USGS c. United States Geologic Survey. Everglades depth estimation network. Available from http://sofia.usgs.gov/eden/nexrad.php (accessed 2015).

USGS d. United States Geologic Survey. National water information system. Available from http://waterdata.usgs.gov/fl/nwis (accessed 2015).

Valiela, I, JC, K Foreman, JM Teal, B Howes, and D Aubrey. 1990. Transport of groundwater-borne nutrients from watersheds and their effects on coastal waters. *Biogeochemistry* 10, (3): 177-97.

Valiela, I, Kenneth F, M LaMontagne, D Hersh, J Costa, P Peckol, B DeMeo-Andreson, C D'Avanzo, M Babione, and C-H Sham. 1992. Couplings of watersheds and coastal waters: Sources and consequences of nutrient enrichment in Waquoit Bay, Massachusetts. *Estuaries* 15, (4): 443-57.

White, WN. 1932. *A method of estimating ground-water supplies based on discharge by plants and evaporation from soil: Results of investigations in Escalante Valley, Utah*. Vol. 659: US Government Printing Office.

Wilson, AM, and JT Morris. 2012. The influence of tidal forcing on groundwater flow and nutrient exchange in a salt marsh-dominated estuary. *Biogeochemistry* 108, (1-3): 27-38.

Winter, TC, JW Harvey, OL Franke, and WM Alley. 1998. *Ground water and surface water: A single resource*. Denver, Colorado: U.S. Geological Survey.

Zapata-Rios, X., and RM Price. 2012. Estimates of groundwater discharge to a coastal wetland using multiple techniques: Taylor Slough, Everglades National Park, USA. *Hydrogeology Journal* 20, (8): 1651-68.